THE IMPORTANCE OF PI(3,5)P2 IN MITOTIC EXIT

by

Şeyma Nur Bektaş

A Dissertation Submitted to the
Graduate School of Sciences and Engineering
in Partial Fulfillment of the Requirements for
the Degree of

Doctor of Philosophy

in

Molecular Biology and Genetics

KOÇ ÜNİVERSİTESİ

March 7, 2024

THE IMPORTANCE OF PI(3,5)P2 IN MITOTIC EXIT

Koç University

Graduate School of Sciences and Engineering

This is to certify that I have examined this copy of a doctoral dissertation by

Şeyma Nur Bektaş

and have found that it is complete and satisfactory in all respects,
and that any and all revisions required by the final
examining committee have been made.

Committee Members:

Dr. Ayşe Koca Çaydaşı (Advisor)

Prof. Dr. Nurhan Özlü

Dr. Tuğba Bağcı Önder

Prof. Dr. Zeynep Petek Çakar

Dr. Bilgin Taşkın

Date: 07.03.24

To my lovely family, who have always supported me

ABSTRACT

The Importance of PI(3,5)P2 in Mitotic Exit

Şeyma Nur Bektaş

Doctor of Philosophy in Molecular Biology and Genetics

March 7, 2024

Phosphoinositides are evolutionarily conserved signaling lipids that are critical for many aspects of cellular biology. Phosphatidylinositol-3,5-bisphosphate (PI(3,5)P2), one of the rarest phosphoinositides, is synthesized on vacuole/lysosome membranes through the phosphorylation of Phosphatidylinositol-3-phosphate (PI3P) by the Fab1 kinase. PI(3,5)P2 plays key roles in various cellular processes, including vacuole/lysosome structure and function, stress response, autophagy, transcriptional regulation, and membrane trafficking. Dysregulation of PI(3,5)P2 production has been implicated in various human diseases such as amyotrophic lateral sclerosis and cancer, highlighting the significance of PI(3,5)P2 for human health.

The work presented in this thesis discovers that PI(3,5)P2 is crucial for a timely mitotic exit in budding yeast. Our data shows that reduced levels of PI(3,5)P2 results in delayed mitotic exit and lethality in cells with compromised mitotic exit activity. Conversely, overproduction of PI(3,5)P2 rescues the prolonged anaphase and lethality of mitotic exit mutants. Mechanistically, we find that PI(3,5)P2 regulates the localization of the mitotic exit inhibitor Kin4. Accordingly, high levels of PI(3,5)P2 causes recruitment of Kin4 to the vacuole periphery. We further show that this process is dependent on Atg18, a known effector of PI(3,5)P2. Thus, this study unravels a novel link between PI(3,5)P2 and cell cycle progression in budding yeast.

ÖZETÇE

Mitotik Çıkışta PI(3,5)P2'nin Önemi

Şeyma Nur Bektaş

Moleküler Biyoloji ve Genetik, Doktora

7 Mart, 2024

Fosfoinosititler, hücresel biyolojinin birçok alanı için kritik öneme sahip evrimsel olarak korunmuş lipitlerdir. PI(3,5)P2 (Fosfatidilinozitol-3,5-bisfosfat), en nadir fosfoinosititlerden biri olup, Fosfatidilinozitol-3-fosfat'ın (PI3P) koful/lizozom membranlarında Fab1 kinaz tarafından fosforile edilmesiyle sentezlenir. PI(3,5)P2, koful/lizozom yapısı ve fonksiyonu, stres yanıtı, otofaji, transkripsiyonel düzenleme ve membran taşımacılığı dahil olmak üzere çeşitli hücresel süreçlerde önemli roller oynar. PI(3,5)P2 üretiminin disregülasyonu, amiyotrofik lateral skleroz ve kanser gibi çeşitli insan hastalıkları ile ilişkilendirilmiştir, bu da PI(3,5)P2'nin insan sağlığı açısından önemini vurgulamaktadır.

Bu tezde sunulan çalışma, PI(3,5)P2'nin tomurcuklanan mayada mitozdan çıkış zamanlaması için önemli olduğunu ortaya çıkarıyor. Verilerimiz, azalmış PI(3,5)P2 seviyelerinin mitozdan çıkışta gecikmeye ve mitotik çıkış aktivitesi bozulmuş hücrelerde ölüme neden olduğunu göstermektedir. Tersine, PI(3,5)P2'nin aşırı üretimi, mitotik çıkış mutantlarının uzamış anafaz fenotipini ve ölümcüllüğünü kurtarmaktadır. Mekanistik olarak, PI(3,5)P2'nin mitozdan çıkış inhibitörü Kin4'ün lokalizasyonunu düzenlediğini bulduk. Buna göre, PI(3,5)P2'nin yüksek seviyeleri, Kin4'ün koful periferine çekilmesine neden olmaktadır. Bu sürecin, PI(3,5)P2'nin bilinen bir efektörü olan Atg18'e bağlı olduğunu da gösteriyoruz. Bu nedenle, bu çalışma, mayada PI(3,5)P2 ile hücre döngüsü ilerlemesi arasında yeni bir bağlantıyı ortaya çıkarıyor.

The data presented in this thesis is published in the “Open Biology” journal under the title “The signalling lipid PI(3,5)P2 is essential for timely mitotic exit”.

(doi:10.1091/mbc.9.10.2803)

ACKNOWLEDGEMENTS

I extend my sincere gratitude to my esteemed mentor, Dr. Ayşe Koca Çaydaşı, whose unwavering support and patience have made this research possible. I am fortunate to have benefited not only from her imparted methods and principles throughout my doctoral studies but also from her invaluable lessons on navigating adversities and deriving meaning from mistakes in life.

I am deeply thankful to the esteemed members of my thesis supervisory committee and defense jury for their generous allocation of time and expertise.

I express my heartfelt gratitude to Prof. Dr. Sreeparna Banerjee, who has always believed in my potential to become a successful scientist and supported me throughout my undergraduate studies at METU.

To my laboratory colleagues, who illuminated the long and exhausting nights of doctoral life with their energy, I extend my sincere appreciation. Though we may now be scattered in different places, I hope all is well with each of you. To Betül, I deeply miss the days we would embark on projects fueled by evening excitement, yet couldn't finish by nightfall. Barış, thank you for your meticulous work with microscopic experiments. You are a remarkable person, and I wish you the best. Hüseyin, thank you for uplifting the lab's energy with your contagious laughter and colorful excitement. Cansu, I consider myself incredibly fortunate to have had your comforting presence during the toughest times. You are a true gem, and may everything turn out in your favor. With Idil, sometimes words were unnecessary; a simple embrace sufficed to carry us through. I miss your empathy and friendship the most. Haroon, I am grateful for your guidance and support during the initial stages of my doctoral journey, especially for sharing your secret methodologies. The moments we shared, whether in laughter or tears, have been invaluable, and I've learned a great deal from them. I hope we'll have the opportunity to reunite someday.

To my dear family, who alleviated the burdens of this arduous journey, I am forever grateful. Mom, you are the beacon behind every beautiful aspect of my life; your support has been immeasurable. Since childhood, you've never discouraged my boundless dreams; instead, you've understood and supported me. None of this would have been possible without you, and you know it; thank you for being my pembe yanak☺. Father, you've taught me the importance of resilience and integrity, even in the face of adversity. I've drawn strength from this during the most challenging times; thank you for being there, for we still need you and your teachings. To my brother, who patiently awaited my return from the lab during those prolonged nights, I remember vividly the excitement in my heart as you taught me about cell division for the first time; I was barely ten years old, but do you remember? Thank you for instilling a passion for science and for your assistance. To my cousin Esra, whom I've been in close contact with almost every day since childhood, you are my greatest fortune. "They will understand one day," we used to say; I think we've succeeded!

To my spouse, whose unconditional love and support have been my cornerstone, you are my better half. Thank you for nurturing the "life" aspect in the work-life balance. To my beloved daughter, despite the challenges, we've produced something beautiful together. Your little fingers are present on every page of this thesis; I love you dearly.

Finally, I extend my gratitude to The Scientific and Technological Research Council of Turkey (TUBITAK) for providing me with the scholarship throughout my doctoral studies. This project was funded by the TUBITAK 219Z100 awarded to Ayşe Koca Çaydaşı.

Additionally, I thank Mrs. Emine Büyükdurmuş and Mrs. Zehra Puntar for their patient and tolerant responses to all our inquiries.

TABLE OF CONTENTS

LIST OF TABLES

LIST OF FIGURES

ABBREVIATIONS

APC/C: Anaphase-Promoting Complex/Cyclosome

CDK: Cyclin Dependent Kinase

CKI: Cyclin Dependent Kinase Inhibitor

FEAR: Fourteen Early Anaphase Release

GAP: GTPase Activating Protein

GEF: Guanine Exchange Factor

MEN: Mitotic Exit Network

MT: Microtubule

MTOC: Microtubule Organizing Center

PI(3,5)P2: Phosphatidylinositol 3,5-bisphosphate

SPB: Spindle Pole Body

SPOC: Spindle Position Checkpoint

Chapter 1

INTRODUCTION

1.1 The Cell cycle

The cell cycle refers to the series of events that occur in a cell during cell division. During this process, genomic material is duplicated and segregated into two daughter cells, and daughter cells are physically separated (Alberts B, 2002). Along the way, new proteins and other essential components are synthesized for the cell to divide. The cell cycle is the fundamental mechanism through which single-celled organisms replicate, playing a pivotal role in the growth and development of multicellular organisms (McIntosh, 2016). Its significance extends to tissue regeneration, repair, and the replenishment of damaged or senescent cells within the adult organism It is vital for tissue renewal, repair, and replacement of damaged or dead cells in the adult organism. Understanding the cell cycle and its regulation is fundamental to understand various diseases, including cancer (Matthews et al., 2022).

1.1.1 Phases of the Cell Cycle

The cell cycle can be divided into two main phases: interphase, where the cell prepares for division by duplicating its genome and centrosomes, grows, and the mitotic phase where nuclear segregation is happen (Hartwell et al., 1973). Interphase is further divided into three subphases; G1, S and G2 phase. In G1 (Gap) phase, cell grows and after getting bigger enough or when receives environmental signals to divide, it passes to the S phase (Johnston, 1977). In the S phase (Synthesis phase) the cell duplicates its DNA to make sure that each cell has a complete set of DNA (Bell & Dutta, 2002). In addition to DNA, the centrosome and its equivalent structure in yeast SPB (spindle pole body) duplicate during the S phase. Also in yeast, bud emerges in this phase (Johnston, 1977). In G2 (Gap2) cell grows and gets prepared for the M (Mitosis) phase of the cell cycle, in which a series of events occur under highly controlled mechanisms for chromosome segregation and cell division (Hartwell et al., 1973).

The M phase, or mitotic phase, is the final stage of the cell cycle and involves the separation of the replicated chromosomes into two identical sets (mitosis, karyokinesis) and the division of the cytoplasm (cytokinesis) to produce two daughter cells. The process of mitosis is divided into distinct stages: prophase, pro-metaphase, metaphase, anaphase, and telophase (Alberts B, 2002). Chromosomes are condensed in prophase while centrosomes separated to opposite sites. In prometaphase, a transition period between prophase and metaphase, nuclear envelope breakdown (NEB) occurs. NEB does not happen in yeast as they undergo close-mitosis (Ferreira & Maiato, 2021). In metaphase, the replicated chromosomes align along the metaphase plate with the attached spindle fibers, ensuring their proper distribution to the daughter cells. Anaphase is the stage when sister chromatids are separated to the poles by spindle

fibers. Anaphase can be divided into two stages anaphase A and anaphase B. In anaphase A, sister chromatids are separated towards the poles of cell and in anaphase B, spindle poles move apart, further separating the chromatids (Scholey et al., 2016). After chromosome segregation, cytokinesis takes place where physical separation of two daughter cells occurs. The contractile ring is formed by actin filaments, and myosin motor proteins drive its contraction, resulting in cell division (Scholey et al., 2016)

1.1.2 Cyclin Dependent Kinases

Cyclin-dependent kinases (CDKs) are master regulators of the cell cycle. To be catalytically active, CDKs interact with proteins named cyclins forming cyclin-CDK protein complexes. These complexes are responsible for driving the progression of the cell cycle by phosphorylating target proteins involved in various cell cycle processes. Cyclins undergo periodic synthesis/degredation during specific stages of the cell cycle while CDK levels are stable (Simmons Kovacs et al., 2012). The activation of the next and inhibition of the previous cyclin-CDK complex providing directionality to the cell cycle. This tightly regulated process ensures that the cell cycle progresses in a unidirectional manner and maintains the fidelity of cell division (Nasmyth & Dirick, 1991).

Cyclins can be categorized depending on the cell cycle phase their levels peak (Table 1.1). Cyclins binding to CDKs induce a conformational change. The T-loop moves away from the catalytic site as a result of this conformational change, and making it accessible to substrates. The catalytic site becomes "phosphorylation competent," which means it can now catalyze the transfer of phosphate groups to target proteins (Morgan, 1997). Activation of CDKs also involves the phosphorylation of a specific residue within the CDK, known as the T-loop. T loop contains threonine or tyrosine rich catalytic domain that needs to be phosphorylated for fully active CDK. To achieve fully state of CDK, T-loops needs to be phosphorylated by CDK activating kinase (CAK) (Morgan, 1997). CAK phosphorylates the threonine residue of CDK, that causes a further conformational change allows stabilization of its active conformation which enhance the catalytic activity. This phosphorylation induces a conformational change in the CDK, allowing it to bind and phosphorylate its target proteins involved in cell cycle progression (Morgan, 1997). Conversely, CDKs can also be inhibited through phosphorylation at different sites, typically by kinases called CKI’s (Table 1.1). These inhibitory phosphorylation’s can be reversed by the action of phosphatases which remove the inhibitory phosphate groups, allowing the CDK to become active once more (Bloom & Cross, 2007)

Table 1.1 Cyclins and CDK partners are listed with cyclin dependent kinase inhibitors (CKI) in both human and budding yeast (Bai et al., 2017).

Cyclin (Human)	**Cyclin (Yeast)**	**Phase of Cell Cycle**	**CDK (Human)**	**CDK (Yeast)**	**CKI (Human)**	**CKI (Yeast)**	**Function**
Cyclin D	Cln1, Cln2, Cln3	G1 phase	CDK4, CDK6	Cdc28	p21, p27 p15,p18	Sic1	Controls G1 phase progression and inhibits CDK activity
Cyclin E	-	G1/S transition	CDK2	-	p21, p27	-	Regulates G1/S transition and prevents premature S phase entry
Cyclin A	Clb5, Clb6	S phase	CDK2, CDK1	Cdc28	p21, p27	-	Ensures proper DNA replication and progression through S phase
Cyclin B	Clb1, Clb2, Clb3, Clb4	G2/M transition	CDK1	Cdc28	p21, p27, p16	-	Controls G2/M transition and prevents premature mitosis

1.2 Yeast as a model for cell cycle studies

Budding yeast, *Saccharomyces cerevisiae*, is used as a model organism to study the complexities of the cell cycle. It has conserved proteins that govern cell cycle regulatory mechanisms including cyclin dependent kinases (CDKs), cyclins and checkpoint proteins. Their genome is fully sequenced, and molecular techniques are well established including selective gene deletion, gene overexpression, labelling fluorescently tagged proteins. Highly standardized and effective molecular biology methods are developed for genome editing, such as gene deletions and epitope tagging, facilitated by its high rate of homologous recombination. It can be maintained in a haploid stage, which enables targeted gene editing; as well as in a diploid state, which enables genetic complementation experiments via yeast mating. The availability of temperature-sensitive mutants and the ability to control temperature-sensitive gene

function by changing the growth temperature provide a powerful tool for studying essential genes. Budding yeast has a quick generation time approximately 90 minutes under optimal conditions (Hinnebusch & Johnston, 2011). This provide large-scale experiments can be efficiently carried out and cell cycle events can be observed in a short period of time. The ease of observing cell cycle stages based on cellular morphology, along with the ability to synchronize cells at specific phases, makes budding yeast a valuable model organism for studying the cell cycle and its regulation. Additionally, its asymmetric cell division allows for investigating cellular asymmetry and differential gene expression.

1.2.1 Yeast life cycle

The life cycle of budding yeast involves both asexual and sexual reproduction. They primarily reproduce asexually by a process known as budding, where a smaller daughter cell is produced as an outgrowth of the mother cell. The daughter cell matures and separates from the mother, growing to full size before it itself can bud (Herskowitz, 1988). Both haploid and diploid *S.cerevisiae* undergoes budding. Two haploid cells of opposite mating types (a and α) merge to form a diploid cell. This diploid, under certain environmental conditions, can sporulate (Merlini et al., 2013). During sporulation, the diploid cell undergoes meiosis to produce four haploid spores encapsulated. Each of these spores can germinate into a new haploid yeast cell when conditions are favorable, and the cycle repeats. These alternating stages of asexual and sexual reproduction allow yeast to adapt to changing environments, contributing to their success as a species (Botstein & Fink, 2011).

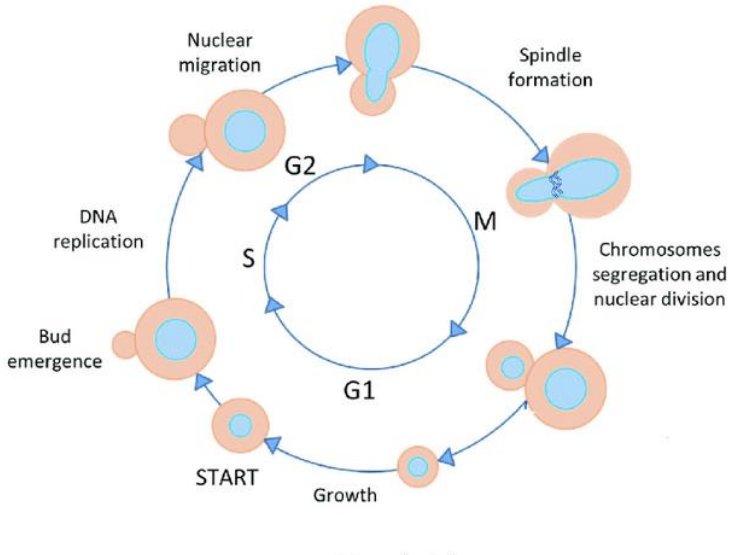

Figure 1.1. The life cycle of budding yeast. It consists of G1, S, G2 and M phase (Alberts B, 2002).

1.2.2 Budding Yeast Cell Cycle

In budding yeast Cdc28 also known CDK1 is the main kinase. It interacts with two types of cyclin, G1 cyclins and B cyclins. G1 cyclins consist of Cln1, Cln2, Cln3 and B type cyclins are Clb1-6 (Nasmyth & Dirick, 1991). G1 phase of the cell cycle events are regulated by G1 cyclins-CDK1 complexes. This activation plays a role in G1-S transition (Hartwell et al., 1973). B type cyclins-CDK1 complexes are involved in regulation of S, G2 and M phases. Throughout the entire process of mitosis in yeast, nuclear envelope remains stable. This type of division called closed mitosis. During closed mitosis, SPB's are embedded in the nuclear envelope. In budding yeast asymmetric division occur, where the cell initiates the division process by forming a bud that emerges from a mother cell. Bud grows in size as the cell cycle progress (Hartwell et al., 1973).

1.3 The Entry to the Cell Cycle

The entry into the cell cycle is a critical decision point as it determines whether a cell commits to a new round of cell division (Johnston et al., 1977). The decision to enter the cell cycle primarily occurs at a point in the G1 phase known as 'Start' and it is not reversible. At 'Start', cells integrate various internal and external signals to decide whether to proceed with the cell cycle or to exit into a quiescent state known as G0. This decision is tightly linked to cell size in yeast cells (Zetterberg & Larsson, 1985). Yeast cells must reach a critical size before they can pass 'Start', emerge a bud and start DNA synthesis. Since this decision mostly depends on size of the cell, smaller cells need more time to reach start point. For higher eukaryotes, start point is also known as the 'Restriction Point' or 'R'. Unlike in yeast, the transition through the 'R' point in mammalian cells is less influenced by cell size and more dependent on growth factor signals. After passing the R point, cells are committed to DNA synthesis and they no longer depend on external growth factors for the remainder of the cell cycle (Johnson & Skotheim, 2013). Start point decisions are governed by CDK-cyclin complexes in both budding yeast and higher eukaryotes.

In budding yeast, Cln3 is an activator for progression through the 'Start' phase in a manner that is dependent on its dosage (Cross & Tinkelenberg, 1991). Insufficient levels of Cln3 can lead to prolonged G1 phase and delayed initiation of bud formation (Sommer et al., 2021). Cln3 associates with CDK1 to form CDK1-Cln3. Active CDK1-Cln3 phosphorylates the transcriptional inhibitor Whi5 promoting its dissociation from the transcription factor SBF (Swi4/Swi6) and MBF (Baetz & Andrews, 1999). Consequently, this leads to SBF dependent slight transcriptional activation of the two G1 cyclins, namely Cln1 and Cln2 in budding yeast (Quilis & Igual, 2012). Cln1 and Cln2 associates with the CDK and cause further inactivation of Whi5 and activation of more SBF and MBF. This results in accumulation of Cln1 and Cln2 which further activate CDK1. Activated CDK1 phosphorylates Sic1, an inhibitor of DNA replication (Barberis et al., 2005). Phosphorylation of Sic1 leads to its proteasomal degradation. Degradation of Sic1 allows the activation of pre-replication complex (pre-RC) which initiates DNA replication (Ferrell, 2011).

In human, growth factors bind to receptor tyrosine kinases on the cell surface leading to activation of RAS and MAPK pathway. RAS is a small GTPase, initiates cascade signaling to MAPK (mitogen activated protein kinase) that activates ERK (Extracellular signal regulated kinase). Active ERK translocate to nucleus and activate transcription factors such as Elk1, c-Myc which induce to transcribe Cyclin D, Cdk4-6 and DNA replication factors. Cyclin D associate with CDK4-6 and forms a complex during G1. Cyclin D with CDK4-6 phosphorylates pRb and this causes a conformational change in pRb causing it to release of E2F transcription factors. After its release from pRb, E2F becomes active and initiates transcription of S phase required genes such as DNA polymerase, MCM proteins, Cdc6. Initiation of DNA replication marks the transition from G1 to S phase.

1.3.1 DNA Synthesis once and only once

DNA replication occurs only once per cell cycle to ensure accurate transmission of genetic information. Initiation of DNA replication occurs at specific regions of DNA called replication origins. Replication origins are recognized by the origin recognition complex (ORC) which recruits pre-replication complex (Pre-RC) (Tsakraklides & Bell, 2010). Pre-RC contain ORC, Cdc6, Cdt1 which promote DNA replication by phosphorylating the MCM complex. MCM complex is composed of six subunits and functions as the DNA helicase (Riera et al., 2017; Tsakraklides & Bell, 2010). Once the Pre-RC is formed, DNA unwinding is initiated by the MCM helicase complex (Froelich et al., 2014). This creates a replication bubble, with replication forks. Active Cdk1/Clb5-6 phosphorylates Sld2 and Sld3 which recruits DNA polymerases for initiation of replication (Bell & Labib, 2016). DNA polymerases, such as Pol α, Pol δ, and Pol ε, along with other replication factors like pCNA, are recruited to the replication origin. DNA replication occurs bidirectionally. Leading strand is synthesized continually in the same direction while lagging strand is synthesized discontinuously in short fragments named Okazaki fragments. These fragments are ligated by ligase later. Replication continues till converging replication forks meet (Dewar & Walter, 2017). During termination process, DNA synthesis is finished, and replication machinery resolved.

The CDK activity is responsible for controlling the timing of DNA replication and preventing re-replication. During the G1-S transition, replication origins are primed and bound by licensing factors. Upon reaching the G1/S transition, S phase cyclins levels are increased and activates CDK that results in phosphorylation of MCM complexes onto replication origins. (Küntzel et al., 1996). This phosphorylation inhibits reloading MCM onto already replicated origins thereby preventing rereplication. As long as CDKs are active throughout S, G2, and M, the licensing factors remain disabled, thereby preventing prereplication.

1.3.2 Spindle pole bodies and the Centrosome

Spindle pole bodies (SPB) in yeasts and centrosomes in animal cells are specialized organelles that serves as the microtubule organizing center (MTOC) (Barberis et al., 2005).

Centrosomes are found on cytoplasm near the nucleus of animal cells. Centrosomes are composed of a pair of centrioles (mother and daughter centrioles) (Figure 1.1). Centrioles have barrel like shape and consist of nine microtubule triplets. (Nigg & Stearns, 2011). (Fu et al., 2015). They are surrounded by pericentriolar material (PCM) which serves as an anchor for the microtubules. Centrosome duplication begins in the G1 phase (Figure 1.1). At the end of G2 duplicated centrosomes surrounding by PCM are present (Fu et al., 2015) (Figure 1.2).

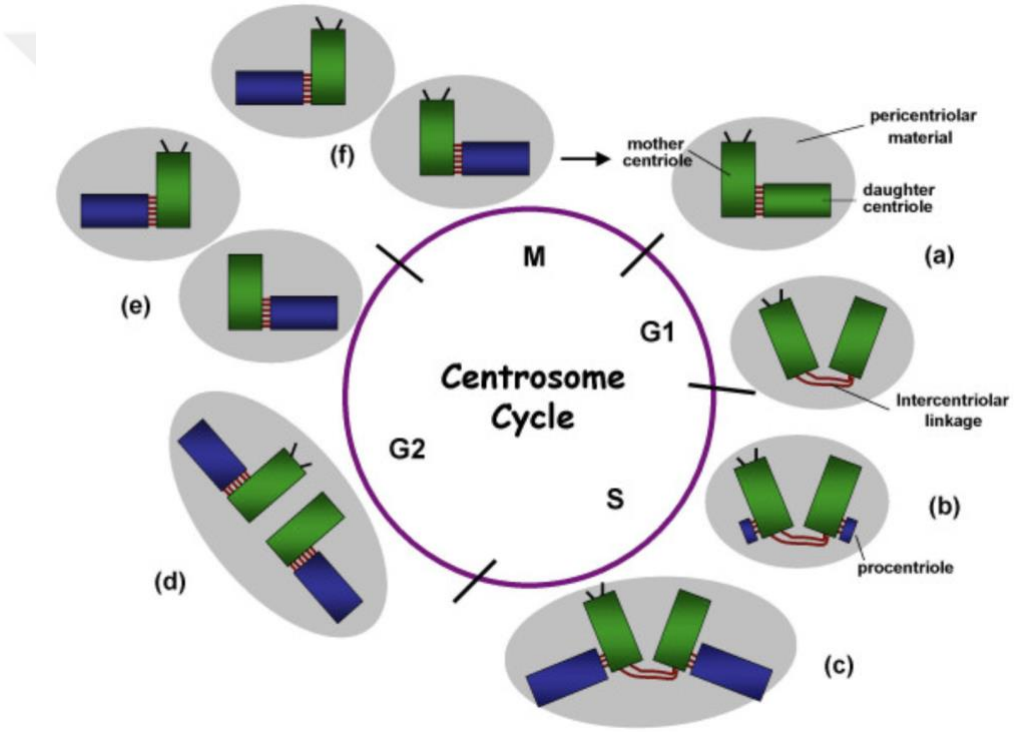

Figure 1.2 The Centrosome Duplication The centrosome is composed of both mother and daughter centrioles (colored green) that are linked together by an intercentriolar linkage (shown in red). They are embedded within the pericentriolar material (PCM) (depicted in grey), which serves as an anchor for the microtubules. The mother centriole can be identified by the presence of appendages (represented by black lines). During the G1 phase, cells undergo a loss of their orthogonal arrangement (a). As they progress from G1 to S phase, a procentriole (shown in blue) forms perpendicularly to each centriole (b). In the S phase, the newly formed centrioles elongate (c). Upon reaching the G2 phase, the two recently formed centriole pairs separate from each other (d). By the G2/M transition, the pericentriolar material is also divided between the centrioles (e). At the end of the cell cycle, the daughter centrioles acquire appendages and behave similarly to mother centrioles during the subsequent cycle (f). This figure is taken from (Crasta & Surana, 2006).

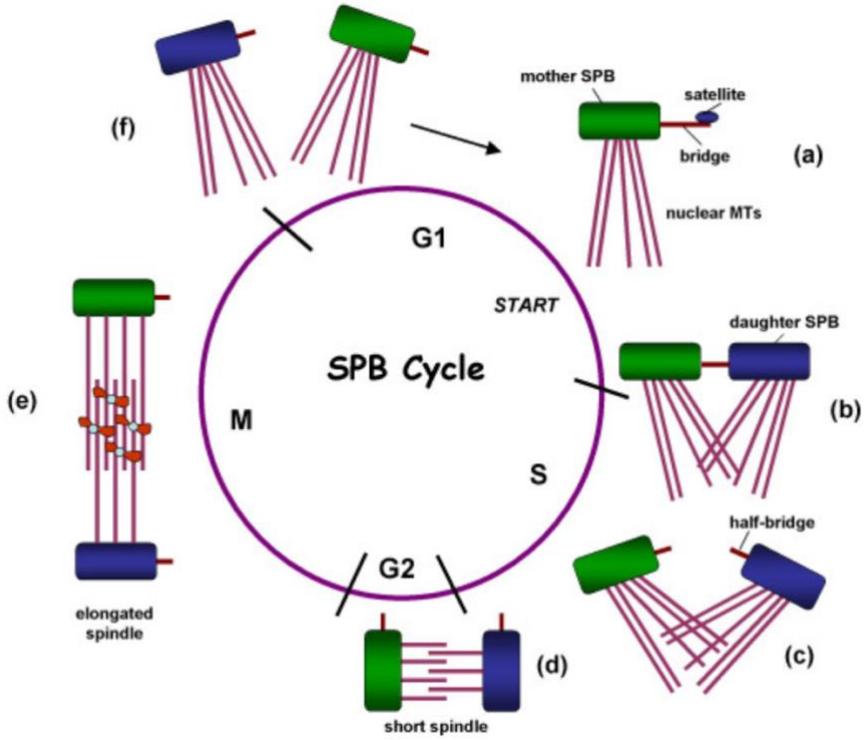

Figure 1.3 The Spindle Pole Body (SPB) Duplication. During the G1 phase, before the START phase, the distal end of the half-bridge (colored red) belonging to the mother SPB (colored green) captures a satellite (depicted as a blue oval) (a). At S phase, the satellite grows in size, eventually become a daughter SPB (blue colored) (b). In the late S phase the bridge that is connecting the SPBs is severed causing the SPBs move away from each other (c) creates a short spindle (d). In mitosis, the spindle poles continue to move apart, elongating the spindle (e). After spindle disassembly at the end of the cycle, each cell obtains a SPB (f). This figure taken from (Crasta & Surana, 2006).

The SPB is structurally distant from the centrosome. The SPB consists of a central plaque, embedded in the nuclear envelope. SPBs nucleate nuclear and cytoplasmic microtubules. Nuclear microtubules nucleate from the inner plaque of the SPB and radiate into the nucleus to perform spindle assembly. Cytoplasmic microtubules nucleate from the outer plaque of the SPB and extend towards the cytoplasm to function in cell polarity, cytoskeletal organizations, cellular transportation (Fraschini, 2018). Other than these roles, SPB functions in mitotic exit as a scaffold protein.

Duplication of SPBs is also tightly regulated for ensuring the formation of two functional SPBs one for each daughter cell. A new SPB duplicate from the old one. This process involves the recruitment of specific proteins like Spc42, Spc29 and form a scaffold for assembly to the site of SPB (Geymonat et al., 2020). Then a duplication plaque, a structure that functions as a precursor to mature SPB is formed. Duplication plaque then undergoes several structural changes finally become the fully matured SPB apparatus at late S phase (Jaspersen & Winey, 2004). CDK1 control the timing and progression of SPB duplication in coordination with other events.

1.4 M-phase

After completion of DNA replication cells enter G2 phase to prepare for M phase by synthesizing proteins required for spindle assembly and chromosome segregation. Mitotic phase aims to proper segregation of sister chromatids (Maiato et al., 2017). M-phase requires activation of the mitotic cyclin-dependent kinase (CDK) complex. The M-CDK complex, composed of cyclin B and Cdk1, drives the transition from the G2 phase to the M phase of the cell cycle. Cyclin B is synthesized during G2 phase. Initially M-CDK complex is inactived by Wee1 inhibitory kinase at Cdk1 at a T14 and Y15 residues. Cdc25 removes the inhibitory phosphate groups from Cdk1 to enable activation of Cdk1 (Alberts B, 2002).

1.4.1 Metaphase to Anaphase Transition

In order for sister chromatids to separate cohesin needs to be cleaved. Cohesin is a protein complex that holds sister chromatids together. Cohesin ring consists of four subunits (Smc1, Smc3, Scc1, Scc3) that form the cohesin ring.

A protease called Separase (Esp1 in yeast) cleaves cohesin ring at the metaphase to anaphase transition to allow sister chromatid segregation (Nasmyth & Haering, 2009). Securin (Pds1) binds to Separase to inhibit catalytic activity of Separase. At the metaphase to anaphase transition, Anaphase Promoting Complex (APC/C) with the Cdc20 subunit ubiquitinate the Securin causing its proteasomal degradation. This happens only after all chromatids are aligned at metaphase plane properly. Proteasomal degradation of Securin by APC/C activates the Separase (Agarwal & Cohen-Fix, 2002). Separase cleaves the Scc1 subunit of Cohesin ring that results in separation of sister chromatids (Uhlmann et al., 2000). In budding yeast, Separase also promotes initial activation of Cdc14 (termed the Cdc14 Early Anaphase release or FEAR) other than its catalytic function (Queralt et al., 2006) which will be discussed in details later.

All chromosomes must be bipolarly attached to the mitotic spindle to allow equal segregation of chromosomes and thus to avoid aneuploidy. Spindle assembly checkpoint (SAC) prevents improper chromosome segregation by inactivating the APC/C-Cdc20 until correct attachment happen (Musacchio & Salmon, 2007). SAC is composed of network of proteins including Mad1, Mad2, Mad3, Bub1, Bub3, BubR1 (yeast homolog of Mad3), and Mps1 (De Antoni et al., 2005). Mad1 is recruited to unattached kinetochores and forms a complex with Mad2. Mad2 has two conformations one is the open and the other is close (Lénárt & Peters, 2006). When Mad1 bind the Mad2 it induces to conversion from O-Mad2 to C-Mad2 which indudes formation of the mitotic checkpoint complex (MCC) together with BubR1, Bub3 and Cdc20. Cdc20 is inhibited by MCC therefore Securin is not degraded, Separase stays inactive and Cohesin cannot be cleaved. Once all chromosomes are attached correctly, SAC is silenced by dissociation of MCC from kinetochores to allow the Cdc20 to activate APC/C and initiate anaphase. Under low tension, anaphase onset is delayed by Bub1 and Bub3. Interestingly, this delay persists in the absence of other SAC proteins (Mad1, Mad2, Mad3) (Proudfoot et al., 2019).

1.4.2. Mitotic Spindle formation and Chromosome segregation

Mitotic spindles are responsible for segregation of chromosomes to the daughter cells. It is composed of microtubules as well as microtubule associated proteins. Microtubules are fibers that are made up α-tubulin and β-tubulin proteins that form α/β-tubulin dimers. α/β-tubulin dimers oligomerize coming head to toe forming linear protofilaments and protofilaments interact laterally make a hollow cylinder of 2.5 nm diameter. Microtubules have a polar structure where all α/β-tubulin dimers have the same orientation. Both α- and β-tubulin can bind GTP, whereas only β-tubulin can hydrolyze the GTP to GDP. β-tubulin designates the plus end of the microtubules. The other end marked with α-tubulin is the minus end. Elongation occurs with the addition of tubulin subunits at the plus end, allowing its growth.

α/β-tubulin can self-assemble in vitro into microtubules when a critical concentration is reached, whereas microtubule organizing centers (MTOCs) provide sites for microtubule nucleate even below this critical concentration (Mitchison & Kirschner, 1984). Nucleation sites of microtubules consist of gamma tubulin ring complex. Gamma tubulin ring complex provides a template for nucleation of microtubules where gamma tubulin recruits α/β-tubulin dimers. Gamma tubulin anchors the minus end of the microtubules.

Microtubules organize into the mitotic spindle in the M-phase. Mitotic spindle is composed of a bi-polar array microtubules that emanate from the MTOC. The plus end of microtubules may interact with kinetochores forming kinetochore microtubules. They may as well interact with the plus end of the microtubules originated from opposing MTOC to form interpolar microtubules. This interaction results in lateral antiparallel array in midzone. Kinetochore microtubules and interpolar microtubules are critical for chromosome segregation to the opposing poles of the cells. In addition to these two classes of microtubules that originate from MTOC, there is also a third class: the astral microtubules. Astral microtubules emerge from the MTOCs and elongate towards the poles to cell cortex, to provide positioning of the spindles in the cell.

During mitosis the stability of microtubules change. Microtubules, show dynamic instability as they alternate between stages of expansion and shrinking (Lénárt & Peters, 2006). The loss of the GTP cap at the plus end can result in catastrophe, which causes shrinkage and is followed by rescue, which causes growth to restart. Microtubule-associated proteins (MAPs) and motor proteins control the dynamics and organization of microtubules. Some MAPs like Tau and MAP2 promote microtubule stability by binding the surface of microtubule and prevent depolymerization (Akhmanova & Steinmetz, 2015). Conversely stathmin destabilize the microtubules and promote their disassembly. Nocodazole, an agent that disrupt assembly of new microtubules by binding and inhibiting beta tubulin. It is widely used in cell cycle studies as well as clinical research. During mitosis, the stability of the microtubules change in a controlled manner to allow for spindle formation and chromosome segregation.

Chromosomes are attached to the spindle microtubules at their kinetochores, a centromeric heterochromatin region. The stabilization of kinetochore microtubule

attachment is provided by Ndc80 complex composed of Ndc80, Nuf2, Spc24, Spc25 (Janke et al., 2001). They mediate the link between kinetochore and microtubules. Ndc80 directly interact with microtubules and Nuf2 stabilize the attachment.

For chromosome alignment along the metaphase plate and for chromosome segregation, mitotic spindle applies three main forces on chromosomes. First, microtubules at plus end near kinetochores are depolymerize after anaphase onset, while the plus tip is hold by the Ndc80 complex (Tooley & Stukenberg, 2011). This generates a force to pull chromosomes to the poles. This is not ATP driven rather the energy required for the poleward force is come from the hyrolyzes of GTP (Zhu et al., 2009). Secondly, microtubule flux generates a force. Microtubule flux stem from continous polymerization and depolymerization of microtubules at different rates to end of the microtubule. Until anaphase onset, dimers are added to the plus tip of the kinetochore microtubules whereas dimers are dissociated at the minus tip. This generates a flux of dimer towards to poles which creates a pulling force and generates tension at the kinetchores (Gardner et al., 2011). Thirdly, a polar ejection forces act on chromosome arms and help their alignment. Motor proteins on microtubules push the chromosome arms away from the spindle poles (Khodjakov & Rieder, 1996). The polar ejection forces contribute to the alignment of chromosomes at the metaphase plate and their subsequent separation during anaphase. By exerting outward forces on the chromosome arms, the polar ejection forces help maintain tension and ensure proper alignment and segregation of the chromosomes. Polar ejection forces work in conjunction with other mechanisms, such as kinetochore-microtubule attachments and spindle assembly checkpoint signaling, to ensure accurate chromosome movements during mitosis.

1.4.3 Spindle Positioning

The development of cell polarity mediated by the small GTPase Cdc42, is the first step in the spindle positioning process. At the cell cortex, Cdc42 is crucial in determining where the daughter cell will form.

Correct spindle positioning is essential in asymmetric cell division in yeast. The division site is determined in a way that spindle oriented mother to bud axis (Palmer et al., 1992). This achieved by two pathways in budding yeast. One requires Kar9, a microtubule binding protein and another requires the minus end directed motor dynein. Kar9 pathway facilitating the sliding of astral microtubule ends and active during metaphase. Bim1, plus end directed motor protein acts as an adaptor protein and binds to Kar9 facilitates Kar9 to bind Myo2. Myo2 moving along the actin cables, moves microtubules' plus ends in the direction of the bud (Hwang et al., 2003).

On the other hand, dynein dependent pathway is more active at anaphase and compensates the absence of Kar9. Dyn1 is a minus end directed protein found growing end of microtubules. The transportation of Dyn1 to the daughter cortex is performed by Kip2/Bik1 complex (Carvalho et al., 2004). Kip2 is a plus end directed kinesin while Bik1 is a plus end targeted protein. Dynein tail is stabilized by Num1 to the daughter cortex while free motor domains of Dyn1 responsible for pulling microtubules toward bud (Adames & Cooper, 2000).

Simultaneous deletion of *KAR9* and *DYN1* results in lethality while their single deletion is not lethal, indicating that the two pathways are redundant.

In mammals cellular shape and contact with neighboring cells influence spindle orientation. Cortical proteins are involved and operates spindle orientation at metaphase. The myristoylated G-protein subunit, Gαi, binds to the plasma membrane, and its membrane association may be contingent upon the participation of the guanine exchange factor Ric-8. Gαi-GDP, in its nucleotide-bound form, functions as a cortical anchor for the protein known as Pins, wherein it engages with the C-terminal GoLoco motifs of Pins. Pins serves as a docking platform for Mud through its N-terminal tetratricopeptide repeats. Notably, Mud establishes an interaction with the dynein/dynactin complex, thereby facilitating the minus-end directed motor activity that underpins the generation of the pulling force within this intricate cellular process (Bergstralh & St Johnston, 2014).

1.4.4 Mitotic Exit and Cytokinesis

The mitotic cyclin-dependent kinase (CDK) complex has to be inactivated and CDK dependent phosphorylation has to be reversed for the transition from M to G1 phase. (Visintin & Amon, 2001).

Anaphase promoting complex (APC) is a large subunit E3 ubiquitin ligase, activated at the onset of the anaphase. APC is found as a complex with its regulatory subunits called Cdh1 and Cdc20 (Pfleger & Kirschner, 2000) After chromosomes are properly aligned, APC/C is activated through its subunit Cdc20 (Jaspersen et al., 1998). APC/C-Cdc20 ubiquitinylates cyclin A and cyclin B, as well as the Securin, and target them for degradation at the proteosome. For full degradation of B-type cyclins in yeast APC/C-Cdh1 is required. APC/C-Cdh1 facilitates the degradation of Clb2 in budding yeast. Degradation of the cyclins causes of the mitotic CDK inactivation which is how cells exit mitosis biochemically (Pfleger & Kirschner, 2000). In addition to M-CDK inactivation, M-CDK phosphorylation's must be reversed by phosphatases. This is driven by Cdc14 in yeast (Li et al., 1997). Mitotic exit in yeast, which is the main focus of this thesis will be explained in the next section in detail.

Mitotic exit is followed by cytokinesis during which the cytoplasm of the dividing cell is divided into two daughter cells. This stage include two important events, actomyosin ring construction and formation of septum (equivalate of localized ECM in human) (Moyano-Rodríguez et al., 2022). The contractile ring made up of actin filaments and the myosin motor protein. Sliding of myosin motor protein on actin filaments results in constriction of the contractile ring. Septin ring is formed at adjacent of the actomyosin ring to support and help to guide the cleavage furrow. Cleavage furrow forms by invagination of plasma membrane at the division site while actomyosin ring constricts (Burgess & Chang, 2005). The plasma membrane components are transported to the cleavage furrow that results in ingrowth of the membrane. Finally cleavage furrow is completely gone and a new cell is separated (Burgess & Chang, 2005).

1.5 Mitotic Exit in Budding Yeast

Mitotic exit in budding yeast is achieved by inactivation of cyclin-CDK complexes and dephosphorylation of CDK substrates. APC/Cdc20 and APC/Cdh1 targets cyclin B for degradation that leads to inactivation of CDK1. Sic1, CDK inhibitor protein provides a direct inhibition of CDK. Likewise a prereplication complex Cdc6 also inhibits M-Cdk (Calzada et al., 2001). Transcription of Sic1 and Cdc6 is governed by Swi5 at late mitosis.

In budding yeast mitotic exit is achieved by the activity of the phosphatase Cdc14. Cdc14 dephosphorylates Sic1, and its transcription factor Swi5. This dephosphorylation event leads to the stabilization of Sic1 and enables the activation of *SIC1* transcription, which is dependent on Swi5 (Aerne et al., 1998). Cdc14 also dephosphorylates Cdh1, which results in activation of APC that causes a ubiquitination of mitotic cyclins.

Activation of Cdc14 is tightly controlled by the FEAR (Cdc Fourteen Early Anaphase Release) and MEN (Mitotic Exit Network) pathways in budding yeast. These pathways promote the release of Cdc14 from its inactive state and facilitate its function in regulating mitotic exit.

1.5.1 Cdc Fourteen Early Anaphase Release (FEAR)

Cdc14 is bounded by a nucleolar inhibitory protein called Net1 (also known as Cfi1) until metaphase to anaphase transition. By the help of FEAR pathway Cdc14 releases partially from nucleus to nucleolus. The FEAR pathway includes several proteins and protein complexes, notably the Esp1 (Separase), Slk19 and Spo12. Before anaphase, Spo12 and interactor protein of Spo12; Fob1 stabilizes the Cdc14 and Cfi1/Net1 interaction (Stegmeier et al., 2004). By the activation of APC/C at anaphase onset, Esp1 is released from Pds1 (Securin) and form a complex with Slk19 (Figure 1.3). This complex results in downregulation of $PP2A^{Cdc55}$ that further allows Clb1/2-CDK phosphorylate Cfi1/Net1. Cdc5, polo like kinase, becomes active at early anaphase, after sister chromatid separation. Cdc5 phosphorylates Cfi/Net1, that prevents Net1 binding to Cdc14 (Botchkarev et al., 2017). The process of phosphorylating Cfi1/Net1 reduces its binding affinity for Cdc14. Similarly, the phosphorylation of Spo12 is thought to contribute to the dissociation of Fob1 from the complex formed by Cdc14 and Cfi1/Net1.

Activation of Cdc14 through the FEAR (Cdc fourteen early anaphase release) network is not crucial and not sufficient for exit from mitosis (Stegmeier et al., 2004). This state of Cdc14 is responsible for dephosphorylation of Cdk targets like Ask1, Sli5, Fin1, Ase1 that facilitate rDNA segregation, stabilizing anaphase spindle, promoting formation of spindle midzone.

1.5.2 Mitotic Exit Network (MEN)

In budding yeast, the Mitotic Exit Network (MEN) is a signaling pathway that is essential for full release of Cdc14 in late anaphase and thus for mitotic exit. MEN is

closely related to Hippo pathway in mammals (Baro et al., 2017). The MEN pathway components become active during late anaphase. It consists of proteins named Tem1, Cdc15 and Dbf2/Mob1 that are activated sequentially, to finally promote fully release of the phosphatase Cdc14 from the nucleolus into the cytoplasm (Figure1.3).

MEN components are localized at the outer plague of the SPBs. SPB localization of the MEN proteins is crucial for MEN function. Accordingly, impairment of SPB localization of the MEN components results in inhibition of the MEN (Gruneberg et al., 2000), and thus inhibition of the mitotic exit.

Tem1 is a small GTPase, a central regulator of the MEN pathway. It predominantly localizes to spindle pole bodies. Cdc15 is a protein kinase homolog of mammalian sterile 20 related kinase. Cdc15 phosphorylates C terminus site of Dbf2 which activates its catalytic activity. Mob1 is a regulatory protein of Dbf2.

Dbf2 is a kinase that is homolog of mammalian Dbf2 related kinase. Dbf2 forms a complex with Mob1, a regulatory subunit of Dbf2 and phosphorylates Cfi1/Net1 and Cdc14 thereby hindering its nuclear localizing signal. MEN proteins predominantly localize to daughter SPB through the scaffold protein Nud1.

Cdc14's release during early anaphase is orchestrated by FEAR which results partial release of Cdc14. At the very downstream of MEN pathway Cdc14 fully releases from nucleolus to cytosol. Cdc14 full release leads to dephosphorylation of its targets Cdh1, Sic1 and Swi5.

MEN activity is promoted by the FEAR network. During cell cycle stages prior to anaphase Cdc15 is inhibitory phosphorylated. This inhibits the mitotic exit role of Cdc15 until FEAR released Cdc14 dephosphorylates Cdc15.

MEN is inhibited in the mother cell compartment by the Spindle position checkpoint (SPOC) which will be discussed below. MEN is activated in the bud by MEN activating proteins Lte1, Ste20. Lte1 is a putative guanine nucleotide exchange factor (GEF) for Tem1. Ste20 is a p21-activate protein kinase (PAK). When FEAR is not active, mitotic exit requires Lte1 and Ste20 for proper exit from mitosis (Caydasi et al., 2017).

1.5.3. Spindle Position Checkpoint (SPOC)

The spindle position checkpoint (SPOC) is a crucial mechanism in budding yeast that makes sure the mitotic spindle is elongated along the mother-to-daughter axis before cells exit from mitosis (Caydasi & Pereira, 2012). This procedure is essential for preserving genomic stability by preventing unequal chromosome partitioning, which can result in multiploidy, euploidy and aneuploidy.

When the anaphase spindle is misaligned, SPOC prevents cell cycle progression by inhibiting the MEN at the level of Tem1. The most downstream SPOC components are Bfa1 and Bub2 which together form the Bfa1-Bub2 GAP (GTPase activating protein). Bfa1-Bub2 GAP complex promotes GTP hydrolysis of Tem1, thus Tem1 is inhibited by the active Bfa1-Bub2 GAP (Pereira & Schiebel, 2005). As Tem1 activity is crucial for mitotic exit, cells cannot get out of mitosis when Bfa1-Bub2 is activated.

Bfa1-Bub2 GAP complex is regulated by two kinases: Cdc5 and Kin4. Cdc5 is a polo like kinase which phosphorylates Bfa1. Phosphorylation of Bfa1 by Cdc5 disrupts Bfa1-Bub2 GAP activity, leading to mitotic exit. Kin4 phosphorylates Bfa1 which in turn enhances ability of Bfa1-Bub2 to inhibit Tem1 (Caydasi et al., 2010).

SPOC components Kin4, Bfa1-Bub2, Cdc5 localizes to the SPBs. Kin4 is a serine/threonine kinase, undergoes specific changes in its localization (Caydasi & Pereira, 2012). Kin4 localizes to the mother cortex most of the time during the cell cycle (Jill E. Falk et al., 2011). Along with this mother cortex localization, Kin4 also localizes to following structures in a cell cycle dependent manner: in G1/S, Kin4 transiently localizes at the new bud site (J. E. Falk et al., 2011). During anaphase in cells with a correctly position spindle, Kin4 transiently localizes to mother SPB whereas, when anaphase spindle is misaligned, Kin4 localizes to both SPBs (Pereira & Schiebel, 2005). At late anaphase/telophase Kin4 localizes to the bud neck. The proper localization of Kin4 is crucial for the activity of the SPOC as symmetrically localized Kin4 mutants inhibit MEN even if there is no spindle misalignment in the absence of Lte1 (Chan & Amon, 2010).

When the spindle is correctly aligned, the SPB localization of Tem1 and Bfa1-Bub2 is preferentially at the dSPB (daughter SPB). When there is spindle misalignment, Kin4 phosphorylation of Bfa1 at S150 and S180 residues causes a decrease in the level of SPB localization of Bfa1 and Bub2 (Caydasi & Pereira, 2009). Phosphorylation of Bfa1 by Kin4 forms a binding site on Bfa1 for Bmh1. Bmh1 binding to Bfa1 removes most of Bfa1 from the dSPB which leads symmetric localization of Bfa1 when the spindle is mispositioned (Caydasi et al., 2014). This localization change prevents Bfa1 from its inhibitory phosphorylation of Cdc5 likely through the protein phosphatase 1 (PP1) Glc7. Glc7 in complex with its regulatory subunit Bud14 dephosphorylates Cdc5 phosphorylated Bfa1 (Kocakaplan et al., 2021). Finally, active Bfa1-Bub2 GAP complex inhibits Tem1 GTPase, therefore inhibits mitotic exit.

Kin4 catalytic activity requires Elm1 which is a kinase that phosphorylates Kin4 from its threonine residue. This phosphorylation found on T loop of Kin4, results in activation of its catalytic function (Caydasi et al., 2010) (Moore et al., 2010). In contrast, the proper localization of Kin4 requires the protein phosphatase PP2A with its regulatory subunit Rts1. The PP2A-Rts1 complex facilitates the localization of Kin4 to the mother spindle pole body (mSPB) and the cortex of the mother cell by dephosphorylating Kin4 (Chan & Amon, 2009).

Kin4 localization to the daughter cell bound SPB in an anaphase is prevented by Lte1. Lte1 localizes to the bud cortex, which is controlled by Rho GTPase Cdc42 and its effector proteins Cla4, a protein kinase (Seshan & Amon, 2005). Phosphorylation of Lte1 by Cla4 results in interaction with Cdc42 which stabilizes the Lte1 at the bud cortex (Geymonat et al., 2010). The asymmetric distribution of Kin4 in the mother cell and Lte1 in the daughter cell eventually ensures spatial regulation of Tem1 activity by modulating the function of Bfa1-Bub2.

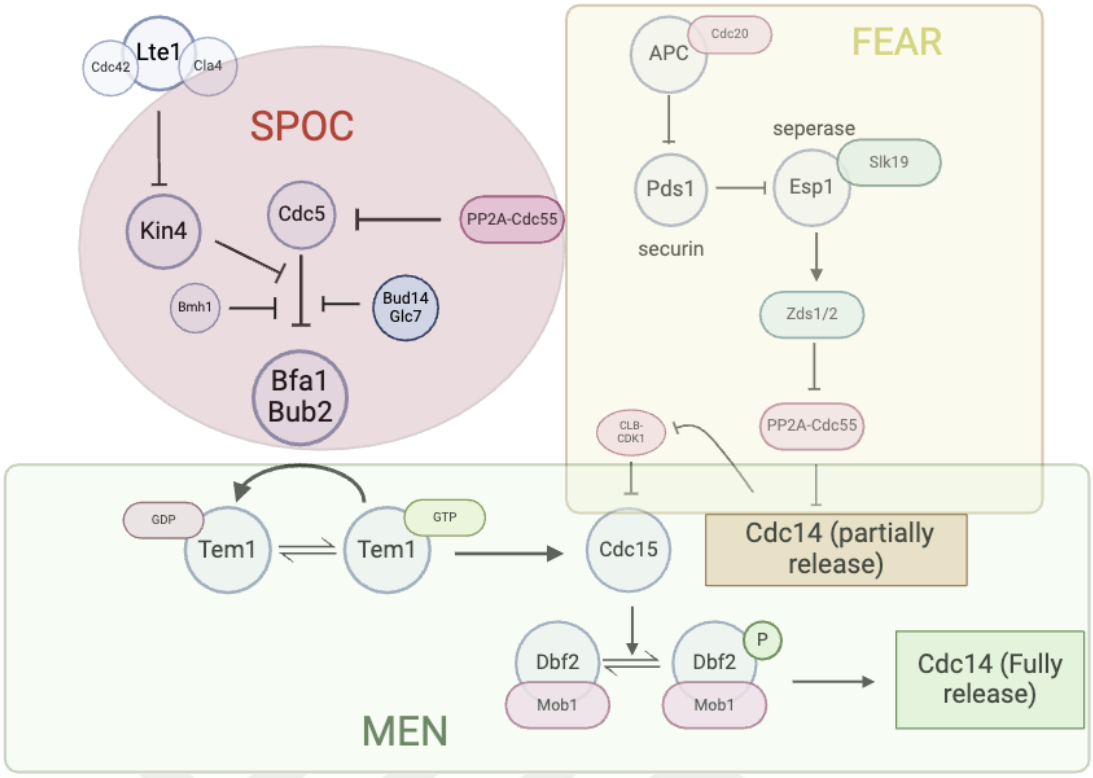

Figure 1.4: Pathways controlling the exit from mitosis in budding yeast. Fear provides partial release of Cdc14 while MEN triggers the fully release. SPOC inhibits the mitotic exit when there is a misalignment. See text for details.

1.6 Phosphatidylinositol 3,5-bisphosphate

A family of acidic phospholipids found in membranes are made up of phosphorylated phosphatidylinositol derivatives known as phosphoinositide. Phosphatidylinositol (PI) is a relatively uncommon phospholipid compared to phosphatidylcholine and phosphatidylethanolamine, but it plays a crucial role in cellular processes. Phosphatidylinositol accounts for 10–20% of all cellular phospholipids (J. Hasegawa et al., 2017).

The intracellular localization and activity of the PIs are governed by the differential phosphorylation. The fundamental building block of the PIs is, non-phosphorylated phosphatidylinositol, which is present in all eukaryotic cells at the cytoplasmic face of the ER, the Golgi, mitochondria, and microsomes (De Craene et al., 2017). They have crucial roles in controlling almost every cellular process as important second messengers' precursors. They also regulate ion channels, vesicular transporting by roles in membrane fusion/fission secretion events (Balla et al., 2009). It is still unclear what role the PIs in the nucleus play, and new researches have focused on the highly phosphorylated inositols that also seem to regulate a number of nuclear processes (Balla et al., 2009). Controlling the subcellular distribution, regulation, and activation states of the enzymes involved in their synthesis and conversion (kinases and phosphatases) is

essential for the PIs' metabolism to be finely regulated timely and locally, which is necessary for them to perform these functions (De Matteis et al., 2005).

Cells have been found to contain seven PIs that are phosphorylated differently at the 3-, 4-, and 5-hydroxyls of the inositol head group (Kim et al., 2011). They are named according to their phosphorylation sites. PI is phosphorylated at position 3 to produce PI3P, which is necessary for endosomal transport as well as the formation and sorting of multivesicular bodies (MVBs). To synthesize bisphophorylated PI, additional phosphorylation can be applied to these monophosphorylated PIs. As a result, Phosphatidylinositol 3,5-bisphosphate (PI(3,5)P2) or, Phosphatidylinositol 4,5-bisphosphate (PI(4,5)P2) can be formed. PI(4,5)P2, mostly studied, primarily produced by PI4P phosphorylation and is function in the control of the actin cytoskeleton and endocytosis. Compared to other derivatives PI(3,5)P2 is the least abundant and less is known.

1.6.1 Synthesis of PI(3,5)P2

PI(3,5)P2 is one of the least understood PI. Low cellular levels of PI(3,5)P2 and lack of specific dyes and/or sensor for detection of PI(3,5)P2 constitutes challenges for studying PI(3,5)P2. Despite their low levels under basal conditions, upon hyperosmotic shock $PI(3,5)P_2$ levels up to 20 fold and after 30 min it returns to normal levels (Jin et al., 2016). This indicates that $PI(3,5)P_2$ levels are tightly controlled.

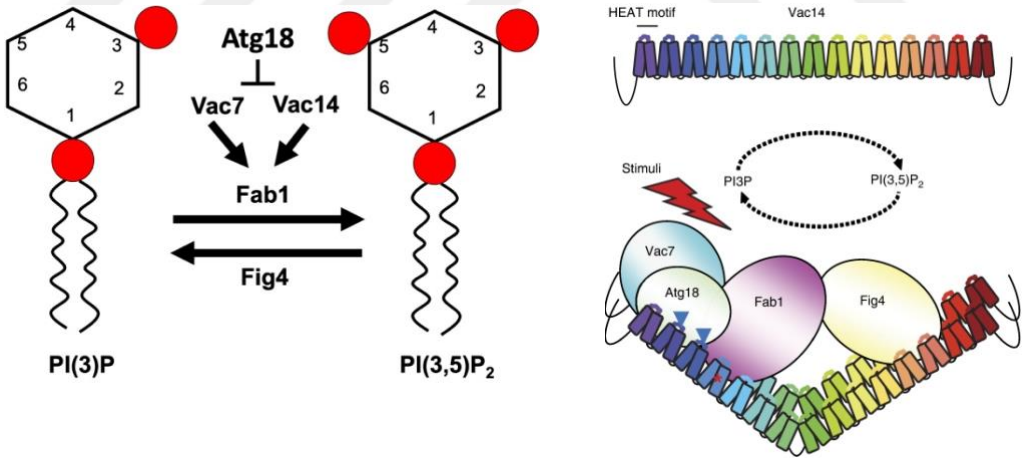

Figure 1.5: Schematic representation of synthesis of PI(3,5)P2 from PI(3)P. Regulatory proteins of the synthesis of PI(3,5)P2: Atg18, Vac7, Vac14, Fab1, Fig4. (See details in the text) (Jin et al., 2008).

PI(3,5)P2 is produced via a conserved mechanism from yeast to human. PI(3,5)P2 is synthesized through the conversion of PI3P to PI(3,5)P2 by the 1-phosphatidylinositol-3-phosphate 5-kinase (PIKfyve in human Fab1 in yeast). PIKfyve/Fab1 phosphorylates the fifth hydroxyl group of the inositol ring on PI3P, resulting in the formation of PI(3,5)P2. Phosphatase Fig4/Sac3 (human/yeast) hydrolyzes this phosphate group converting PI(3,5)P2 back to PI3P (Balla, 2013) (J. D. Gary et al., 1998). The Vac14 protein, conserved in both yeast and human, acts as a scaffold protein. Vac7 is a yeast specific component of the Fab1 regulatory complex. Deletion of Vac7, Vac14 or Fab1 results defective vacuole morphology and decreased amount of PI(3,5)P2. Hence, Vac7 and Vac14 are positive regulators that increase the synthesis of PI(3,5)P2 by activate lipid kinase Fab1 (Jin et al., 2016).

Fab1, Vac14, Fig4/Sac3, and Vac7 all in all called PAS complex. PAS complex components are localized to vacuole membrane in yeast, endosomes and lysosome in human (Bonangelino et al., 2002). Each component of the PAS complex of yeast is discussed in detail below:

Fab1

Fab1 is the conserved lipid kinase found on vacuole/lysosome membranes. It catalyzes the transfer of a phosphate group from ATP to PI3P resulting PI(3,5)P2 (McCartney et al., 2014). Regulatory proteins of Fab1 are Vac14 and Fig4. Fab1's association with PI3P-enriched membranes is critical for its kinase activity. Membrane targeting is facilitated by the FYVE domain and is regulated by Vac14. Mutations in Fab1 lead to a decrease in PI(3,5)P2 levels and defects in vacuole acidification, endocytosis, and autophagy.

Vac7

Vac7 is a transmembrane protein that is specific to yeast. It has a critical role in the organization and maintenance of the vacuolar membrane. It is responsible for the regulation of vacuolar shape, size, and inheritance. The segregation of vacuole is impaired in cells that has defects in Vac7 (Bonangelino et al., 1997). Loss of function mutants of Vac7 leads to abnormal vacuole morphology. It is the part of PAS complex, studies shows the levels of PI(3,5)P2 diminished in the absence of Vac7 similar to Fab1 (J. Hasegawa et al., 2017).

Vac14

Vac14 is a conserved regulatory protein that involved in synthesis and regulation of PI(3,5)P2. It serves as a scaffold protein that brings Fab1, Vac7, Fig4 and Atg18 together (Jin et al., 2017). Vac14 is composed of HEAT repeats, which are protein-protein interaction domains. Vac14 binds to PIKfyve and Fig4 and it is required for the binding PIKfyve to PI3P. Mutations in Vac14 causes a decrease in PI(3,5)P2 (Simon A. Rudge et al., 2004).

Fig4

Fig4 localizes to vacuolar/lysosomal membrane and interacts with Fab1 and Vac14. These interactions ensure the localization and activation of Fig4. Vac14-Fig4 directly interact each other and this interaction is essential for its activity since Vac14 stabilizes Fig4 and promotes its association with endosomal membranes, allowing it to access PI(3,5)P2. Fig4 has dual function: (1) through phosphatase activity it dephosphorylates PI(3,5)P2 and increase the level of PI3P. (2) through its interaction with Vac14 and Fab1/PIKfyve, it positively affect the Fab1 activity (Botelho et al., 2008).

The synthesis of PI(3,5)P2 by Fab1 kinase is regulated through phosphorylation of Fab1. PIKfyve (Fab1) is phosphorylated by mTORC1 in mammalian cells (Rivero-Ríos & Weisman, 2022) and in yeast (Chen et al., 2021). It has been suggested that PIKfyve activated through phosphorylation by AKT and promotes vesicle trafficking to lysosomes (Er et al., 2013). In yeast Pho85/CDK5 phosphorylates directly and activates Fab1, protects against stress induced elevated levels of PI(3,5)P2 (Jin et al., 2017). It is also shown that, Ivy1, the inverted BAR protein, inhibit Fab1 through binding Ypt7. Suggest Ivy1 controls the synthesis of PI(3,5)P2 via Fab1 inhibition (Malia et al., 2018).

The known diseases associated with mutations in proteins involved in the synthesis of PI(3,5)P2 are shown in the table below. For instance, SAC3 (also known as Fig4) is associated with Charcot-Marie-Tooth disease, type 4J, indicating a potential role of this gene in the development or progression of this neurological disorder. Similarly, ARPIKFYVE (also known as Vac14) is linked to Striatonigral degeneration, childhood-onset, suggesting a connection between this gene and the manifestation of this specific neurodegenerative condition. Additionally, PIKFYVE (also known as Fab1) is associated with Corneal fleck dystrophy, indicating its potential involvement in the pathogenesis of this ocular disorder.

Table 1.2 Diseases associated with mutations in proteins involved in the synthesis of PI(3,5)P2

GENE	Description	Disease
SAC3 (Fig4)	**PHOSPHOINOSITIDE 5-PHOSPHATASE**	**Charcot-Marie-Tooth disease, type 4J Amyotrophic lateral sclerosis**
ARPIKFYVE (Vac14)	**ASSOCIATED REGULATOR OF PIKFYVE**	**Striatonigral degeneration, childhood-onset**
PIKFYVE (Fab1)	**PHOSPHATIDYLINOSITOL 3-PHOSPHATE 5-KINASE, TYPE III**	**Corneal fleck dystrophy**

1.6.2 Cellular Functions of PI(3,5)P2

$PI(3,5)P_2$ is involved in various functions, including membrane trafficking, stress response, regulation of ion homeostasis by Ca+2 signalling, selective autophagy (Jin et al., 2016) and cell cycle.

1.6.2.1 Vacuolar Membrane Dynamics

PI(3,5)P2 involved in membrane dynamics by regulating vacuolar morphogenesis and fusion. In particular, it promotes the fusion of vacuolar compartments by facilitating the assembly of the soluble N-ethylmaleimide-sensitive factor attachment protein receptor (SNARE) complex, which is essential for membrane fusion events (Duex et al., 2006).
PI(3,5)P2 plays a role in regulating vacuolar size, function, and fusion/fission events. When Fab1 is defective in kinase function, vacuoles become abnormally large (S. A. Rudge et al., 2004). Likewise, the loss of Fab1/PyKfive activity leads to significantly enlarged endo-lysosomal compartments in mammalian cells and mouse tissues. In terms of vacuolar homeostasis, PI3P is known to inhibit vacuolar fusion, while PI(3,5)P2 promotes vacuolar fission (J. D. Gary et al., 1998). As a result, the deletion or loss of function of Fab1 kinase leads to a deficiency in PI(3,5)P2, causing abnormally large vacuoles due to the inhibition of the fission pathway. Additionally, *atg18Δ* yeast cells fail to fragment their vacuoles under salt stress, indicating that both Atg18 and PI(3,5)P2 are involved in membrane fission.

1.6.2.2 Vacuolar Acidity

Vph1 is a vacuolar H(+)-ATPase (V-ATPase) that plays a key role in regulating vacuolar pH V-ATPases are large multi-subunit complexes that use ATP hydrolysis to pump protons across biological membranes, generating an electrochemical gradient that is used to drive a range of cellular processes. Yeast mutants *fab1Δ* and *vac14Δ* exhibit a notable decrease in V-ATPase assembly and function, both under iso-osmotic conditions and during hyper osmotic stress (Cooke et al., 1998). The cytosolic N-terminal domain of Vph1 is also drawn to membranes in a PI(3,5)P2-dependent way. PI(3,5)P2 has been found to directly interact with and activate the V-ATPase, promoting the transport of protons into the vacuole (Banerjee et al., 2019). These findings indicate that PI(3,5)P2 is required for assembly and function of Vph1. Regulating Vph1 activation is essential for vacuolar acidification which is crucial for selective degradation of cargo ensuring the correct luminal environment for cargo processing. Dysfunction of acidity cause lysosomal diseases leading thrombosis in mice (Junya Hasegawa et al., 2017).

1.6.2.3 Endosome Maturation

Endosomal maturation involves the dynamic transformation of early endosomes into late endosomes, which subsequently fuse with lysosomes to degrade their content. This process is essential for maintaining cellular homeostasis, recycling membrane components, and regulating the degradation of signaling receptors (Huotari & Helenius, 2011). Early endosomes are formed from plasma membrane; pinged like bud. After that depending on internalized substance, endosomes get matured and fused with lysosome or vacuole in yeast, to become late endosome. Multivesicular bodies are responsible for degradation of proteins that are ubiquitylated. The transition of early to late endosomes required Fab1 kinase activity since PI(3,5)P2 conversion from PI3P is essential for this process (Wallroth & Haucke, 2018).

1.6.2.4 Nutrient Sensing through TORC1

Target of Rapamycin Complex 1 (TORC1) is a critical component of the nutrient-sensing and
signaling pathway in eukaryotic cells. One of the primary functions of TORC1 is to regulate cell growth and proliferation in response to nutrient availability and energy status. In the presence of abundant nutrients, TORC1 becomes active and stimulates cell growth by promoting protein synthesis, ribosome biogenesis, and other anabolic processes. Conversely, under conditions of nutrient scarcity, TORC1 activity is suppressed, leading to a consequent reduction in cell growth (Loewith & Hall, 2011). Furthermore, TORC1 plays a crucial role in metabolic regulation, encompassing lipid, glucose, and amino acid metabolism. The kinase complex supports anabolic processes such as lipogenesis and glycogenesis while inhibiting catabolic processes like lipolysis and autophagy. In this manner, TORC1 helps maintain a balance between the synthesis and degradation of cellular components (Noda, 2017). As a conserved protein kinase complex, TORC1 influences a wide array of cellular processes to ensure the optimal allocation of resources, thereby promoting cell growth and proliferation under favorable

conditions. In yeast, it consists of Kog1, Tor1, Tor2 and Kog1 along with Lst8 and Tco89 (Noda, 2017). The complex senses and integrates signals from various sources, such as amino acids, nitrogen, carbon, and energy status. Upon activation by these signals, TORC1 phosphorylates a range of downstream target proteins to regulate key processes, including protein synthesis, ribosome biogenesis, nutrient transport, and autophagy. In budding yeast, the key protein targeted by TORC1 is Sch9 a functional homolog of mammalian S6 kinase. Phosphorylation of Sch9 by TORC1 promotes protein synthesis and ribosome biogenesis, thereby supporting cell growth and proliferation (Takeda & Matsuura, 2018). The Integrity of the vacuolar membrane and the levels of PI(3,5)P2 are essential for proper Sch9 localization and function. PI(3,5)P2 is shown to control the localization of Sch9 by recruiting Sch9 to vacuole which facilitates TORC1 phosphorylation (Takeda & Matsuura, 2018). However, in response to nutrient deficiency or cellular stress, yeast TORC1 activity leads to a shift in cellular processes toward a more conservative mode. Under such conditions, TORC1-mediated inhibition of autophagy is relieved, allowing the degradation and recycling of cellular components to maintain cellular homeostasis (Takeda & Matsuura, 2018). Furthermore, the complex represses mRNA translation and promotes stress resistance and cell survival pathways. This results in the dephosphorylation and activation of the autophagy-initiating proteins, which in turn allows for the formation of the autophagosome, a double-membraned vesicle that engulfs cellular components targeted for degradation. The autophagosome then fuses with a lysosome (in mammals) or vacuole (in yeast) to form an autolysosome, where the engulfed components are degraded and their constituent molecules are recycled back into the cytosol for reuse (Loewith & Hall, 2011).

1.6.2.5 Transcription Regulation and Chromatin Remodelling Functions

The transcriptional activity of a gene is controlled by transcriptional regulatory complexes that form and disassemble on the gene, thereby influencing chromatin structure. PI(3,5)P2 is shown to be involved transcriptional regulation. Tup1 and Cti6 were identified as specific binding partners of PI(3,5)P2 (Han & Emr, 2011). Tup1, which interacts with various transcriptional regulators such as the histone deacetylase (HDAC) and SAGA complexes, is crucial for determining the activated or repressed chromatin state of numerous genes, including GAL1 (Han & Emr, 2011). GAL1 is a gene in the budding yeast that encodes for galactokinase, an enzyme involved in galactose metabolism. The transcriptional regulation of GAL1 is tightly controlled in response to environmental conditions, such as the presence or absence of galactose. PI(3,5)P2 has been reported to play an essential role in converting the repressed chromatin structure, mediated by Tup1 (TLE1 in human), into an activated chromatin structure containing the SAGA complex at the GAL1 promoter when the Gal4 activation pathway is compromised. This conversion is crucial for the regulation of GAL1 transcription in response to galactose availability (J. Hasegawa et al., 2017).

1.6.2.6 Translocation of RNA molecules

Translocation of RNA granules refers to the movement of RNA granules within a cell to ensure their proper localization and function. RNA granules are membrane-less,

dynamic structures composed of RNA molecules (such as mRNA) and RNA-binding proteins (Weber & Brangwynne, 2012). It has been shown that RNA granules can transported via on lysosome in mammallian cell (Liao et al., 2019). ANXA11, a phospholipid-binding protein, is identified as the molecular tether that links RNA granules to lysosomes. It exerts its function by binding both the lysosomal membrane and the RNA granule component. This binding only occur when PI(3,5)P2 and Ca+2 channel is tethered on vacuole (Liao et al., 2019). After binding on lysosome, transportation of RNA granules proceeds via motor proteins.

1.6.2.7 Roles in Calcium Signalling

PI(3,5)P2 has emerged as an important player in modulating the activity of various calcium channels. The calcium signaling and homeostasis are significantly regulated by PI(3,5)P2's interactions with calcium channels (Bagur & Hajnóczky, 2017). Voltage-gated calcium channels (VGCCs) and transient receptor potential (TRP) channels are the two main classes of calcium channels that PI(3,5)P2 has been demonstrated to interact with.

Transient receptor potential channels are a diverse family of non-selective cation channels that mediate calcium influx in response to various stimuli, such as temperature, pressure, and ligand binding. They are ubiquitously expressed in many cell types and contribute to a wide range of physiological processes. One example of a TRP channel modulated by PI(3,5)P2 is the TRPML1 channel in mouse fibroblasts. A member of the mucolipin subfamily predominantly localized in lysosomes and late endosomes (Dong et al., 2010). TRPML1 is a Ca2+-permeable channel that plays a critical role in lysosomal calcium release, which in turn regulates lysosomal membrane trafficking, fusion, and fission events.

1.6.2.8 Autophagy Related Functions

Autophagy is a highly conserved cellular process that is responsible for self degradation and recycling of cellular components. Autophagy is essential for homeostasis. Impaired autophagy leads neurodegenerative diseases like Parkinson's and Huntington diseases. Among the various molecules involved in autophagy regulation, PI(3,5)P2 has emerged as a crucial player (J. Hasegawa et al., 2017). Autophagy has several steps including membrane formation for autophagasome, maturation, fusion with lysosome, cargo selection for degradation.

PI(3,5)P2 localizes to membrane of early autophagosomes. It recruits effector proteins for the formation and expansion of autophagosomes, acting as a signalling lipid. WIPI (WD-repeat protein interacting with phosphoinositides) WIPI1 and WIPI2 interact with PI(3,5)P2 on autophagosomal membrane and with this interaction nucleating and elongation of the autophagosomes initiate in mammalian cell. In yeast, Atg18 binds to PI(3,5)P2 on the autophagosomal membrane to contribute the expansion and closure of the autophagosome (Jin et al., 2016).

Autophagy related Atg18 protein negatively regulates PI(3,5)P2 levels. Autophagy dependent degradation process after tethering of the autophagasome to the lysosome. Acidity of the lysosome lumen is also regulated by PI(3,5)P2, which creates another link with autophagy and PI(3,5)P2.

PI(3,5)P2 is involved in mediating the tethering and fusion of autophagosomes with lysosomes. PI(3,5)P2 interacts with specific effector proteins, such as the HOPS (homotypic fusion and protein sorting) complex and the SNARE (soluble N-ethylmaleimide-sensitive factor attachment protein receptor) proteins, which are essential for membrane fusion (Baskaran et al., 2012).

Selective autophagy is another event that PI(3,5)P2 indirectly plays a role. It is highly controlled mechanism which specific cellular components such as damaged organelles or protein aggregates should be targeted and degraded (Strømhaug et al., 2004). This provide the recruitment of Atg8/Lc3 to the autophagosamal membrane facilitating the cargo recognition and autophagosome formation (Balderhaar & Ungermann, 2013). This recruitment to the site occurs via activation of Ypt7 the effector protein of PI(3,5)P2.

Conversely PI(3,5)P2 also plays an inhibitory role in autophagy. Sch9 branch of TORC1 is activated by PI(3,5)P2 this causes TORC1 dependent inhibiton of autophagy. This requires vacuolar localization of Sch9 which is performed by PI(3,5)P2 (Novarina et al., 2021).

1.6.2.9 Cell Cycle Entry

Mitotic division is a process in which in addition to segregation of nucleus, many other organelles are also segregated. This inheritance ensures that organism has organelles. Vacuole segregation is a process that occurs during the cell cycle to ensure that daughter cells inherit functional vacuoles (Yui Jin & Lois S. Weisman, 2015). The segregation process varies depending on the type of organism, but in general, it involves the division of vacuoles and their proper distribution to the daughter cells. The vacuole in mother cell should reach a specific size at early G1. Vacuole inheritance in yeast cells begin with G1 phase via Cdk1 a small vacuole in mother prepare to elongate and transport complex also formed. The vacuole is moved by a transport complex called the vacuole transport complex, which consists of three components: Myo2, a myosin V motor; Vac8, a protein anchored to the vacuole membrane; and Vac17, an adaptor protein that connects Myo2 and Vac8 (Catlett & Weisman, 1998). At S phase it becomes the vacuole in the mother extend toward bud. As the bud grows, vacuole also extend and goes towards to bud (Weisman, 2003). At G2 stage Vac17 is ubiquitylated and transportation of the vacuole is finished. During cytokinesis mother and daughter cells separate and have functional vacuoles. This inheritance is not essential for cell cycle since when inheritance fails, cell generates a new vacuole (Y. Jin & L. S. Weisman, 2015). In other words, daughter cell cannot become a mother cell if vacuole is not present but it does not have to inherit. When they lack both vacuole gene (*VAC17*) and vacuole formation gene (*PEP12*) they found cells are inviable. In the absence of Vac17, newly synthesized vacuoles of daughter cell exhibit differences. Sch9 is found on vacuoles and

phosphorylated by TORC1 (Loewith et al., 2002). The newly synthesized vacuole lacks Fab1 and Sch9, indicating that the newly synthesized vacuole is not yet matured. Vacuoles that are newly synthesized lack Fab1, which in turn prevents the recruitment of Sch9, leading to a delay in the G1/S phase (Yui Jin & Lois S. Weisman, 2015). Therefore, the localization of TORC1-Sch9 and the signaling originating from the vacuole through PI(3,5)P2 play crucial roles in regulating the initiation of mitosis.

Recent findings highlight the essential function of BUR1, a gene encoding the cyclin-dependent kinase (CDK) in conjunction with the cyclin Bur2, in the progression of the cell cycle mediated by the vacuole. Cells with defective Bur1 exhibit an inability to phosphorylate Sch9 on the vacuole, causing a significant delay in the mitotic cycle. Furthermore, Bur1 functions in parallel with TORC1 to phosphorylate Sch9 on the vacuole membrane (Jin et al., 2022). It is important to note that the vacuole-mediated progression of the cell cycle relies on the presence of Sch9 on the vacuole, a requirement facilitated by the presence of PI(3,5)P2.

Chapter 2

MATERIAL AND METHODS

2.1 Yeast Specific Methods

2.1.1 Yeast Strains and Plasmids

The yeast strains and plasmids used in this study are listed in Table 5.3. Gene deletions and C- terminal tagging were performed using cassette PCR genome editing method (Knop et al., 1999). *TUB1* N-terminally tagged with GFP or mCherry was integrated into the genome at the corresponding auxotrophy gene as extra copy. For strains involving genetic deletions, confirmation was achieved through yeast colony PCR or PCR from yeast chromosomal DNA. In the case of tagging with fluorophores, confirmation was conducted using microscopy (Janke et al., 2004).

2.1.2 Yeast Growth and Media

Composition of all growth media is described in Table 5.5. Yeast strains were cultured at 30 °C in YPAD media, unless otherwise specified. For the microscopy experiments filter sterilized SC-Complete media was used. Temperature sensitive mutants were grown at 23°C until the experiment where temperature sensitive phenotype is examined. Yeast strains taken from -80°C glycerol stocks were streaked onto appropriate solid agar plates (Sherman, 1991). Once the cells had grown on the solid agar, they were transferred into the corresponding liquid medium. The aim was to establish a logarithmically growing culture, often referred to as the log-phase. This was achieved by allowing the liquid culture to incubate overnight at the proper temperature for a duration of 12 to 18 hours, allowing the cells to progress from their initial state to reach the stationary phase. Culture's optical density (OD) at 600nm was measured using a spectrophotometer (PG Instruments, T60 Visible Spectrophotometer). Then, cultures were diluted to an OD600 value of 0.15-0.2 in fresh medium. Log-phase culture was obtained when the OD600 of the culture had reached 0.8-1.0. This OD600 range ensured that the yeast cells from stationary culture divided at least 2 times in the fresh medium.

2.1.3 Preparation of Yeast Competent Cells and Transformation

Competent cell of yeast was prepared using Lithium acetate and PEG (polyethylene glycol) method (Ito et al., 1983). To achieve this, first 50 ml from the log phase culture (OD600 of 1) was centrifuged at 3200 rpm for 2 minutes at room temperature. Supernatant of the culture was removed, and the cell pellet was washed with 20 ml sterile dH_2O. For this, cell pellets were resuspended in water, centrifuged at 3200 rpm for 2 minutes and supernatant was aspirated. Then, cells were resuspended with 20-25ml LiSORB and centrifuged at 3200 rpm for 2 minutes at room temperature. Supernatant was aspirated. Pellet was subjected to another round of centrifugation to eliminate excess LiSORB. After getting rid of all LiSORB via aspiration, cell pellet was resuspended in a solution of 300 µl LiSORB and 50 µl denatured Salmon Sperm DNA per pellet coming from 50 ml log phase culture of 1 OD600. The amount of LiSORB

and Salmon Sperm DNA was scaled depending on the initial log phase culture amount. After resuspension step, the competent cells were either used immediately for transformation (freshly prepared ones more efficient) or preserved at -80°C for later use. To obtain the denatured salmon sperm DNA, salmon sperm DNA solution was heated at 95°C for 5 minutes followed by a 5 minute incubation on ice.

Transformation was performed using competent cells and cassette PCR products or linearized integration plasmids. To achieve high efficiency, 50 µl competent cell was transformed with 5 µl cassette PCR product or 5 µl linearized plasmid. Briefly, DNA was mixed with the competent cells and cells were incubated at room temperature for 15 minutes. Subsequently, 300µl LIPEG was introduced to the cell mixture, and mixed via vortexing. After an incubation of 15 minutes at room temperature, 35µl DMSO (Fisher Scientific #BP231-1) was added to this mixture, contents were vortexed and immediately placed in a 42°C water bath for 15 minutes (12 minutes for the temperature sensitive strains). After this incubation period, cells were centrifuged at 3200 rpm for 2 minutes at room temperature. Supernatant was aspirated. Finally, cell pellet was resuspended in 200µl 1X sterile PBS and plated out on auxotrophic selective agar plate. If the selection marker is antibiotic resistance, cells were transferred to the non-selective liquid medium for recovery, grown over night, and plated out on selective agar plates. Plates were incubated at an appropriate temperature until transformant colonies were visible (at least 2 days).

2.1.4 Yeast Growth Assay (Drop Test)

Cultures were grown in 1-5 mL medium for 24h-48h. Then yeast cultures were diluted to a value of 1.0 OD600 using 1X PBS. Following this, the 1 OD dilution was serially diluted 10-fold using sterile 1X PBS to obtain $1,10^{-1},10^{-2}$,10^{-3}, 10^{-4} OD600 cell suspensions. 10 µl of each dilution was carefully spotted on appropriate agar plates. These plates were then incubated at proper temperatures for a period ranging from 1-3 days. Finally, plates were imaged using a photo-scanner.

2.2 PCR Based Methods

2.2.1 Cassette PCR

Every PCR procedure was carried out using the Biometra T advance Twin Analytik Jena PCR machine. When performing gene deletions, S1/S2 primers (see Table 5.2) were employed. In the case of C- terminal tagging, S2/S3 and S1/S4 primers were utilized respectively.

For the construction of 50 µl PCR product, following reaction mixture was prepared (Knop et al., 1999):

5 µl of 20 ng/ µl plasmid template

3.2 µl of forward S1 or S3 primers (10 µm)

3.2 µl of reverse S2 or S4 primers (10 µm)

0.6 µl of the polymerase enzyme mixture which composed of 2x µl Taq DNA Polymerase (5U/ µL, NEB #M0273L)+ 1x µl Vent (2U/µL, NEB #M0254S)

8.75 µl of 2mM dNTPs mix (NEB #N0446S)

5 µl of 10X PCR buffer and 24.25 µl dH_2O.

The Cassette PCR conditions were as follows (Knop et al., 1999):

1: Initial Denaturation: 2 min at 95°C

2: Denaturation: 30 sec. at 95°C

3: Annealing: 30 sec at 52°C

4: Elongation: X min at 68°C; x refers to the duration of elongation and is determined by calculating 1 min for every 1000 bp of the expected product size.

Steps 2 to 4 were repeated for 9 times.

5: Denaturation: 30 sec at 95°C.

6: Annealing: 30 sec at 52°C.

7: Elongation: X min and each step incrementally increased by 20 sec at 68°C.

These steps (5 to 7) were repeated 19 times.

8. Hold at 4°C. After this step it can be used or stored at -20°C for further usage. The PCR products were visualized using 0.8% agarose gel prepared in 1X TAE buffer.

2.2.2 Colony PCR

Colony PCR was performed from colonies were picked from agar plates. Colonies were added in 50 µl Sarkosyl/NaOH solution composed of 0.01% Sarkosyl lauryl sulfate in 0.02 M NaOH, vortexed and boiled at 95°C for 15 min while shaking. This mixture was used as the template DNA source in the colony PCR.

Colony PCR reaction mixture was prepared to construct 25 µl PCR product as following:

Template DNA: 0.6 µl

Gene-specific forward primer (10 µM): 1.25 µl

Gene-specific reverse primer (10 µM): 1.25 µl

10X PCR buffer: 2.5 µl

2 mM dNTP mixture: 2.5 µl

Taq DNA polymerase (5U/µL): 0.2 µl

Double-distilled water: 16.7 µl

Colony PCR cycle conditions were:

1: 5 min at 95°C for initial denaturation:

2: 30 sec at 95°C for denaturation

3: 30 sec at X°C for annealing.

(X was calculated for each primer set as; $Tm - 5 = 2(A+T)+4(G+C) - 5$)

4: X min at 68°C

(X was calculated as 1 min per 1000bp of the expected PCR product size).

5: Steps 2-to-4 were repeated 30 times.

6. 3 min at 68°C for final elongation.

7. Hold at 4°C. After this step it can be used or stored at -20°C for further usage.

After finishing the PCR, the PCR product was run on 0.8% agarose gel prepared with 1X TAE buffer.

2.2.3 Cloning FAB1 in pRS315

FAB1 was amplified from genomic DNA, using the following primers designed to contain XhoI and SacII restriction enzyme sites at their 5' ends as flanking sequences:

Forward Primer: 5'ccgctcgagACGCTAGACCAATTAGTCGC 3' (primer name: Fab1-Xho1), The Fab1-Xho1 primer binds 594 bases upstream of the START codon on the template DNA strand: 5' - GCTCGAG - 3'

Reverse Primer: 5' tctccgcggCAGTGGCCGAGTGGTTAAG 3' (primer name: Fab1-Sac2)

the Fab1-Sac2 primer binds 254 bases downstream of the STOP codon on the template DNA strand: 5' - CCGCGG – 3'

The *FAB1* gene was amplified utilizing NEB Phusion Polymerase using following PCR conditions:

- Nuclease-free water: 28.5 µl
- 5X Phusion GC Buffer: 10 µl
- 2 mM dNTPs: 5 µl
- 10 µM Forward Primer (Fab1-Xho1): 2.5 µl
- 10 µM Reverse Primer (Fab1-Sac2): 2.5 µl
- Template DNA: 2 µl
- Phusion DNA Polymerase: 0.5 µl

Thermocycling conditions specific to *FAB1* amplification:

- Initial Denaturation: 98°C 30 seconds
- 25-35 Cycles: 98°C 10 seconds
56°C 30 seconds
72°C 30 seconds
- 4°C hold

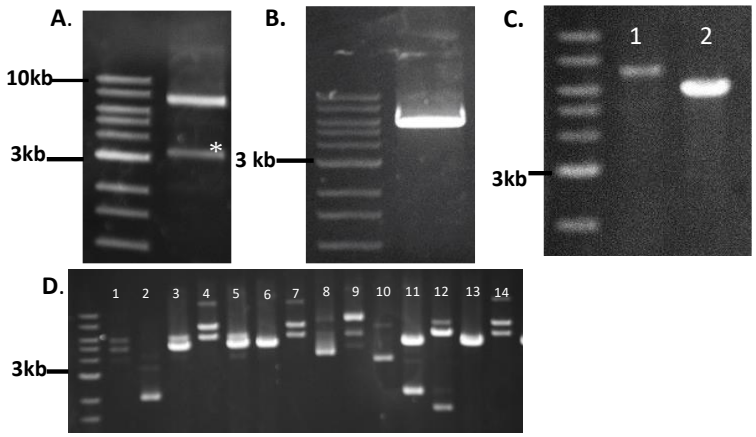

Figure 2.1: Agarose Gel Electrophoresis Results for Molecular Cloning of the *FAB1* gene into pRS315 plasmid. (A) PCR product of *FAB1* gene for generating insert. The *FAB1* gene was amplified utilizing genomic DNA and NEB Phusion Polymerase using Fab1-XhoI and Fab1-SacII primers. *non-specific band, which is eliminated via gel excision method. (B) Agarose gel image of pRS315 that is digested using XhoI and SacII enzymes. (C) Lane 1: Gel analysis of insert DNA (Upper band of A was gel extracted, digested with XhoI and SacII and purified with PCR purification kit. Lane 2: backbone DNA: Band from B was gel extracted. (D) Control digestion of obtained plasmids. Ligation product was transformed in DH5-alpha *E.coli* competent cells. Plasmids were isolated from 14 colonies and control digestion was performed using XhoI and SacII. Lane 4, Lane 7 and Lane 14 have expected bands, others have nonspecific bands.

PCR product was run on agarose gel and the band corresponding to the expected size of *FAB1* (7.4 kb), as depicted in Figure 2.1, was excised and purified using a gel extraction kit. Subsequently, the purified DNA was digested with XhoI and SacII enzymes, followed by purification using a PCR purification kit (MN #740588.50) (Figure 2.1.C, lane 1). Simultaneously, the plasmid pRS315, utilized as the backbone, was subjected to restriction enzyme digestion with XhoI and SacII. Gel electrophoresis was applied to the digested product of plasmid pRS315 (Figure 2.1.B). The expected band for backbone (5.9 kb) was purified from the gel. The pre-ligation states of the vector seen as (1) and backbone (2) are illustrated in Figure 2.1.C. The purified (Figure 2.1.C, lane2). *FAB1* insert and the linearized pRS315 vector were mixed in a molar ratio (3:1) optimized for ligation efficiency. The ligated product was transformed into competent *Escherichia coli DH-5alpha* cells, and plasmids were isolated from colonies and positive clones were identified through control digestion with XhoI and SacII (Figure 2.1.D). Another set of control digestion was performed using BamHI and HpaI enzymes separately (data not shown). Expected bands after digestion with BamHI were 4140bp and 9167bp. Expected bands after digestion with HpaI were 6855bp, 4215bp and 2237bp. Two positive plasmids exhibiting expected fragments after the aforementioned digestions were named as pSE001-1 and pSE001-2.

2.2.4 Point Mutations of FAB1

To introduce a point mutation into *FAB1* plasmid (PSE001), the site directed mutagenesis PCR was performed.

For 50 µl PCR reaction, the following components were combined:

5 µl of plasmid template plasmid pSE001, (5 ng/µl)

1.5 µl forward primer (FAB1-T2250A, FAB1-F1833L) (10 µM)

1.5 µl reverse primer (FAB1-E183L-REV, FAB1-T2250A-REV) (10 µM)

1.5 µl of Turbo PFU DNA Polymerase (Agilent #600250)

4 µL of 2 mM dNTPs mix (NEB #N0446S)

5 µL of a 10X PFU Turbo Buffer

31.5 µL of double-distilled water (dH_2O)

PCR conditions were:

- Initial Denaturation: 95°C 30 seconds
- 16 Cycles: 95°C 30 seconds
  56°C 1 minutes
  68°C 28 minutes
- 4°C hold

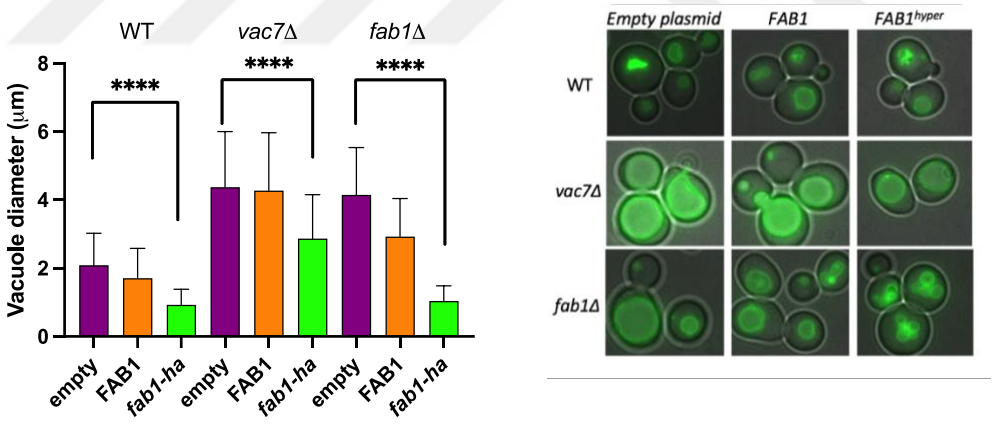

Figure 2.2: Functionality assay of pSE001 and pSE002. We initially tagged the VPH1 gene, a vacuolar marker, with green fluorescent protein (GFP) in wild-type (WT), *vac7*Δ, and *fab1*Δ strains. Subsequently, these strains were separately transformed with an empty plasmid (pRS315), a plasmid carrying wild type *FAB1* (pSE001), and a plasmid having the hyperactive *FAB1* (*fab1-ha*) (pSE002) mutant. From left to right strain names; SEY045, SEY044, SEY046, SEY060, SEY061, SEY062, SEY043, SEY042, SEY047. (see Table 5.1 for descriptions).

After PCR amplification the final product was treated with 2µl DpnI (Thermo Fisher Scientific #ER1705) incubated overnight at 37°C. After that, 10 µl of the reaction was

transformed to 100 µl DH-5alpha *E. coli* competent cells. From that transformants, single colonies were picked, plasmids were isolated and sequenced using Fab1-seq1 and Fab1-seq2 primers (Table 5.2) to confirm the mutation. The plasmid with desired mutations were named as PSE002. These mutations were expected to result in a hyperactive version of Fab1 (*fab1-ha*) (Duex et al., 2006). The hyperactive mutant Fab1 rescues the enlarged vacuole phenotype in *vac7*Δ and *fab1*Δ mutants (Duex et al., 2006). *FAB1* and *fab1-ha* functionality was tested based on the vacuole sizes using Vph1-GFP as a vacuole marker (Figure 2.2). Wildtype *FAB1* in pSE001 partially rescued enlarged vacuoles in *fab1*Δ and did not rescue the enlarged vacuoles of *vac7*Δ, whereas *fab1-ha* in pSE002 fully rescued both the *fab1*Δ and *vac7*Δ enlarged vacuole phenotypes.

Following transformation, vacuolar diameters were measured using Image J measure tool. A minimum 100 cell was counted for each strain. $p<0.0001$ according to ordinary one way ANOVA.

2.2.5 Subcloning of fab1-ha (pSE002) into pRS305

The subcloning of pSE002 into pRS305 was conducted with several steps. Firstly, pSE002 was subjected to restriction enzyme digestion with XhoI and SacII. Expected band (7.45 kb) was extracted and purified with digestion purification kit (MN #740588.50). pRS305 was also digested and linearized with XhoI and SacII. Expected band was seen on gel electrophoresis and gel extraction purification was performed via the kit (MN #740588.50). For the ligation, pSE002 insert and the linearized pRS305 vector were mixed in a molar ratio (3:1) optimized for ligation efficiency. The ligated product was transformed into competent *Escherichia coli DH-5alpha* cells, and plasmids were isolated from colonies and positive clones were identified through control digestion with XhoI and SacII. Expected bands were seen around 7.5 kb and 5.4 kb. Second digestion was performed for confirmation, employing the EcoRI enzyme with expected restriction fragment sizes of 8.5kb and 4.45kb. A positive result was obtained from one plasmid (pSE003) which was subsequently cleaved with Eco91L enzyme for genome integration.

2.2.6 Yeast Chromosomal DNA Isolation

Yeast chromosomal DNA was obtained by first culturing the cells to stationary phase in appropriate media. Subsequently, 1 ml culture was centrifuged at 3200 rpm for two minutes, and the supernatant was carefully aspirated. The pellet was then resuspended in 1 mL distilled water and centrifuged again as before, with subsequent removal of the supernatant by aspiration. The resulting pellet was resuspended in 750 µl P1 buffer, 1 µl mercaptoethanol, and 0.15 mg Zymolase 20 T (MP Biomedicals, LLC #320921). This mixture was incubated at 37 °C with occasional mixing for 1-2 hours.

Following this enzymatic treatment, 150 µl P2 buffer was introduced to the mixture with careful mixing, followed by incubation at 65 °C for 20 minutes. The sample was then placed on ice for 10 min. Subsequently, 150 µl P3 buffer was added with careful mixing, and the mixture was incubated on ice for an additional 15 minutes. The

resulting sample was centrifuged at 14000 rpm for 5 minutes, and the supernatant was carefully transferred to a new eppendorf tube.

To precipitate the chromosomal DNA, 450 µl isopropanol (ACS #0312.2500) was added to the supernatant. The mixture was gently mixed and incubated for 5 minutes at room temperature, followed by centrifugation at 14000 rpm for 15 minutes. The supernatant was then discarded, and 1 ml of 70% molecular ethanol is added. The sample was centrifuged once more, and the supernatant was removed. The remaining sample was left to air dry until all liquid has evaporated. Subsequently, 20 µl of pre-heated (65°C) dH_2O was added to elute the chromosomal DNA, which was then stored at -20 °C for future use.

2.2.7 Plasmid DNA Isolation

For the bacterial plasmid isolation, miniprep method was used (Sambrook et al., 1989). Briefly, a single *E. coli* colony was inoculated in 3 ml TY-liquid medium with suitable antibiotics and incubated overnight at 37°C. From this overnight culture, 2 ml of culture was pelleted through centrifugation at 6000 rpm for 5 min at room temperature. Supernatant was carefully aspirated. 300 µl P1 buffer was added to pellet and vortexed. After that, 300 µl P2 buffer was added to the mixture and mixed gently via inversion. Immediately, 300 µl P3 buffer was added, mixed via inversion, and centrifuged at 14000 rpm for 10 min. The supernatant of this step was carefully transferred to the new tubes that contains 500 µl isopropanol (ACS #0312.2500), mixed by inversion/rotation, and centrifuged at 14000 rpm for 20 min. The supernatant was discarded, 500 µl %70 Ethanol was added and centrifuged at 14000 rpm for 1 min. Supernatant was discarded, and the pellet was air dried. Finally, pellet was dissolved in 20 µl pre heated dH_2O. The plasmid DNA can be stored at -20°C after this step.

2.2.8 Agarose Gel Electrophoresis

A 0.8% agarose gel was prepared by boiling 0.4 grams of agarose (SIGMA A9539) in 50 ml of TAE buffer using a microwave oven until all agarose is solubilized. Agarose solution was poured in trays containing combs and let sit until it solidifies. Gel was placed in a chamber that contains 1XTAE. DNA samples mixed with loading dye were carefully loaded into the wells. A DNA ladder (NEB N3232L) was also loaded in one of the wells to serve as the reference marker. The electrophoresis process was carried out at 100 volts for approximately 45 min, followed by an incubation period in an ethidium bromide (EtBr) solution for a minimum of 15 min at room temperature. The gels were visualized using a gel documentation system (Carestream) under ultraviolet (UV) light.

2.3 Microscopy Based Techniques

For all microscopy experiments, Carl ZEISS Axio Observer 7 motorized inverted epifluorescence microscope with an XL incubation and environmental control chamber was used. Microscope had Colibri 7 LED light source, Axiocam 702 monochrome

camera, 63X and 100X plan apochromat immersion oil lenses. Filter sets include a combination of 95 (GFP/Cherry), 20 (Rhodamin), FITC, and DAPI filters. For the analysis of GFP-Tubulin, Kin4-GFP, Vph1-mCherry 63X oil immersion objective was used.

For all time-lapse experiments cells were cultured in filter sterilized SC-complete medium and kept in log phase for at least 24 hours before the experiment. 200 µl of a 6% solution of Concanavalin A (Con A) was evenly applied to the glass surface of petri dishes with glass bottoms (specifically, WvR 10810-054 Matsunami dishes). Following a 10 min incubation period at room temperature, the Con A solution was removed, and the glass surface was rinsed with dH_2O 5-to-6 times. Subsequently, a 200 µl aliquot of logarithmic-phase culture 0,5 of OD600 was pipetted onto the glass surface. Glass bottomed petri dish was incubated for 30-40 minutes at appropriat temperature depending on designed experiment (mainly at 30°C exception was *lte1Δ* at 21°C). Subsequently, the remaining culture was aspirated, and the glass surface was gently washed with pre-warmed fresh medium (filter sterilized SC-Complete) 5 times to eliminate unattached cells. Finally, 3 ml of filter sterilized SC-Complete medium was added on the cells and the petri dish was relocated to the microscope chamber, which had been pre-heated to 30°C (for *lte1Δ* it was at 21°C). To ensure equilibration, glass bottom petri dishes containing the cellular specimens were maintained within the microscope chamber for a minimum of 30 min prior to the imaging process. Specific areas of interest were selected, and time lapse experiment was started. GFP- Tubulin timelapse was performed using the 63x objective, 2x2 binning and the FITC filter. 488 nm LED intensity was adjusted to %20 and exposure time was set to 60 ms. Images were acquired with 1 min intervals. For each timepoint, 10-13 z-stacks of 0.3 µm thickness were acquired in the FITC channel. A brightfield image was taken as a reference at the middle point of the z-stacks.

For the quantifications of time lapse analysis, z-stacks were sum projected using Image j software. Cells that misaligned their spindle at any timepoint were excluded from analysis. The duration of anaphase is defined as the time elapsed between the moment when rapid spindle elongation begins in the cell and the moment when the mitotic spindle disassembles.

For measurement of spindle elongation dynamics, spindle length of was measured at each time point, by measuring the distance between the two poles of the spindles using Image j software. Measurements from different cells were aligned according to the anaphase onset point. Mean spindle length as a function of time was plotted via GraphPad Prism software.

For the still image analysis of cells, 1 ml log phase culture grown in SC-Complete filter sterilized medium was centrifuged at 3200 rpm for 1 min, pellet was resuspended in 20 µl of SC-Complete filter sterilized medium. 2 µl of this concentrated cell suspension was pipetted on slides and sandwiched with a cover slip to obtain a wet-mount sample. Kin4-GFP imaging was performed using 63X objective lenses and FITC filters. LED intensity was 30% and exposure time was 200 ms. For Spc42-eQFP, LED intensity was 30% and exposure time was 120 ms. For VPH1-3mCherry, LED intensity was 25% and exposure time was 150ms.

In the localization experiment of Kin4, all quantifications were performed using log phase cultures. Minimum 100 anaphase cells were counted for each experiment. 13 z-stacks of 0.3 µm thickness were taken for each stage position with 63x lenses. The visualization of SPBs in all cells was achieved through SPB marker Spc42 labeled with EQFP, Tubulin labeled with mCherry, and Kin4 labeled with GFP.

2.3.1 Statistical Analysis

All statistical analysis were done via GraphPad Prism 9. One way ANOVA or unpaired two tailed students's t-test was applied depending on the number of samples to compare.

Chapter 3

RESULTS

3.1 Defects in the Fab1-Complex cause synthetic lethality in mitotic exit impaired cells

Phosphatidylinositol (3,5) biphosphate, often abbreviated as PI(3,5)P2, is a type of phosphoinositide, which is a class of lipid molecules found in cell membranes (Di Paolo & De Camilli, 2006). PI(3,5)P2 specifically refers to the phosphorylated form of phosphatidylinositol that has phosphate groups attached to the 3 and 5 positions of the inositol ring. This lipid is primarily localized in the vacuolar and lysosomal membranes within a cell (Dove et al., 2009).

Despite being one of the least abundant phosphoinositide derivative in a cell (J. Hasegawa et al., 2017), PI(3,5)P2 plays pivotal roles in various cellular processes such as vacuole/endolysosome structure, transcriptional regulation, membrane trafficking and stress response (J. Hasegawa et al., 2017). Remarkably, literature to date has not ascribed any mitotic function to PI(3,5)P2.

Vac7, Vac14 and Fab1 are proteins responsible for the PI(3,5)P2 production (Dove et al., 2002; J. D. Gary et al., 2002). They form a protein complex, hereafter will be named as the Fab1-complex. Absence of any Fab1-complex components causes decreased level of PI(3,5)P2 (Jin, 2017). In previous genome-wide genetic screens, *VAC7* and *VAC14* genes were found to become essential in combination with mitotic exit mutants in budding yeast (Caydasi et al., 2017; Costanzo et al., 2019). This led us hypothesize that PI(3,5)P2 may exert regulatory control over mitotic exit in yeast.

Exit from mitosis in budding yeast is governed by the mitotic exit network (MEN) (de Bettignies & Johnston, 2003). Lte1, a positive regulator of the MEN, is essential for mitotic exit at cold temperatures (<15 ^{o}C) (Shirayama et al., 1994). In order to understand whether low levels of PI(3,5)P2 impairs growth of mitotic exit defective cells, first we deleted *VAC7* in *lte1*Δ cells and assessed their growth through a colony growth assay. In the first growth assay, *lte1*Δ cells were complemented with *LTE1* on a *URA3*-based CEN-plasmid (pRS316-*LTE1*), therefore *lte1*Δ phenotype is observed on 5 FOA plates which negatively selects for *URA3* (Figure 3.1A). While wild type (WT) cells grew well at all temperatures, *lte1*Δ cells showed slow growth at 18°C (Figure 3.1.A), which is in line with the literature (Shirayama et al., 1994). Growth of *vac7*Δ cells was overall slower than WT cells at all temperatures (Figure 3.1). Deletion of *VAC7* in *lte1*Δ cells resulted in lethality at 18°C and 23°C, and growth impairment at 30°C and higher temperatures (Figure 3.1.A). Similar lethality was observed in a second growth assay where *vac7*Δ was complemented with pRS416-*VAC7* (Figure 3.1B). Subsequently, we sought to investigate whether the lethality observed in *vac7*Δ is attributed to loss of function of the Fab1-complex. To explore this, we analyzed effects of other Fab1-complex components on growth of *lte1*Δ. Similar growth lethality was observed in *vac14*Δ*lte1*Δ cells (Figure 3.1C).

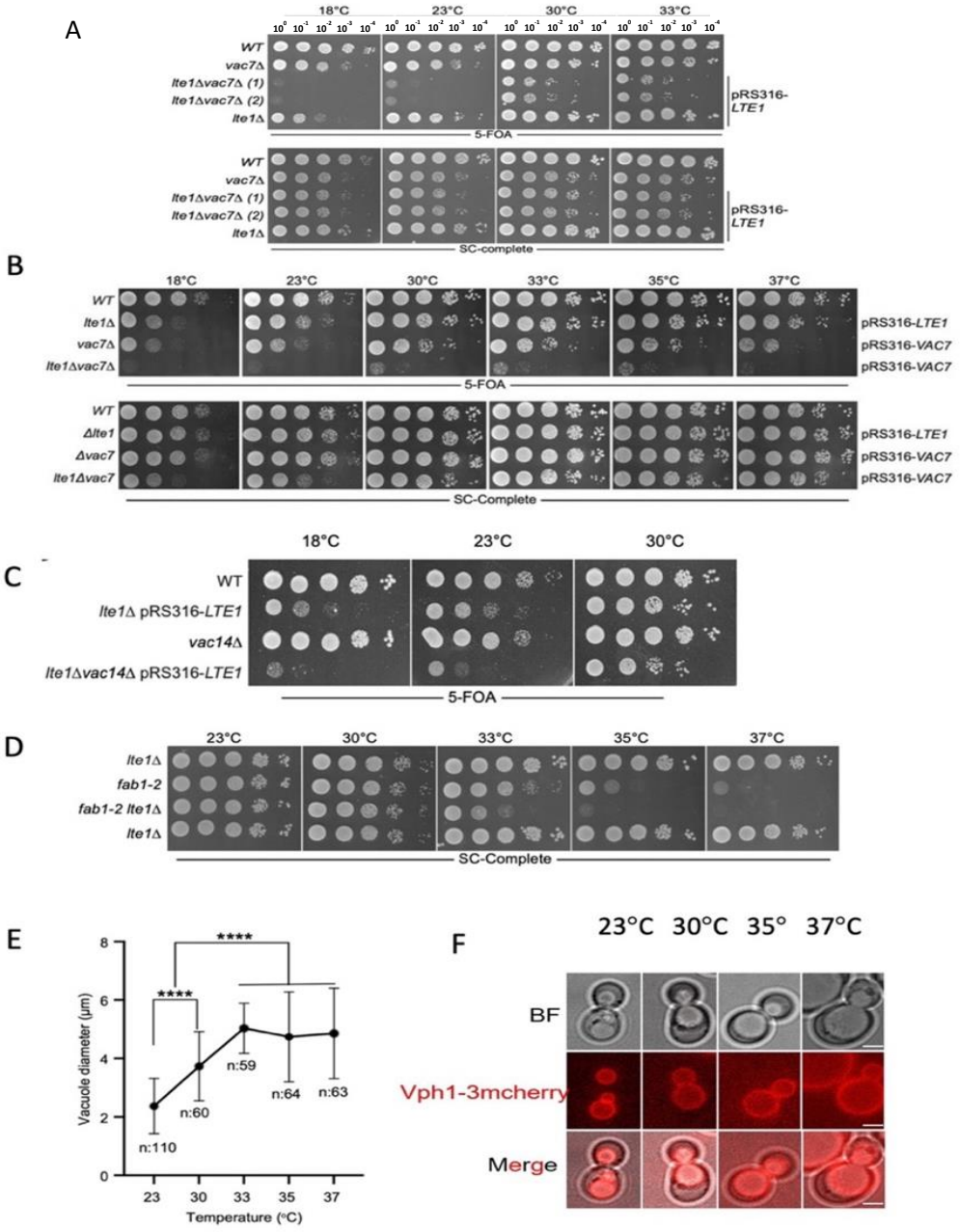

Figure 3.1 Deleting *VAC7* causes growth impairment with mitotic exit defective cells. **(A-B-C)** Serial dilutions from left to right $10,10^{-1},10^{-2},10^{-3},10^{-4}$ of indicated strains were spotted on appropriate plates. Deleting *VAC7* in *lte1*Δ cells resulted in lethality at 18°C and 23°C. All strains contain pRS316-*LTE1*. Stains analyzed were WT (ESM356), *vac7*Δ (SEY023), *lte1*Δ *vac7*Δ (SEY025 and SEY075), *vac14Δ* and *lte1*Δ (FAY145). **(D)** Impairing the activity of *FAB1* by using a temperature sensitive mutant caused synthetic lethality with *lte1*Δ. Stains analyzed were *lte1*Δ (SEY202), *fab1-2* (672-5-2-2), *lte1*Δ *fab1-2* (SEY199). **(E-F)** Confirmation of the *fab1-2* strain by measuring the vacuole diameter with different temperatures. ****p<0.0001 according to ordinary ANOVA. **(F)** From log phase culture indicated strains are observed under fluorescent

microscopy. Representative images of the *fab1-2* used in E. Vph1-3mCherry used as a vacuole marker. Scale bars are 3 μm.

FAB1 deletion causes severe growth defects (J. D. Gary et al., 1998). Therefore, we took advantage of the temperature-sensitive mutant of *FAB1* (*fab1-2)* to observe phenotypes after inhibition of Fab1. *fab1-2* is lethal at 37°C and shows growth defects at 35°C (Yamamoto et al., 1995). When examining the growth assay of *fab1-2* cells, we confirmed its lethality at 37°C (Figure 3.1D). Upon deletion of *LTE1* in *fab1-2* cells, lethality was observed at 35°C (Figure 3.1D). To have a better understanding of *fab1-2* temperature sensitivity we measured vacuole sizes (Figure 3.1E), as vacuole enlargement is an indication of Fab1 loss of function (Jonathan D. Gary et al., 1998). Vacuole diameter started increasing from 30°C, and reached ~5μm at 33°C and above (Figure 3.1E). This suggests significant loss of Fab1 function at 33°C and above temperatures. Consistent with this, growth of *lte1Δ fab1-2* cells were severely impaired at 33°C (Figure 3.1D).

3.2 VAC7 deletion delays mitotic exit in lte1Δ cells

We observed growth defects in *lte1*Δ*vac7*Δ (Figure 3.1). We next asked whether mitotic exit is delayed in these cells. For this, we analyzed the timing of mitotic exit in cells using time-lapse microscopy at 30°C. Anaphase duration was determined as the interval between the beginning of rapid spindle elongation and the beginning of spindle breakdown. Anaphase took 19 minutes in wild type and *lte1*Δ cells, while *vac7*Δ cells took longer (22 minutes) (Figure 3.2A). On the other hand, *lte1*Δ*vac7*Δ cells, had significantly longer anaphase which took around 30 min (Figure 3.2A). Further, we asked whether this delay was due to defects in mitotic exit. We reasoned that if this were the case, deletion of mitotic exit inhibitors would rescue the growth lethality and prolonged anaphase phenotypes of *lte1*Δ*vac7*Δ. To test this, we deleted mitotic exit inhibitors *BFA1* or *KIN4* in *lte1*Δ*vac7*Δ. Growth lethality of *lte1*Δ*vac7*Δ was rescued by deletion of *BFA1* or *KIN4* (Figure 3.2C). Moreover, the deletion of *BFA1* also rescued the prolonged anaphase duration of *lte1*Δ*vac7*Δ (Figure 3.2D). This data confirmed our hypothesis that *lte1*Δ*vac7*Δ is defective in exit from mitosis.

Next, we asked whether the duration of anaphase is longer in *lte1*Δ*vac7*Δ due to any defect in spindle elongation dynamics. To address this question, we measured the spindle length over time in WT, *vac7*Δ*, lte1*Δ*, lte1*Δ*vac7*Δ cells. Spindle lengths were plotted for each cell every minute and aligned with respect to the anaphase onset (t=5min). Graphs were divided into three phases as PI, PII, and PIII, representing the fast, slow, and final phases of spindle elongation, respectively. Spindle elongation dynamics were calculated by assessing the slope of the spindle elongation curve in each phase. Comparison of the phase specific slopes did not yield a significant difference (Figure 3.2E). Thus, we conclude that the increased anaphase duration of *lte1*Δ*vac7*Δ cells is unlikely to be due to spindle elongation defects.

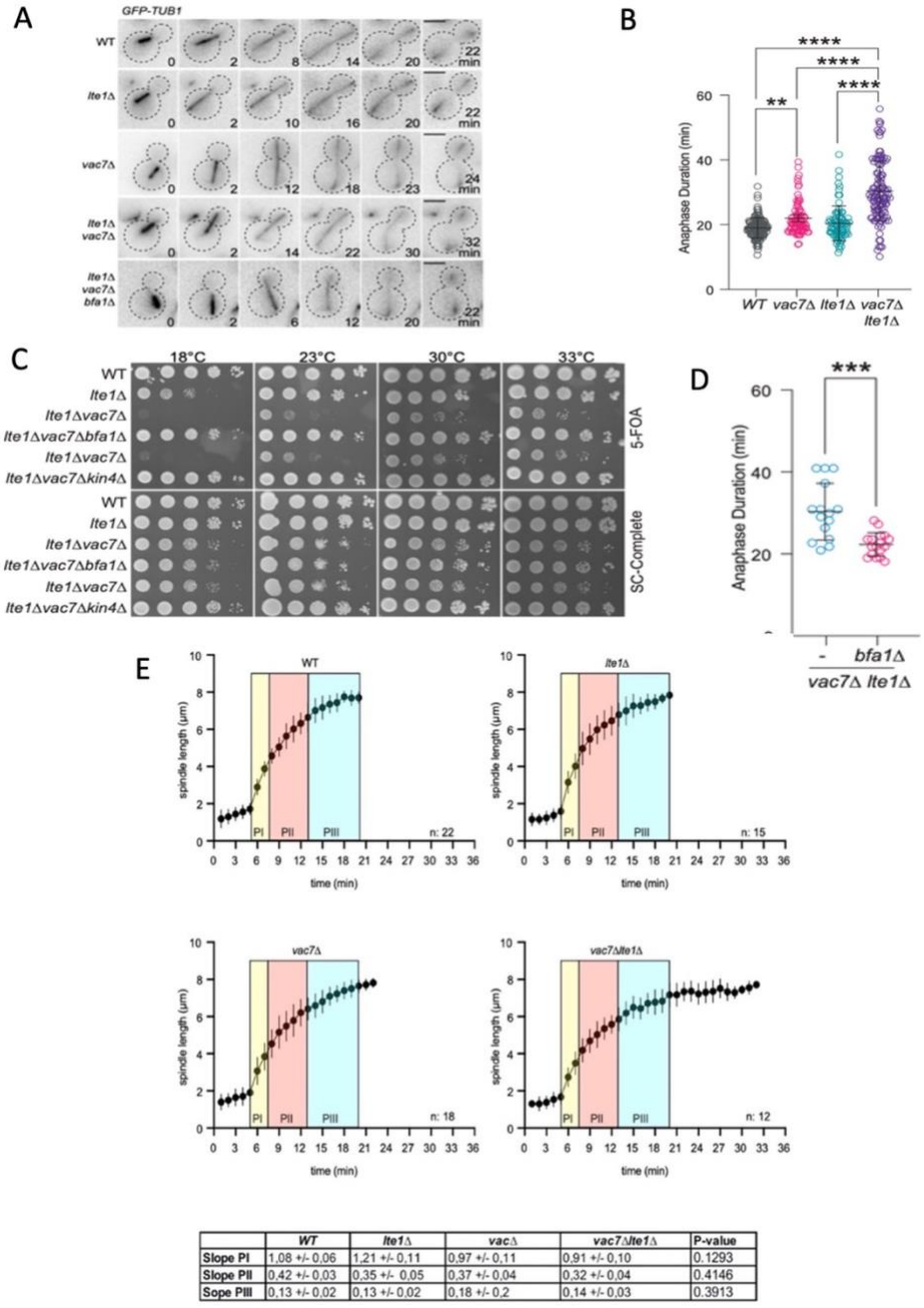

	WT	lte1Δ	vacΔ	vac7Δlte1Δ	P-value
Slope PI	1,08 +/- 0,06	1,21 +/- 0,11	0,97 +/- 0,11	0,91 +/- 0,10	0.1293
Slope PII	0,42 +/- 0,03	0,35 +/- 0,05	0,37 +/- 0,04	0,32 +/- 0,04	0.4146
Sope PIII	0,13 +/- 0,02	0,13 +/- 0,02	0,18 +/- 0,2	0,14 +/- 0,03	0.3913

Figure 3.2 Anaphase duration is longer in *lte1*Δ *vac7*Δ. **(A)** Representative still images from time-lapse series of indicated cells at 30°C. GFP-Tubulin (GFP-TUB1) used as a marker for mitotic progression. Time point zero marks 2 minutes before anaphase onset. Last time points shown are the time of spindle breakdown. Dashed lines show cells outline. Scale bars are 3 μm. (**B)** Dot plots for anaphase duration of individual cells at 30°C. Anaphase duration was calculated as the time elapsed between the onset of anaphase and spindle breakdown. Lateral black lines show the mean. Error bars are standard deviation. Sample sizes are 136, 82, 81 and 119 cells for *SEY037, SEY036, BBY024, SEY034* respectively. Ordinary one-way ANOVA was performed with Tukey's multiple comparison test. ** p<0.01, ****p<0.0001. **(C)** Deletion of the mitotic exit

inhibitors *BFA1* and *KIN4* rescue synthetic lethality of *lte1*Δ *vac7*Δ. All *lte1Δ* strains are complemented with pRS316-*LTE1*. Drops done on 5-FOA plates to lose the centromeric plasmid. WT (ESM356), *vac7*Δ (SEY023), *lte1*Δ *vac7*Δ (SEY025), *lte1*Δ *vac7*Δ *bfa1*Δ (SEY040), *lte1*Δ *vac7*Δ *kin4*Δ (SEY080). **(D)** Anaphase duration of *lte1*Δ *vac7*Δ is rescued by the deletion of the mitotic exit inhibitors *BFA1* and *KIN4.* Dot plots showing anaphase duration of indicated cells at 30°C. Lateral black lines show the mean. Error bars are standard deviation. Sample sizes are 15 and 17 for *lte1*Δ*vac7*Δ and *lte1*Δ*vac7*Δ*bfa1*Δrespectively. Unpaired two-tailed t-test was performed. ***p=0.0001. **(E)** The spindle lengths of indicated cells were measured from the timelapse series (refer to Figure 2B) and plotted against time. The graph depicts the mean spindle length, with error bars indicating standard deviation. "n" represents the sample size. Phases PI, PII, and PIII refer to the first (fast), second (slow), and final phases of spindle elongation, respectively. The slopes (μm/min +/- standard error) of phases PI, PII, and PIII were determined through simple linear regression analysis.

3.3 Mitotic Exit is Delayed in the Absence of PI(3,5)P2

The absence of Vac7 in mitotic exit defective cells is associated with both growth lethality and anaphase delay. This might bring the question of whether this stems from function of Vac7 in PI(3,5)P2 synthesis. To understand whether defects are due to a lack of PI(3,5)P2, we used the hyperactive allele of *FAB1* (*fab1-ha*) (Duex et al., 2006). It was previously shown that cells that have *fab1-ha* do not require Vac7 for the production of PI(3,5)P2 (Duex et al., 2006). Therefore, I cloned *FAB1* in a yeast vector under its own promoter and terminator, and using site directed mutagenesis I mutated *FAB1* at FAB1-T2250A, FAB1-F1833L residues (See materials methods, Figure 2.2). *fab1-ha* containing integration vector was integrated into the *leu* locus in the yeast genome to have cells stably expressing the hyperactive. Remarkably, *fab1-ha* rescued the lethality observed in *lte1*Δ*vac7*Δ cells (Figure 3.3A). In addition, *fab1-ha* alleviated anaphase delay in the absence of *VAC7* (*BEKDAŞ, B. (2023); [Master Thesis], (*Figure 3.3B) and in *lte1*Δ*vac7*Δ cells (Figure 3.3C). *fab1-ha* rescue of both the anaphase delay and growth defects of *vac7*Δ suggests that it is the lack of PI(3,5)P2 that causes mitotic exit defects in *vac7*Δ cells. We conclude that PI(3,5)P2 is required for a timely mitotic exit.

*3.4 Overproduction of PI(3,5)P2 rescues cold sensitivity of lte1*Δ

We observed that *fab1-ha* rescued mitotic exit defects of *vac7*Δ (Figure 3.4). This prompted us to investigate whether it could also alleviate the cold sensitivity of *lte1*Δ cells. For this, we conducted growth assays and measured the anaphase duration of *lte1*Δ at 21°C using the *fab1-ha* plasmid. Cold sensitivity of *lte1*Δ was rescued by *fab1-ha* (Figure 3.4A). Similarly, *fab1-ha* mitigated the anaphase delay in *lte1*Δ at cold temperatures (Figure 3.4B). This indicates that overproduction of PI(3,5)P2 promotes mitotic exit of *lte1*Δ cells.

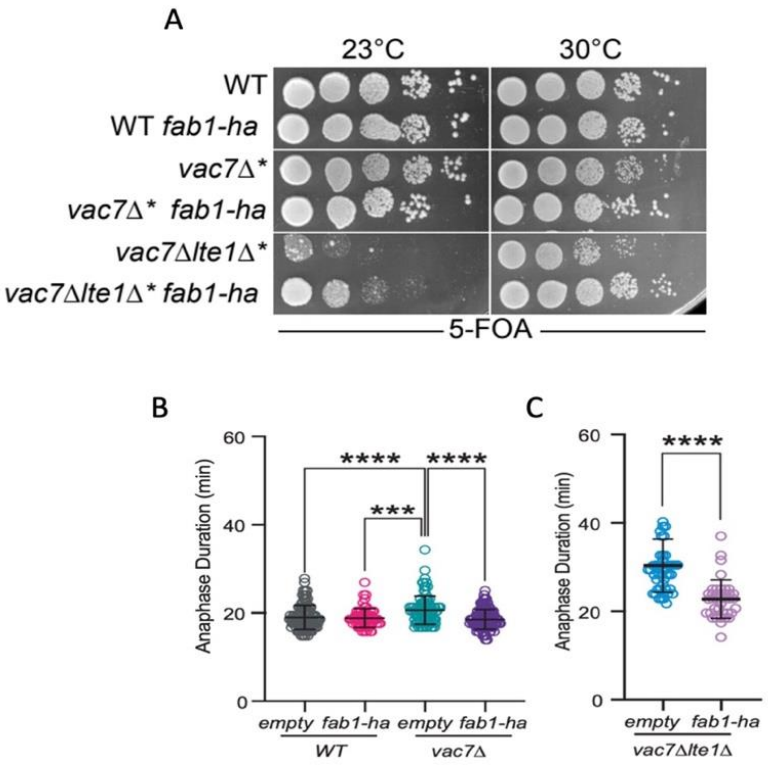

Figure 3.3. Hyperactive *FAB1* allele (*fab1-ha*) rescues *lte1*Δ *vac7*Δ growth lethality and anaphase delay. Synthetic lethality of *lte1*Δ*vac7*Δ is rescued by addition of *fab1-ha*. *vac7*Δ* and *lte1*Δ* indicates that the strain contains pRS416-*VAC7* and pRS316-*LTE1* respectively. Indicated strains in SEY228, SEY250, SEY214, SEY213, SEY230 and SEY162; **(A)** *fab1-ha* rescues anaphase delay of *vac7*Δ **(B)** and *lte1*Δ *vac7*Δ **(C)**. Anaphase duration of indicated strains (SEY258, SEY259, SEY264, SEY260, SEY149, SEY143) was calculated and plotted. Ordinary one-way ANOVA was performed with Tukey's multiple comparison test. *** $p<0.001$, **** $p<0.0001$

3.5 Overproduction of PI(3,5)P2 rescues cold sensitivity of lte1Δ via Atg18

Atg18 is a known effector protein of PI(3,5)P2 (Obara et al., 2008). We were curious to determine whether PI(3,5)P2 drives mitotic exit of *lte1*Δ cells through the PI(3,5)P2 binding protein Atg18. To understand this, we examined strains used in Figure 3.4A, both with and without Atg18. Our findings revealed that Atg18 is necessary for this rescue (Figure 3.4C). This suggests that PI(3,5)P2 functions through Atg18 to facilitate the exit of mitotic exit-defective cells from mitosis.

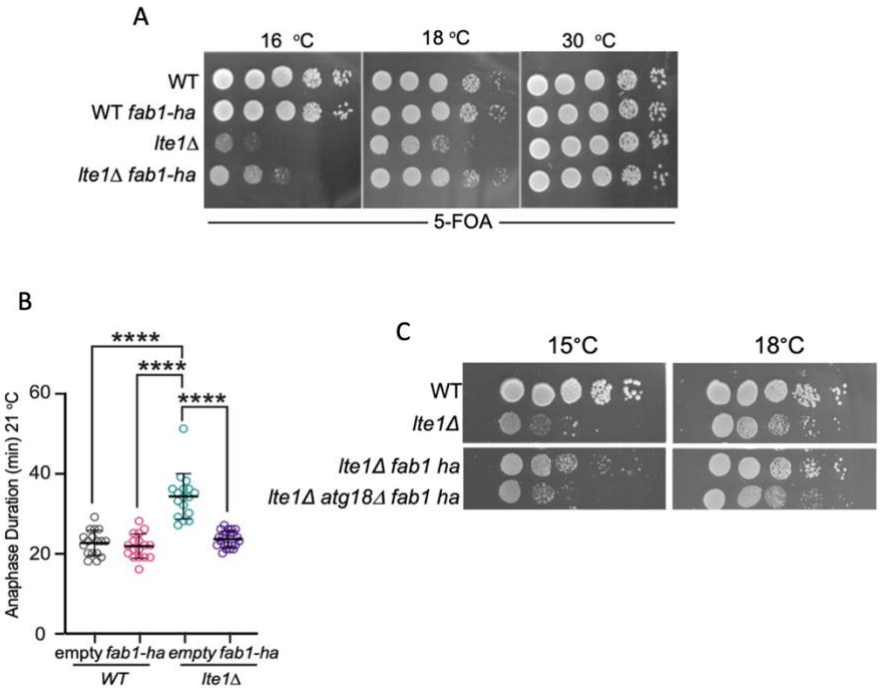

Figure 3.4. Hyperactive Fab1 (*fab1-ha*) rescues mitotic exit of *lte1Δ* cells through Atg18. **(A)** *fab1-ha* rescues cold sensitivity of *lte1*Δ at 18°C and 16°C. WT(SEY228), WT *fab1-ha* (SEY250), *lte1*Δ (SEY215), and *lte1*Δ *fab1- ha* (SEY216). **(B).** Anaphase delay of *lte1*Δ is rescued by the addition of *fab1-ha* at 21°C. (n>80, 3 independent experiments each, P<0.0001). WT(SEY258), WT *fab1-ha* (SEY259), *lte1*Δ (SEY262), and *lte1*Δ *fab1-ha* (SEY261). **(C).** Atg18 is required for growth rescue of *lte1*Δ by *fab1-ha***.**

3.6 Kin4 localization is changed by increased level of PI(3,5)P2

Under normal conditions, Kin4 exhibits asymmetric localization, accumulating predominantly at the daughter spindle pole body (SPB) to aid in establishing proper spindle positioning and orientation (D'Aquino et al., 2005). However, in the absence of Lte1, Kin4 localized on both daughter and mother SPB (Bertazzi et al., 2011). We wondered if introducing *fab1-ha* could rescue the cold sensitivity of *lte1*Δ by affecting Kin4 SPB localization. For this we quantified Kin4 localization at the SPBs of *lte1*Δ and *fab1-ha* bearing *lte1*Δ. As expected, during anaphase, Kin4 localized on both SPBs in *lte1*Δ cells (Figure 3.5A-3.5B). Kin4 SPB localization in *fab1-ha* expressing *lte1*Δ cells was not different than that in *lte1*Δ cells (Figure 3.5A-B). However, surprisingly, we discovered that Kin4 localizes to vesicle-like structures in the cytoplasm of *lte1*Δ in response to *fab1-ha* expression (Figure 3.5A, 3.5C). We conclude that whereas the localization of Kin4 at the spindle pole body (SPB) remains unchanged, the subcellular localization of Kin4 undergoes a transition to vesicle-like structure(s) following the introduction of *fab1-ha*.

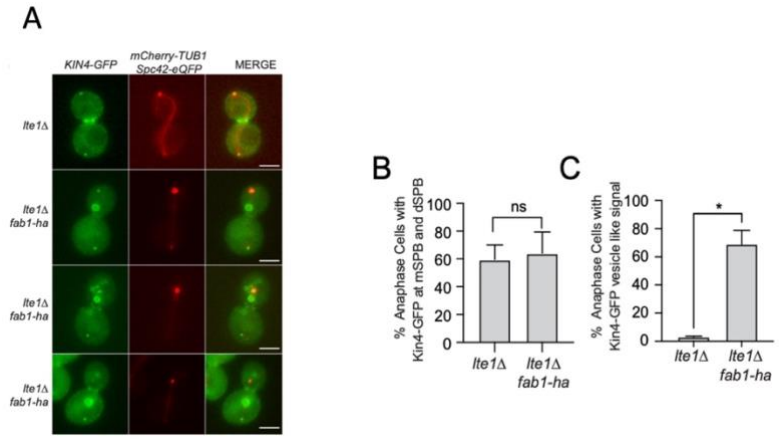

Figure 3.5. Kin4 locates to vesicle-like structures upon *fab1-ha* expression. **(A)** Representative still images of cells that *KIN4* localizes to vesicles by adding *fab1-ha* in the absence of *LTE1*. *KIN4* is seen in green, mCherry used as a tubulin marker and *SPC42* for SPB; both are in red. **(B-C)** Percentages of anaphase cells where *KIN4* is seen at both spindle pole bodies (B) and on vesicle-like structures (C) with or without *fab1 ha* addition in *lte1*Δ**.** Columns show the mean of 3 independent experiments. Error bars are standard deviation. Scale bars are 3µm.

Chapter 4
DISCUSSION

Phosphoinositides are evolutionarily conserved signaling lipids that are crucial for recruiting effector proteins to specific cellular membrane locations (McCartney et al., 2014). Although they constitute a relatively small proportion (approximately 10–20%) of total cellular phospholipids compared to more abundant counterparts like phosphatidylcholine and phosphatidylethanolamine, phosphatidylinositols play an indispensable role in various cellular processes (J. Hasegawa et al., 2017).

PI(3,5)P2, one of the seven phosphatidylinositols, is synthesized on vacuole/lysosome membranes through the phosphorylation of phosphatidylinositol-3-phosphate (PI3P) by the Fab1 kinase (Jin et al., 2016). The levels of PI(3,5)P2, as well as its precursor PI3P dynamically change in response to specific stresses such as osmotic stress (Jonathan D. Gary et al., 2002). In response to the osmotic shock in yeast, PI(3,5)P2 levels are increased at 5-10 minutes after the osmotic exposure (Jin et al., 2016). This rapid elevation is mediated by the Fab1 kinase and involves regulatory proteins within the Fab1 complex, including Vac7, Vac14 and Fig4. While several roles have been attributed to PI(3,5)P2, its role in mitotic exit remains unknown.

The findings presented in this thesis shed light on the pivotal role of PI(3,5)P2 in regulating mitotic exit, emphasizing its significance in coordinating cellular processes essential for cell division. Through elucidating the interactions between PI(3,5)P2 and key proteins such as Atg18 and Kin4, this thesis work provides valuable insights into the mechanisms underlying mitotic exit regulation. The interaction between PI(3,5)P2 and Atg18 emerges as a critical determinant in promoting mitotic exit. Atg18, as a PI(3,5)P2 binding protein, likely facilitates the localization and function of PI(3,5)P2 in the context of mitotic exit regulation. The dependency of *fab1-ha* driven Kin4 vacuole recruitment on Atg18 underscores the significance of this interaction, suggesting that Atg18 acts as a mediator in the process of PI(3,5)P2 mediated regulation of Kin4 localization (Figure 4.1). Elevated PI(3,5)P2 levels, as observed in *fab1-ha* cells, causes Kin4 localization at the vacuole periphery, highlighting the importance of maintaining appropriate PI(3,5)P2 levels for proper Kin4 localization and consequently, efficient mitotic exit (Huda et al., 2023). Conversely, the absence of PI(3,5)P2 in *vac7Δ* cells also perturbs Kin4 localization (Huda et al., 2023). The disruption of Kin4's asymmetric distribution in both *fab1-ha* and *vac7Δ* cells suggests that PI(3,5)P2 plays a crucial role in establishing and maintaining this asymmetry. This observation shows the significance of PI(3,5)P2 mediated regulation in coordinating mitotic exit events between mother and daughter cells, ensuring proper cell division. How PI(3,5)P2 affect Kin4 localizations may have several answers. PI(3,5)P2 might assist in retaining Kin4 within the mother cell by promoting its association with specific cellular membranes or structures. Since Kin4 is primarily localized to vacuolar membranes and the cortex of the mother cell, PI(3,5)P2 could play a role in tethering Kin4 to these locations. PI(3,5)P2 may also contribute to excluding Kin4 from the daughter cell. This could involve mechanisms such as preventing Kin4 from associating with membranes or structures specific to the daughter cell or promoting its removal from these locations.

PI(3,5)P2 may also regulate the association of Atg18 with membranes or structures, thereby influencing its interaction with Kin4 and modulating Kin4 localization. PI(3,5)P2 is known to play roles in membrane trafficking, endosome recycling, and protein sorting. These processes may indirectly affect Kin4 localization by influencing the dynamics of membrane-bound compartments or protein complexes involved in Kin4 distribution. The exact mechanism by which PI(3,5)P2 affects Kin4 localization remains unknown, but it likely involves a complex interplay between PI(3,5)P2, Atg18, cellular membranes, and other regulatory factors involved in cell division and membrane dynamics.

In budding yeast, vacuole segregation occurs prior to the segregation of the nucleus to the daughter cell, indicating its importance in cell cycle progression (Weisman, 2003). Intriguingly, mutants with blocked vacuole segregation can still divide, but the resulting daughter cell lacking a vacuole spends more time in G1 before entering the cell cycle. This delay suggests a regulatory role for vacuole and PI(3,5)P2 in the G1/S transition, highlighting their significance in cell cycle entry (J. Hasegawa et al., 2017). In this study we also demonstrate that, PI(3,5)P2 dependent mechanisms promote mitotic exit (M/G1 transition) (Huda et al., 2023) We propose that the control of mitotic exit by PI(3,5)P2 may serve as a means to coordinate vacuole segregation with mitotic exit. Speculate that the absence of vacuole segregation and consequently the lack of PI(3,5)P2 in the daughter cell compartment could delay mitotic exit, providing cells with additional time to complete vacuole segregation before exiting mitosis. However, the observation that cells can complete cell division in the absence of vacuole segregation suggests that this delay may not entirely guarantee the completion of vacuole segregation before mitotic exit. Therefore, a more detailed analysis of the timing of mitotic exit and vacuole segregation is warranted to ascertain the existence and extent of communication between these processes.

Fab1 inhibitors are used in therapeutic strategies against cancer (Hou et al., 2019). The rationale behind this lies in the understanding that genetically unstable tumor cells often exhibit aberrant cell cycle regulation, including dysregulated mitotic exit. Studies show that inhibitors of PIKfyve cause cytoplasmic vacuolation in dividing cells, including cancer cells (Ikonomov et al., 2019). However, while this vacuolation occurs in all cells, cancer cells are more susceptible to non-apoptotic death due to excessive vacuolation induced by these inhibitors (Ikonomov et al., 2019). PIKfyve has also been implicated in viral entry and infection for certain viruses, including Ebola, Marburg, and SARS-CoV-2. Inhibition of PIKfyve activity prevents viral infection of cultured cells, making it a potential antiviral agent against these pathogens (Rivero-Ríos & Weisman, 2022). Genetic and pharmacological studies demonstrated that deletion of PIKfyve or treatment with apilimod, a specific PIKfyve inhibitor, enhanced the function of dendritic cells. This enhancement was achieved by selectively altering the alternate/non-canonical NF-κB pathway, a signaling pathway involved in immune responses (Jae Eun et al., 2024). This suggests, PIKfyve negatively regulates dendritic cell function and that PIKfyve inhibition can enhance immune responses, potentially improving the efficacy of immunotherapy and vaccine-based treatment strategies (Jae Eun et al., 2024). PI(3,5)P2 dysfunction has been also linked to certain neurological disorders, such as Parkinson’s disease and Alzheimer’s disease. Our work establishing a link between asymmetric cell division through disruption of asymmetric protein distribution may

bring new concepts that could be applicable to other asymmetric cells or asymmetric cell divisions including neuronal cell division and synaptic function, potentially contributing to the pathogenesis of these disorders.

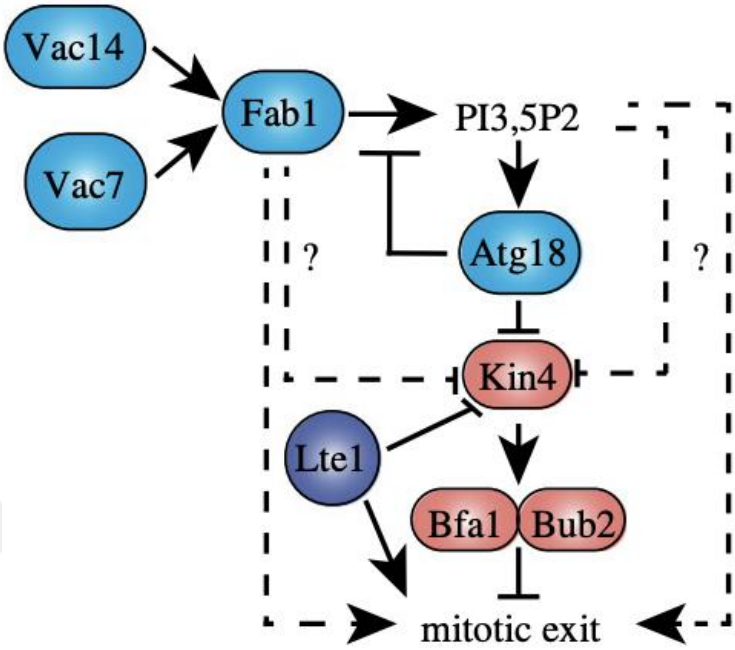

Figure 4.1. Model shows PI(3,5)P2 controls mitotic exit. Lines with arrow heads barbed ends indicate positive and negative regulation respectively. Dashed lines show possible scenarios of Atg18-independent mechanisms. (Huda et al., 2023)

APPENDIX

Table of Strains

Table 5.1: Strains used in this study

Strain Name	**Descriptions**	**Source**
SEY025-2	*MATa ura3-52 his3Δ200 leu2Δ1 lte1Δ::kanMX6 pTH17 (pRS316-LTE1) vac7Δ::hphNT1*	*This study, (Huda et al., 2023)*
SEY026-1	*MATa ura3-52 his3Δ200 leu2Δ1 lte1Δ::kanMX6 pTH17 (pRS316-LTE1) vac14Δ::hphNT1*	*This study, (*Huda et al., 2023*)*
SEY034-2	*MATa his3Δ200 leu2Δ1 lte1Δ::kanMX6 vac7Δ::hphNT1 ura3-52::URA3-GFP-TUB1*	*This study (*Huda et al., 2023*)*
SEY036-1	*MATa ura3-52 his3Δ200 leu2Δ1 lte1Δ::kanMX6 ura3::URA3-GFP-TUB1*	*This study, (*Huda et al., 2023*)*
SEY037-1	*MATa leu2Δ1 his3Δ200 trp1Δ63 ura3-52::URA3-GFP-TUB1*	*This study, (*Huda et al., 2023*)*
SEY040-1	*MATa ura3-52 his3Δ200 leu2Δ1 lte1Δ::kanMX6 pTH17 (pRS316-LTE1) vac7Δ::hphNT1 bfa1Δ::natNT2*	*This study, (*Huda et al., 2023*)*
SEY075-1	*MATa ura3-52 his3Δ200 leu2Δ1 lte1Δ::kanMX6 pTH17 (pRS316-LTE1) vac7Δ::hphNT1*	*This study, (*Huda et al., 2023*)*
SEY080-1	*MATa ura3-52 his3Δ200 leu2Δ1 lte1Δ::kanMX6 pTH17 (pRS316-LTE1) vac7Δ::hphNT1 kin4Δ::his3MX6*	*This study, (*Huda et al., 2023*)*
SEY115-1	*MATa ura3-52 his3Δ200 leu2Δ1 lte1Δ::kanMX6 vac7Δ::hphNT1 ura3::URA3-GFP-TUB1 bfa1Δ::his3MX6*	*This study, (*Huda et al., 2023*)*
SEY128	*MATa fab1-2 his3 leu2 ura3 gal1 VPH1-3xmCherry-kanMX6.*	*This study, (*Huda et al.,

		2023*)*
SEY143-1	*MATa his3Δ200 lte1Δ::kanMX6 vac7Δ::hphNT1 ura3-52::URA3-GFP-TUB1 leu2Δ1::LEU2-fab1-ha*	*This study, (*Huda et al., 2023*)*
SEY149	*MATa his3Δ200 lte1Δ::kanMX6 vac7Δ::hphNT1 ura3-52::URA3-GFP-TUB1 leu2Δ1::LEU2*	*This study, (*Huda et al., 2023*)*
SEY162	*MATa ura3-52 his3Δ200 lte1Δ::kanMX6 pTH17 (pRS316-LTE1) vac7Δ::hphNT1 leu2Δ1::LEU2-fab1-ha*	*This study, (*Huda et al., 2023*)*
SEY199-1	*MATa fab1-2 his3 leu2 ura3 gal1 lte1Δ::his3MX6*	*This study, (*Huda et al., 2023*)*
SEY202-1	*MATa leu2 ura3 his3 gal1 lte1Δ::his3MX6.*	*This study, (*Huda et al., 2023*)*
SEY213	*MATa ura3-52 his3Δ200 trp1Δ63 vac7::his3MX6 leu2Δ1::LEU2-fab1-ha*	*This study, (*Huda et al., 2023*)*
SEY214	*MATa ura3-52 his3Δ200 trp1Δ63 vac7::his3MX6 leu2Δ1::LEU2*	*This study, (*Huda et al., 2023*)*
SEY215	*MATa ura3-52 his3Δ200 lte1Δ::kanMX6 pTH17 (pRS316-LTE1) leu2Δ1::LEU2*	*This study, (*Huda et al., 2023*)*
SEY216	*MATa ura3-52 his3Δ200 lte1Δ::kanMX6 pTH17 (pRS316-LTE1) leu2Δ1::LEU2-fab1-ha*	*This study, (*Huda et al., 2023*)*
SEY228-1	*MATa ura3-52 his3Δ200 trp1Δ63 leu2Δ1::LEU2*	*This study, (*Huda et al., 2023*)*
SEY230-1	*MATa ura3-52 his3Δ200 lte1Δ::kanMX6 pTH17 (pRS316-LTE1) vac7Δ::hphNT1 leu2Δ1::LEU2*	*This study, (*Huda et al., 2023*)*
SEY231-1	*MATa his3Δ200 leu2Δ1 ura3-52::URA3-GFP-TUB1 VPH1-3XmCherry-natNT2 lte1Δ::kanMX6 vac7Δ::hphNT1*	*This study, (*Huda et al., 2023*)*
SEY239-1	*MATa leu2Δ1 his3Δ200 trp1Δ63 ura3-52::URA3-GFP-*	*This study, (*Huda et al.,

	TUB1 VPH1-3XmCherry-kanMX6 lte1Δ::hphNT1	2023*)*
SEY250-1	*MATa ura3-52 his3Δ200 trp1Δ63 leu2Δ1::LEU2-fab1-ha*	*This study, (*Huda et al., 2023*)*
SEY254-1	*MATa ura3-52 leu2Δ1 his3Δ200 trp1Δ63 pRS416-VAC7 vac7Δ::his3MX6*	*This study, (*Huda et al., 2023*)*
SEY256-1	*MATa leu2Δ1 his3Δ200 trp1Δ63 ura3-52::URA3-GFP-TUB1 VPH1-3XmCherry-kanMX6 vac7Δ::klTRP1*	*This study, (*Huda et al., 2023*)*
SEY258-1	*MATa ura3-52 his3Δ200 trp1Δ63 ura3::URA3-GFP-TUB1 leu2Δ1::LEU2*	*This study, (*Huda et al., 2023*)*
SEY259-1	*MATa ura3-52 his3Δ200 trp1Δ63 ura3::URA3-GFP-TUB1 leu2Δ1::LEU2-fab1-ha*	*This study, (*Huda et al., 2023*)*
SEY260-1	*MATa ura3-52 his3Δ200 trp1Δ63 ura3::URA3-GFP-TUB1 vac7Δ::klTRP1 leu2Δ1::LEU2-fab1-ha*	*This study, (*Huda et al., 2023*)*
SEY261	*MATa his3Δ200 lte1Δ::kanMX6 ura3-52::URA3-GFP-TUB1 leu2Δ1::LEU2-fab1-ha*	*This study, (*Huda et al., 2023*)*
SEY262-1	*MATa ura3-52 his3Δ200 lte1Δ::kanMX6 ura3::URA3-GFP-TUB1 leu2Δ1::LEU2*	*This study, (*Huda et al., 2023*)*
SEY264-1	*MATa ura3-52 his3Δ200 trp1Δ63 ura3::URA3-GFP-TUB1 vac7Δ::klTRP1 leu2Δ1::LEU2*	*This study, (*Huda et al., 2023*)*
SEY267	*MATa ura3-52 his3Δ200 KIN4-GFP-his3MX6 SPC42-eqFP-natNT2 lte1Δ::ura3 Cherry-TUB1-klTRP::trp1Δ63 leu2Δ1::LEU2-fab1-ha*	*This study, (*Huda et al., 2023*)*
SEY023-2	*MATa ura3-52 leu2Δ1 his3Δ200 trp1Δ63 vac7Δ::hphNT1*	*This study, (*Huda et al., 2023*)*
SEY024-1	*MATa ura3-52 leu2Δ1 his3Δ200 trp1Δ63 vac14Δ::hphNT1*	*This study, (*Huda et al., 2023*)*
ESM356-1	*MATa ura3-52 leu2Δ1 his3Δ200 trp1Δ63*	*(Pereira et*

		al., 2001)
YPH499	*MATa ura3-52 lys2-801amber ade2-101ochre trp1Δ63 his3Δ200 leu2Δ1*	*(Sikorski & Hieter, 1989)*
FAY145	*MATa ura3-52 his3Δ200 leu2Δ1 lte1Δ::kanMX6 pTH17 (pRS316-LTE1)*	*(Bertazzi et al., 2011)*
4506-9-4-2	*MATa leu2 ura3 his3 gal1*	*(*Yamamoto et al., 1995*)*
672-5-2-2	*MATa fab1-2 his3 leu2 ura3 gal1*	*(*Yamamoto et al., 1995*)*
BBY024-1	*MATa leu2Δ1 his3Δ200 trp1Δ63 ura3-52::URA3-GFP-TUB1 vac7Δ::klTRP1*	*(*Huda et al., 2023*), BEKDAŞ, B. (2023). [Master Thesis].*
AKY4016-1	*MATa ura3-52 leu2Δ1 his3Δ200 KIN4-GFP-his3MX6 SPC42-eqFP-natNT2 lte1Δ::ura3 mCherry-TUB1-klTRP::trp1Δ63*	*This study, (*Huda et al., 2023*)*
AKY4109-1	*MATa his3Δ200 trp1Δ63 KIN4-GFP-his3MX6 SPC42-eqFP-natNT2 ura3-52::URA3-mCherry-TUB1 leu2Δ1::LEU2*	*This study, (*Huda et al., 2023*)*
AKY4110-1	*MATa his3Δ200 trp1Δ63 KIN4-GFP*	*This study, (*Huda et al., 2023*)*
AKY4111	*MATa KIN4-GFP-his3MX6 SPC42-eqFP-natNT2 ura3-52::URA3-mCherry-TUB1 vac7Δ::klTRP1*	*This study, (*Huda et al., 2023*)*
AKY4005	*MATa his3Δ200 trp1Δ63 KIN4-GFP-his3MX6 SPC42-eqFP-natNT2 ura3-52::URA3-mCherry-TUB1*	*This study, (*Huda et al., 2023*)*
SEY042	*SEY038-1 (SEY030 (ESM356 ((Spore 2.1) MATa ura3-52 leu2Δ1 his3Δ200 trp1Δ63., fab1Δ::hphNT2) VPH-GFP-HIS3MX6 + PSE001-1 Selected on sc- leu plates*	*This study*
SEY043	*SEY038-1 (SEY030 (ESM356 ((Spore 2.1) MATa ura3-52 leu2Δ1 his3Δ200 trp1Δ63., fab1Δ::hphNT2) VPH-GFP-HIS3MX6 + PRS315-1 Selected on sc-leu plates*	*This study*
SEY044	*SEY033-1 (ESM 356 VPH-GFP-HIS3MX6) +PSE001-1 Selected on sc-leu plates*	*This study*

SEY045	*SEY033-1 (ESM 356 VPH-GFP-HIS3MX6) +PRS315-1 Selected on sc-leu plates*	*This study*
SEY046	*SEY033-1(ESM 356 VPH-GFP-HIS3MX6) + PSE002-1 (fab1 hyperactive mutant) selected on sc-leu plates.*	*This study*
SEY061	*SEY051-1 (SEY023-2 (ESM356 vac7Δ::hphNT2) VPH1-GFP-his3mx6 + PSE001-1 Selected on sc-leu*	*This study*
SEY060	*SEY051-1 (SEY023-2 (ESM356 vac7Δ::hphNT2) VPH1-GFP-his3mx6) + PRS315 Selected on sc-leu*	*This study*
SEY062	*SEY051-1 (SEY023-2 (ESM356 vac7Δ::hphNT2) VPH1-GFP-his3mx6 +PSE002-1 Selected on sc-leu*	*This study*
SEY047	*SEY038-1(SEY030(ESM356 ((Spore 2.1) MATa ura3-52 leu2Δ1 his3Δ200 trp1Δ63., fab1Δ::hphNT2) VPH-GFP-HIS3MX6) + PSE002-1 (fab1 hyperactive mutant) selected on sc-leu plates.*	*This study*

Table of Primers

Table 5.2: Primers used in this study

Primer Name	**Sequence**
VAC14-S2	CAGGTCCATTTCTTAACCAAAGATGCTTTCAATCAGGTAATGGGTAGTTAATCGATGAATTCGAGCTCG
VAC14-S1	TTGATGCTGCTGTGCTTATCTGCTCAGGCTACAACAGGAACTGGAACATGCGTACGCTGCAGGTCGAC
VAC7-2	ACTATCGCTTCCGCTACTA
VAC7-1	TGTAAGTCTTCCTGGCCAC
VAC7-S2	AAAAAGAAAAATACCCAGCTTTGACGAAAAAGCTACATTCTTAACACTCAATCGATGAATTCGAGCTCG
VAC7-S1	TTATCGTTTCATCTCAGGCAAGTTAAAGCATTTGGGAAACGTGCTAGATGCGTACGCTGCAGGTCGAC
Bfa1-S1	TGCGTACGCTGCAGGTCGACAGAAAAAAGTTCGAAAACTTTTGTAGCAGTTGAAAGTTTTGTATGCTA
Bfa1-S2	TGTACTCAAGATAACGGTAAAGAAACAGTTATAAGAAGGCTAAAGGGCTAATCGATGAATTCGAGCTCG
BFA1-1	GTGATTCAAATGTTGGGTGAGC
BFA1-2	CGAGTTTTAATCCATTCCACCC
S1-Kin4	TCGCATAATATTCTATCAGGACATTCCGTATACCTGAATATATATACATGCGTACGCTGCAGGTCGAC
S2-Kin4	CACTCTATAATATAATGTAATTGTCGATATAACTATGTACTGAAAACTCAATCGATGAATTCGAGCTCG
Kin4-Col1	AATCGCATCGGTGGGAGAG
Kin4-Col2	AACAACTTGCCAGCCAAGAC
FAB1-S1	AATAGCAAGGTAGCTTCCATCCTGTACATGCAAGACCGTCACACAGCATGcgtacgctgcaggtcgac
FAB1-S2	AGTGTATAAAAAAAAGTTACAGAATATAACTTGTACACGTTTATGTATTAatcgatgaattcgagctcg

FAB1-xhoI-fw	ccgctcgagACGCTAGACCAATTAGTCGC
FAB1-SacII-rev	tctccgcggCAGTGGCCGAGTGGTTAAG
Lte1-S1	TTGCTTTACATAGCCTCTAGCCATTCAAAGATTCGCTACCCTGAACCATGcgtacgctgcaggtcgac
Lte1-S2	TTTTTTACAAGAGGAATTTGGGAACTGGAGGAAAGTGGCACAATACCTCAatcgatgaattcgagctcg
Lte1-Col1	GAAGCATGAATTAAGATCATCG
Lte1-Col2	CCGTTGTAGTTATGTACTGAAG
VPH1-S2	TTAATGAAGTACTTAAATGTTTCGCTTTTTTTAAAAGTCCTCAAAATTTAatcgatgaattcgagctcg
VPH1-S3	ATAAAGACATGGAAGTCGCTGTTGCTAGTGCAAGCTCTTCCGCTTCAAGCcgtacgctgcaggtcgac
Fab1-seq1	GACGCAGTTGATGAACCGC
Fab1-seq2	ACCTGCGCAGGTTCGAATC
Pbs2-S1	TAGATACATTATTATATTAAGCAGATCGAGACGTTAATTTCTCAAAGATGcgtacgctgcaggtcgac
Pbs2-S2	TTGTTGTTATATTCACGTGCCTGTTTGCTTTTATTTGGATATTAACGCTAatcgatgaattcgagctcg
Pbs2-Col1	TCCAGACATCAACGTCATAC
Pbs2-Col2	TATATTGACGTCCACATCGC
ATG18-S1	AATAGTGTTCCAGTTAACTCTGTATCCTTTTCTTCTTCGGCCTGACAATGcgtacgctgcaggtcgac
ATG18-S2	GTGTATGCGTTGTGACGTACGGAAGGCAGCGCGAGACACTTCCGTGATCAatcgatgaattcgagctcg
ATG18-1	ATATGCATAAGCACTGACTC
ATG18-2	GTAACGTCACTCCAGTGATC
FAB1-T2250A-	CCTACCGTTGTTGCACCAAGACAATAT

Fw	
FAB1-T2250A-Rev	ATATTGTCTTGGTGCAACAACGGTAGG
FAB1-E1822V-Rev	ACTCCACAACCTGTAAAATCATTATTG
FAB1-F1833L-Fw	ACCTTGAGCAACCTTTGGGCAGATCGA
FAB1-F1833L-Rev	TCGATCTGCCCAAAGGTTGCTCAAGGT

Table of Plasmids

Table 5.3: Plasmids used in this study

Plasmid Name	**Descriptions**	**Source**
pRS416-*VAC7*	pRS416-*VAC7*	(Jin et al., 2008)
pAFS125-*GFP-TUB1*	*GFP-TUB1* in a *URA3* -based integration vector	(Straight et al., 1997)
pRS305	*LEU2*-based integration vector	(Sikorski & Hieter, 1989)
pRS315	*LEU2*-based CEN plasmid	(Sikorski & Hieter, 1989)
pSE001	pRS315-*FAB1*	This study
pSE002	pRS315- *fab1*(T2250A, E1822V , F1833L)	This study
pSE003	pRS305-*fab1*(T2250A, E1822V , F1833L)	This study, (Huda et al., 2023)
pAK010	*mCherry-TUB1-klTRP1* containing integration plasmid.	(Khmelinskii et al., 2007)
pAK011	*mCherry-TUB1-URA3* containing integration plasmid	(Khmelinskii et al., 2007)
pSM903-4	pRS316-*LTE1*	(Höfken & Schiebel, 2002)
pRS316	*URA3-dependent CEN-based yeast-E. coli* shuffle plasmid. *AmpR.*	(Sikorski & Hieter, 1989)

Buffers, Reagents and Compositions

Table 5.4: Compositions of buffer and reagents used in this study

10X PCR Buffer	500mM Tris-HCl pH: 9.2 (Sigma, #T1503), 160mM (NH4)2SO4, 17.5mM MgCl2 (Fisher BioReagents, #BP214)
2mM dNTPs mix	20 µL of dATP (100 mM), 20 µL dCTP (100 mM), 20 µL dTTP (100 mM) and 20 µL dGTP (100 mM), 920 µL dH_2O
LiPEG	100mM LiOAc (Sigma, #L6883), 10mM Tris pH: 8.0, 1mM EDTA pH 8.0, 40% PEG3350 (Sigma, #P4338) dH_2O to complete the desired volume. Filter to sterilize.
LiSORB	100mM Lithium Acetate (LiOAc), 10mM Tris pH: 8.0, 1mM EDTA pH: 8.0, 1M Sorbitol (Merck, #107758), dH_2O to complete the desired volume. Filter to sterilize
P1 Buffer	50mM Tris-HCl pH:8.0, 10mM EDTA pH 8.0, 0.1 mg/mL RNase A
P2 Buffer	200mM NaOH, 1% SDS
P3 Buffer	3M KAc pH: 5.5
1XPBS	137mM NaCl, 2.7mM KCl (Merck, #104936), 10mM Na2HPO4 (Merck, #106575), 1.76mM KH2PO4 (Fisher BioReagents, #BP362). Adjust pH to 7.2-7.4
1XTAE	4.84 g of Tris, 1.14 mL of Glacial acetic acid (Isolab, #901016), 2 mL of 0.5M EDTA pH:8.0 (Sigma, #E5134), ddH2O up to 1000 mL.
Colony PCR lysis buffer	0.01% sarkosyl in 0.02M NaOH

Media/Agar and Compositions

Table 5.5: Media, agar and their compositions

Name	**Description**
TY agar with selective antibiotics (Ampicillin or Kanamycin)	5 g of NaCl (Merck, #106498), 5 g of Yeast Extract (Conda, #1702), 10 g of Tryptone (Biolife, #4122902), 20 g of Agar (Carl Roth, #5210.2), dH_2O up to 1000 mL. 100 µg/mL Ampicillin or 50 Kanamycin µg/mL
SC-X (X= URA, LEU, HIS or TRP)	3.4 g of Bacto Yeast Nitrogen Base (YNB) without amino acids with ammonium sulfate, 1 g of SC-X dropout amino acid mix, 10 g of D-(+)-Glucose, 0.05 g of Adenine hemisulfate salt (Sigma # A9126), dH_2O up to 500 mL
SC-X with selective antibiotics (Geneticin, Nourseothricin, or Hygromycin)	1.7 g of Yeast Nitrogen Base without amino acids without ammonium sulfate (Conda, #1553), 1 g of monosodium glutamic acid, 2 g of dropout amino acid mix, 20 g of D-(+)-Glucose, 20 g of Agar, dH_2O up to 500 mL were mixed and autoclaved, then mixed with 20 g of sterile agar in 500 mL dH_2O. 200 mg/L G418, 100 mg/L Nourseothricin or 300 mg/L Hygromycin into autoclaved agar
TY agar	5 g of NaCl, 5 g of Yeast Extract, 10 g of Tryptone, 20 g of Agar, dH_2O up to 1000 mL
YPD with selective antibiotics (Geneticin, Nourseothricin, or Hygromycin)	10 g of Yeast Extract, 20 g of Peptone, 20 g of D-(+)-Glucose, 20 g of Agar, dH_2O up to 1000 mL. 200 mg/L G418, 100 mg/L Nourseothricin or 300 mg/L Hygromycin in autoclaved agar
TY medium	5 g of NaCl, 5 g of Yeast Extract, 10 g of Tryptone, dH_2O up to 1000 mL
TY medium with selective antibiotics (Ampicillin or	5 g of NaCl, 5 g of Yeast Extract, 10 g of Tryptone, dH_2O up to 1000 mL. 100 µg/mL Ampicillin or 50 Kanamycin µg/mL

Kanamycin)	
YPAD	5 g of Yeast Extract, 10 g of Peptone (Conda, #1616), 10 g of D-(+)-Glucose, 0.05 g of Adenine hemisulfate salt, dH_2O up to 500 mL
5-FOA agar	6.7 g of Yeast Nitrogen Base without amino acids with ammonium sulfate (Conda, #1545), 2 g of SC-URA dropout amino acid mix, 20 g of D-(+)-Glucose, 0.1 g of Uracil (Sigma, #U1128), 1 g of 5- Fluoroorotic acid (USbiological), dH_2O up to 500 mL were mixed and filter-sterilized, then mixed with 20 g of sterile agar in 500 mL dH_2O

BIBLIOGRAPHY

Adames, N. R., & Cooper, J. A. (2000). Microtubule interactions with the cell cortex causing nuclear movements in Saccharomyces cerevisiae. *J Cell Biol*, *149*(4), 863-874. https://doi.org/10.1083/jcb.149.4.863

Aerne, B. L., Johnson, A. L., Toyn, J. H., & Johnston, L. H. (1998). Swi5 Controls a Novel Wave of Cyclin Synthesis in Late Mitosis. *Molecular biology of the cell*, *9*(4), 945-956. https://doi.org/10.1091/mbc.9.4.945

Agarwal, R., & Cohen-Fix, O. (2002). Phosphorylation of the mitotic regulator Pds1/securin by Cdc28 is required for efficient nuclear localization of Esp1/separase. *Genes Dev*, *16*(11), 1371-1382. https://doi.org/10.1101/gad.971402

Akhmanova, A., & Steinmetz, M. O. (2015). Control of microtubule organization and dynamics: two ends in the limelight. *Nat Rev Mol Cell Biol*, *16*(12), 711-726. https://doi.org/10.1038/nrm4084

Alberts B, J. A., Lewis J. (2002). Molecular Biology of the Cell. 4th edition.

Baetz, K., & Andrews, B. (1999). Regulation of Cell Cycle Transcription Factor Swi4 through Auto-Inhibition of DNA Binding. *Molecular and Cellular Biology*, *19*(10), 6729-6741. https://doi.org/10.1128/MCB.19.10.6729

Bagur, R., & Hajnóczky, G. (2017). Intracellular Ca²⁺ Sensing: Its Role in Calcium Homeostasis and Signaling. *Molecular Cell*, *66*(6), 780-788. https://doi.org/10.1016/j.molcel.2017.05.028

Bai, J., Li, Y., & Zhang, G. (2017). Cell cycle regulation and anticancer drug discovery. *Cancer Biology and Medicine*, *14*(4), 348-362. https://doi.org/10.20892/j.issn.2095-3941.2017.0033

Balderhaar, H. J., & Ungermann, C. (2013). CORVET and HOPS tethering complexes - coordinators of endosome and lysosome fusion. *J Cell Sci*, *126*(Pt 6), 1307-1316. https://doi.org/10.1242/jcs.107805

Balla, T. (2013). Phosphoinositides: tiny lipids with giant impact on cell regulation. *Physiol Rev*, *93*(3), 1019-1137. https://doi.org/10.1152/physrev.00028.2012

Balla, T., Szentpetery, Z., & Kim, Y. J. (2009). Phosphoinositide signaling: new tools and insights. *Physiology (Bethesda)*, *24*, 231-244. https://doi.org/10.1152/physiol.00014.2009

Banerjee, S., Clapp, K., Tarsio, M., & Kane, P. M. (2019). Interaction of the late endo-lysosomal lipid PI(3,5)P2 with the Vph1 isoform of yeast V-ATPase increases its activity and cellular stress tolerance. *J Biol Chem*, *294*(23), 9161-9171. https://doi.org/10.1074/jbc.RA119.008552

Barberis, M., De Gioia, L., Ruzzene, M., Sarno, S., Coccetti, P., Fantucci, P., Vanoni, M., & Alberghina, L. (2005). The yeast cyclin-dependent kinase inhibitor Sic1 and mammalian p27Kip1 are functional homologues with a structurally conserved inhibitory domain. *Biochem J*, *387*(Pt 3), 639-647. https://doi.org/10.1042/bj20041299

Baro, B., Queralt, E., & Monje-Casas, F. (2017). Regulation of Mitotic Exit in Saccharomyces cerevisiae. *Methods Mol Biol*, *1505*, 3-17. https://doi.org/10.1007/978-1-4939-6502-1_1

Baskaran, S., Ragusa, Michael J., Boura, E., & Hurley, James H. (2012). Two-Site Recognition of Phosphatidylinositol 3-Phosphate by PROPPINs in Autophagy. *Molecular Cell*, *47*(3), 339-348. https://doi.org/https://doi.org/10.1016/j.molcel.2012.05.027

Bell, S. P., & Dutta, A. (2002). DNA replication in eukaryotic cells. *Annu Rev Biochem*, *71*, 333-374. https://doi.org/10.1146/annurev.biochem.71.110601.135425

Bell, S. P., & Labib, K. (2016). Chromosome Duplication in Saccharomyces cerevisiae. *Genetics*, *203*(3), 1027-1067. https://doi.org/10.1534/genetics.115.186452

Bergstralh, D. T., & St Johnston, D. (2014). Spindle orientation: What if it goes wrong? *Seminars in Cell & Developmental Biology*, *34*, 140-145. https://doi.org/https://doi.org/10.1016/j.semcdb.2014.06.014

Bertazzi, D. T., Kurtulmus, B., & Pereira, G. (2011). The cortical protein Lte1 promotes mitotic exit by inhibiting the spindle position checkpoint kinase Kin4. *J Cell Biol*, *193*(6), 1033-1048. https://doi.org/10.1083/jcb.201101056

Bloom, J., & Cross, F. R. (2007). Multiple levels of cyclin specificity in cell-cycle control. *Nat Rev Mol Cell Biol*, *8*(2), 149-160. https://doi.org/10.1038/nrm2105

Bonangelino, C. J., Catlett, N. L., & Weisman, L. S. (1997). Vac7p, a novel vacuolar protein, is required for normal vacuole inheritance and morphology. *Mol Cell Biol*, *17*(12), 6847-6858. https://doi.org/10.1128/mcb.17.12.6847

Bonangelino , C. J., Nau , J. J., Duex , J. E., Brinkman , M., Wurmser , A. E., Gary , J. D., Emr , S. D., & Weisman , L. S. (2002). Osmotic stress–induced increase of phosphatidylinositol 3,5-bisphosphate requires Vac14p, an activator of the lipid kinase Fab1p. *Journal of Cell Biology*, *156*(6), 1015-1028. https://doi.org/10.1083/jcb.200201002

Botchkarev, V. V., Jr., Garabedian, M. V., Lemos, B., Paulissen, E., & Haber, J. E. (2017). The budding yeast Polo-like kinase localizes to distinct populations at centrosomes during mitosis. *Mol Biol Cell*, *28*(8), 1011-1020. https://doi.org/10.1091/mbc.E16-05-0324

Botelho, R. J., Efe, J. A., Teis, D., & Emr, S. D. (2008). Assembly of a Fab1 phosphoinositide kinase signaling complex requires the Fig4 phosphoinositide phosphatase. *Mol Biol Cell*, *19*(10), 4273-4286. https://doi.org/10.1091/mbc.e08-04-0405

Botstein, D., & Fink, G. R. (2011). Yeast: An Experimental Organism for 21st Century Biology. *Genetics*, *189*(3), 695-704. https://doi.org/10.1534/genetics.111.130765

Burgess, D. R., & Chang, F. (2005). Site selection for the cleavage furrow at cytokinesis. *Trends Cell Biol*, *15*(3), 156-162. https://doi.org/10.1016/j.tcb.2005.01.006

Calzada, A., Sacristán, M., Sánchez, E., & Bueno, A. (2001). Cdc6 cooperates with Sic1 and Hct1 to inactivate mitotic cyclin-dependent kinases. *Nature*, *412*(6844), 355-358. https://doi.org/10.1038/35085610

Carvalho, P., Gupta, M. L., Jr., Hoyt, M. A., & Pellman, D. (2004). Cell cycle control of kinesin-mediated transport of Bik1 (CLIP-170) regulates microtubule stability and dynein activation. *Dev Cell*, *6*(6), 815-829. https://doi.org/10.1016/j.devcel.2004.05.001

Catlett, N. L., & Weisman, L. S. (1998). The terminal tail region of a yeast myosin-V mediates its attachment to vacuole membranes and sites of polarized growth. *Proc Natl Acad Sci U S A*, *95*(25), 14799-14804. https://doi.org/10.1073/pnas.95.25.14799

Caydasi, A. K., Khmelinskii, A., Duenas-Sanchez, R., Kurtulmus, B., Knop, M., & Pereira, G. (2017). Temporal and compartment-specific signals coordinate mitotic exit with spindle position. *Nat Commun*, *8*, 14129. https://doi.org/10.1038/ncomms14129

Caydasi, A. K., Kurtulmus, B., Orrico, M. I., Hofmann, A., Ibrahim, B., & Pereira, G. (2010). Elm1 kinase activates the spindle position checkpoint kinase Kin4. *J Cell Biol*, *190*(6), 975-989. https://doi.org/10.1083/jcb.201006151

Caydasi, A. K., Micoogullari, Y., Kurtulmus, B., Palani, S., & Pereira, G. (2014). The 14-3-3 protein Bmh1 functions in the spindle position checkpoint by breaking Bfa1 asymmetry at yeast centrosomes. *Mol Biol Cell*, *25*(14), 2143-2151. https://doi.org/10.1091/mbc.E14-04-0890

Caydasi, A. K., & Pereira, G. (2009). Spindle alignment regulates the dynamic association of checkpoint proteins with yeast spindle pole bodies. *Dev Cell*, *16*(1), 146-156. https://doi.org/10.1016/j.devcel.2008.10.013

Caydasi, A. K., & Pereira, G. (2012). SPOC alert—When chromosomes get the wrong direction. *Experimental Cell Research*, *318*(12), 1421-1427. https://doi.org/https://doi.org/10.1016/j.yexcr.2012.03.031

Chan, L. Y., & Amon, A. (2009). The protein phosphatase 2A functions in the spindle position checkpoint by regulating the checkpoint kinase Kin4. *Genes Dev*, *23*(14), 1639-1649. https://doi.org/10.1101/gad.1804609

Chan, L. Y., & Amon, A. (2010). Spindle position is coordinated with cell-cycle progression through establishment of mitotic exit-activating and -inhibitory zones. *Mol Cell*, *39*(3), 444-454. https://doi.org/10.1016/j.molcel.2010.07.032

Chen, Z., Malia, P. C., Hatakeyama, R., Nicastro, R., Hu, Z., Péli-Gulli, M.-P., Gao, J., Nishimura, T., Eskes, E., Stefan, C. J., Winderickx, J., Dengjel, J., De Virgilio, C., & Ungermann, C. (2021). TORC1 Determines Fab1 Lipid Kinase Function at Signaling Endosomes and Vacuoles. *Current Biology*, *31*(2), 297-309.e298. https://doi.org/https://doi.org/10.1016/j.cub.2020.10.026

Cooke, F. T., Dove, S. K., McEwen, R. K., Painter, G., Holmes, A. B., Hall, M. N., Michell, R. H., & Parker, P. J. (1998). The stress-activated phosphatidylinositol 3-phosphate 5-kinase Fab1p is essential for vacuole function in S. cerevisiae. *Current Biology*, *8*(22), S1-S2. https://doi.org/10.1016/S0960-9822(07)00513-1

Costanzo, M., Kuzmin, E., van Leeuwen, J., Mair, B., Moffat, J., Boone, C., & Andrews, B. (2019). Global Genetic Networks and the Genotype-to-Phenotype Relationship. *Cell*, *177*(1), 85-100. https://doi.org/10.1016/j.cell.2019.01.033

Crasta, K., & Surana, U. (2006). Disjunction of conjoined twins: Cdk1, Cdh1 and separation of centrosomes. *Cell Division*, *1*, 12. https://doi.org/10.1186/1747-1028-1-12

Cross, F. R., & Tinkelenberg, A. H. (1991). A potential positive feedback loop controlling CLN1 and CLN2 gene expression at the start of the yeast cell cycle. *Cell*, *65*(5), 875-883. https://doi.org/10.1016/0092-8674(91)90394-e

D'Aquino, K. E., Monje-Casas, F., Paulson, J., Reiser, V., Charles, G. M., Lai, L., Shokat, K. M., & Amon, A. (2005). The Protein Kinase Kin4 Inhibits Exit from Mitosis in Response to Spindle Position Defects. *Molecular Cell*, *19*(2), 223-234. https://doi.org/10.1016/j.molcel.2005.06.005

De Antoni, A., Pearson, C. G., Cimini, D., Canman, J. C., Sala, V., Nezi, L., Mapelli, M., Sironi, L., Faretta, M., Salmon, E. D., & Musacchio, A. (2005). The Mad1/Mad2 complex as a template for Mad2 activation in the spindle assembly checkpoint. *Curr Biol*, *15*(3), 214-225. https://doi.org/10.1016/j.cub.2005.01.038

de Bettignies, G., & Johnston, L. H. (2003). The mitotic exit network. *Current Biology*, *13*(8), R301.

De Craene, J.-O., Bertazzi, D. L., Bär, S., & Friant, S. (2017). Phosphoinositides, Major Actors in Membrane Trafficking and Lipid Signaling Pathways. *International Journal of Molecular Sciences*, *18*(3), 634. https://www.mdpi.com/1422-0067/18/3/634

De Matteis, M. A., Di Campli, A., & Godi, A. (2005). The role of the phosphoinositides at the Golgi complex. *Biochim Biophys Acta*, *1744*(3), 396-405. https://doi.org/10.1016/j.bbamcr.2005.04.013

Dewar, J. M., & Walter, J. C. (2017). Mechanisms of DNA replication termination. *Nature Reviews Molecular Cell Biology*, *18*(8), 507-516. https://doi.org/10.1038/nrm.2017.42

Di Paolo, G., & De Camilli, P. (2006). Phosphoinositides in cell regulation and membrane dynamics. *Nature*, *443*(7112), 651-657. https://doi.org/10.1038/nature05185

Dong, X.-P., Wang, X., & Xu, H. (2010). TRP channels of intracellular membranes. *Journal of Neurochemistry*, *113*(2), 313-328. https://doi.org/https://doi.org/10.1111/j.1471-4159.2010.06626.x

Dove, S. K., Dong, K., Kobayashi, T., Williams, F. K., & Michell, R. H. (2009). Phosphatidylinositol 3,5-bisphosphate and Fab1p/PIKfyve underPPIn endo-lysosome function. *Biochem J*, *419*(1), 1-13. https://doi.org/10.1042/bj20081950

Dove, S. K., McEwen, R. K., Mayes, A., Hughes, D. C., Beggs, J. D., & Michell, R. H. (2002). Vac14 controls PtdIns(3,5)P(2) synthesis and Fab1-dependent protein trafficking to the multivesicular body. *Curr Biol*, *12*(11), 885-893. https://doi.org/10.1016/s0960-9822(02)00891-6

Duex, J. E., Tang, F., & Weisman, L. S. (2006). The Vac14p-Fig4p complex acts independently of Vac7p and couples PI3,5P2 synthesis and turnover. *J Cell Biol*, *172*(5), 693-704. https://doi.org/10.1083/jcb.200512105

Er, E. E., Mendoza, M. C., Mackey, A. M., Rameh, L. E., & Blenis, J. (2013). AKT facilitates EGFR trafficking and degradation by phosphorylating and activating PIKfyve. *Sci Signal*, *6*(279), ra45. https://doi.org/10.1126/scisignal.2004015

Falk, J. E., Chan, L. Y., & Amon, A. (2011). Lte1 promotes mitotic exit by controlling the localization of the spindle position checkpoint kinase Kin4. *Proc Natl Acad Sci U S A*, *108*(31), 12584-12590. https://doi.org/10.1073/pnas.1107784108

Falk, J. E., Chan, L. Y., & Amon, A. (2011). Lte1 promotes mitotic exit by controlling the localization of the spindle position checkpoint kinase Kin4. *Proceedings of the National Academy of Sciences*, *108*(31), 12584-12590. https://doi.org/doi:10.1073/pnas.1107784108

Ferreira, L. T., & Maiato, H. (2021). Prometaphase. *Seminars in Cell & Developmental Biology*, *117*, 52-61. https://doi.org/https://doi.org/10.1016/j.semcdb.2021.06.004

Ferrell, James E., Jr. (2011). Simple Rules for Complex Processes: New Lessons from the Budding Yeast Cell Cycle. *Molecular Cell*, *43*(4), 497-500. https://doi.org/10.1016/j.molcel.2011.08.002

Fraschini, R. (2018). Divide Precisely and Proliferate Safely: Lessons From Budding Yeast. *Front Genet*, *9*, 738. https://doi.org/10.3389/fgene.2018.00738

Froelich, C. A., Kang, S., Epling, L. B., Bell, S. P., & Enemark, E. J. (2014). A conserved MCM single-stranded DNA binding element is essential for replication initiation. *Elife*, *3*, e01993. https://doi.org/10.7554/eLife.01993

Fu, J., Hagan, I. M., & Glover, D. M. (2015). The centrosome and its duplication cycle. *Cold Spring Harb Perspect Biol*, *7*(2), a015800. https://doi.org/10.1101/cshperspect.a015800

Gardner, M. K., Zanic, M., Gell, C., Bormuth, V., & Howard, J. (2011). Depolymerizing kinesins Kip3 and MCAK shape cellular microtubule architecture by differential control of catastrophe. *Cell*, *147*(5), 1092-1103. https://doi.org/10.1016/j.cell.2011.10.037

Gary, J. D., Sato, T. K., Stefan, C. J., Bonangelino, C. J., Weisman, L. S., & Emr, S. D. (2002). Regulation of Fab1 Phosphatidylinositol 3-Phosphate 5-Kinase Pathway by Vac7 Protein and Fig4, a Polyphosphoinositide Phosphatase Family Member. *Molecular biology of the cell*, *13*(4), 1238-1251. https://doi.org/10.1091/mbc.01-10-0498

Gary, J. D., Sato, T. K., Stefan, C. J., Bonangelino, C. J., Weisman, L. S., & Emr, S. D. (2002). Regulation of Fab1 phosphatidylinositol 3-phosphate 5-kinase pathway by Vac7 protein and Fig4, a polyphosphoinositide phosphatase family member. *Mol Biol Cell*, *13*(4), 1238-1251. https://doi.org/10.1091/mbc.01-10-0498

Gary, J. D., Wurmser, A. E., Bonangelino, C. J., Weisman, L. S., & Emr, S. D. (1998). Fab1p Is Essential for PtdIns(3)P 5-Kinase Activity and the Maintenance of Vacuolar Size and Membrane Homeostasis. *Journal of Cell Biology*, *143*(1), 65-79. https://doi.org/10.1083/jcb.143.1.65

Gary, J. D., Wurmser, A. E., Bonangelino, C. J., Weisman, L. S., & Emr, S. D. (1998). Fab1p is essential for PtdIns(3)P 5-kinase activity and the maintenance of vacuolar size and membrane homeostasis. *J Cell Biol*, *143*(1), 65-79. http://www.ncbi.nlm.nih.gov/pubmed/9763421

http://www.ncbi.nlm.nih.gov/pmc/articles/PMC2132800/pdf/9807012.pdf

Geymonat, M., Peng, Q., Guo, Z., Yu, Z., Unruh, J. R., Jaspersen, S. L., & Segal, M. (2020). Orderly assembly underpinning built-in asymmetry in the yeast centrosome duplication cycle requires cyclin-dependent kinase. *Elife*, *9*, e59222. https://doi.org/10.7554/eLife.59222

Geymonat, M., Spanos, A., Jensen, S., & Sedgwick, S. G. (2010). Phosphorylation of Lte1 by Cdk prevents polarized growth during mitotic arrest in S. cerevisiae. *J Cell Biol*, *191*(6), 1097-1112. https://doi.org/10.1083/jcb.201005070

Gruneberg, U., Campbell, K., Simpson, C., Grindlay, J., & Schiebel, E. (2000). Nud1p links astral microtubule organization and the control of exit from mitosis. *The EMBO Journal*, *19*(23), 6475-6488. https://doi.org/https://doi.org/10.1093/emboj/19.23.6475

Han, B. K., & Emr, S. D. (2011). Phosphoinositide [PI(3,5)P2] lipid-dependent regulation of the general transcriptional regulator Tup1. *Genes Dev*, *25*(9), 984-995. https://doi.org/10.1101/gad.1998611

Hartwell, L. H., Mortimer, R. K., Culotti, J., & Culotti, M. (1973). Genetic Control of the Cell Division Cycle in Yeast: V. Genetic Analysis of cdc Mutants. *Genetics*, *74*(2), 267-286.

Hasegawa, J., Strunk, B. S., & Weisman, L. S. (2017). PI5P and PI(3,5)P(2): Minor, but Essential Phosphoinositides. *Cell Struct Funct*, *42*(1), 49-60. https://doi.org/10.1247/csf.17003

Hasegawa, J., Strunk, B. S., & Weisman, L. S. (2017). PI5P and PI(3,5)P₂: Minor, but Essential Phosphoinositides. *Cell Structure and Function*, *42*(1), 49-60. https://doi.org/10.1247/csf.17003

Herskowitz, I. (1988). Life cycle of the budding yeast Saccharomyces cerevisiae. *Microbiol Rev*, *52*(4), 536-553. https://doi.org/10.1128/mr.52.4.536-553.1988

Hinnebusch, A. G., & Johnston, M. (2011). YeastBook: an encyclopedia of the reference eukaryotic cell. *Genetics*, *189*(3), 683-684. https://doi.org/10.1534/genetics.111.135129

Hou, J. Z., Xi, Z. Q., Niu, J., Li, W., Wang, X., Liang, C., Sun, H., Fang, D., & Xie, S. Q. (2019). Inhibition of PIKfyve using YM201636 suppresses the growth of liver cancer via the induction of autophagy. *Oncol Rep*, *41*(3), 1971-1979. https://doi.org/10.3892/or.2018.6928

Höfken, T., & Schiebel, E. (2002). A role for cell polarity proteins in mitotic exit. *Embo j*, *21*(18), 4851-4862. https://doi.org/10.1093/emboj/cdf481

Huda, M., Bektas, S. N., Bekdas, B., & Caydasi, A. K. (2023). The signalling lipid PI3,5P₂ is essential for timely mitotic exit. *Open Biology*, *13*(9), 230125. https://doi.org/doi:10.1098/rsob.230125

Huotari, J., & Helenius, A. (2011). Endosome maturation. *Embo j*, *30*(17), 3481-3500. https://doi.org/10.1038/emboj.2011.286

Hwang, E., Kusch, J., Barral, Y., & Huffaker, T. C. (2003). Spindle orientation in Saccharomyces cerevisiae depends on the transport of microtubule ends along polarized actin cables. *J Cell Biol*, *161*(3), 483-488. https://doi.org/10.1083/jcb.200302030

Ikonomov, O. C., Sbrissa, D., & Shisheva, A. (2019). Small molecule PIKfyve inhibitors as cancer therapeutics: Translational promises and limitations. *Toxicology and Applied Pharmacology*, *383*, 114771. https://doi.org/https://doi.org/10.1016/j.taap.2019.114771

Ito, H., Fukuda, Y., Murata, K., & Kimura, A. (1983). Transformation of intact yeast cells treated with alkali cations. *J Bacteriol*, *153*(1), 163-168. https://doi.org/10.1128/jb.153.1.163-168.1983

Jae Eun, C., Yuanyuan, Q., Ilona, K., Jiali, Y., Jonathan, G., Yi, B., Mahnoor, G., Jean Ching-Yi, T., Tomasz, M., Sahr, Y., Abhijit, P., Houjun, X., JiaJia, Z., Shuang, W., Sara, G., Linda, V., Heng, L., Gaopeng, L., Yang, Z., . . . Arul, M. C. (2024). PIKfyve controls dendritic cell function and tumor immunity. *bioRxiv*, 2024.2002.2028.582543. https://doi.org/10.1101/2024.02.28.582543

Janke, C., Magiera, M. M., Rathfelder, N., Taxis, C., Reber, S., Maekawa, H., Moreno-Borchart, A., Doenges, G., Schwob, E., Schiebel, E., & Knop, M. (2004). A versatile toolbox for PCR-based tagging of yeast genes: new fluorescent proteins, more markers and promoter substitution cassettes. *Yeast*, *21*(11), 947-962. https://doi.org/10.1002/yea.1142

Janke, C., Ortiz, J., Lechner, J., Shevchenko, A., Shevchenko, A., Magiera, M. M., Schramm, C., & Schiebel, E. (2001). The budding yeast proteins Spc24p and Spc25p interact with Ndc80p and Nuf2p at the kinetochore and are important for kinetochore clustering and checkpoint control. *The EMBO Journal*, *20*(4), 777-791. https://doi.org/https://doi.org/10.1093/emboj/20.4.777

Jaspersen, S. L., Charles, J. F., Tinker-Kulberg, R. L., & Morgan, D. O. (1998). A late mitotic regulatory network controlling cyclin destruction in Saccharomyces cerevisiae. *Mol Biol Cell*, *9*(10), 2803-2817. https://doi.org/10.1091/mbc.9.10.2803

Jaspersen, S. L., & Winey, M. (2004). The budding yeast spindle pole body: structure, duplication, and function. *Annu Rev Cell Dev Biol*, *20*, 1-28. https://doi.org/10.1146/annurev.cellbio.20.022003.114106

Jin, N., Chow, C. Y., Liu, L., Zolov, S. N., Bronson, R., Davisson, M., Petersen, J. L., Zhang, Y., Park, S., Duex, J. E., Goldowitz, D., Meisler, M. H., & Weisman, L. S. (2008). VAC14 nucleates a protein complex essential for the acute interconversion of PI3P and PI(3,5)P(2) in yeast and mouse. *Embo j*, *27*(24), 3221-3234. https://doi.org/10.1038/emboj.2008.248

Jin, N., Jin, Y., & Weisman, L. S. (2017). Early protection to stress mediated by CDK-dependent PI3,5P(2) signaling from the vacuole/lysosome. *J Cell Biol*, *216*(7), 2075-2090. https://doi.org/10.1083/jcb.201611144

Jin, N., Lang, M. J., & Weisman, L. S. (2016). Phosphatidylinositol 3,5-bisphosphate: regulation of cellular events in space and time. *Biochem Soc Trans*, *44*(1), 177-184. https://doi.org/10.1042/BST20150174

Jin, Y., Jin, N., Oikawa, Y., Benyair, R., Koizumi, M., Wilson, T. E., Ohsumi, Y., & Weisman, L. S. (2022). Bur1 functions with TORC1 for vacuole-mediated cell cycle progression. *EMBO reports*, *23*(4), e53477. https://doi.org/https://doi.org/10.15252/embr.202153477

Jin, Y., & Weisman, L. S. (2015). The vacuole/lysosome is required for cell-cycle progression. *Elife*, *4*, e08160. https://doi.org/10.7554/eLife.08160

Jin, Y., & Weisman, L. S. (2015). The vacuole/lysosome is required for cell-cycle progression. *Elife*, *4*. https://doi.org/10.7554/eLife.08160

Johnson, A., & Skotheim, J. M. (2013). Start and the restriction point. *Curr Opin Cell Biol*, *25*(6), 717-723. https://doi.org/10.1016/j.ceb.2013.07.010

Johnston, G. C. (1977). Cell size and budding during starvation of the yeast Saccharomyces cerevisiae. *J Bacteriol*, *132*(2), 738-739. https://doi.org/10.1128/jb.132.2.738-739.1977

Johnston, G. C., Pringle, J. R., & Hartwell, L. H. (1977). Coordination of growth with cell division in the yeast Saccharomyces cerevisiae. *Exp Cell Res*, *105*(1), 79-98. https://doi.org/10.1016/0014-4827(77)90154-9

Khmelinskii, A., Lawrence, C., Roostalu, J., & Schiebel, E. (2007). Cdc14-regulated midzone assembly controls anaphase B. *J Cell Biol*, *177*(6), 981-993. https://doi.org/10.1083/jcb.200702145

Khodjakov, A., & Rieder, C. L. (1996). Kinetochores moving away from their associated pole do not exert a significant pushing force on the chromosome. *Journal of Cell Biology*, *135*(2), 315-327. https://doi.org/10.1083/jcb.135.2.315

Kim, Yeun J., Guzman-Hernandez, Maria L., & Balla, T. (2011). A Highly Dynamic ER-Derived Phosphatidylinositol-Synthesizing Organelle Supplies Phosphoinositides to Cellular Membranes. *Developmental Cell*, *21*(5), 813-824. https://doi.org/10.1016/j.devcel.2011.09.005

Knop, M., Siegers, K., Pereira, G., Zachariae, W., Winsor, B., Nasmyth, K., & Schiebel, E. (1999). Epitope tagging of yeast genes using a PCR-based strategy: more tags and improved practical routines. *Yeast*, *15*(10B), 963-972. https://doi.org/https://doi.org/10.1002/(SICI)1097-0061(199907)15:10B<963::AID-YEA399>3.0.CO;2-W

Kocakaplan, D., Karabürk, H., Dilege, C., Kirdök, I., Bektas, S. N., & Caydasi, A. K. (2021). Protein phosphatase 1 in association with Bud14 inhibits mitotic exit in Saccharomyces cerevisiae. *Elife*, *10*, e72833. https://doi.org/10.7554/eLife.72833

Küntzel, H., Schulz, A., & Ehbrecht, I. M. (1996). Cell cycle control and initiation of DNA replication in Saccharomyces cerevisiae. *Biol Chem*, *377*(7-8), 481-487.

Lénárt, P., & Peters, J. M. (2006). Checkpoint activation: don't get mad too much. *Curr Biol*, *16*(11), R412-414. https://doi.org/10.1016/j.cub.2006.05.008

Li, L., Ernsting, B. R., Wishart, M. J., Lohse, D. L., & Dixon, J. E. (1997). A Family of Putative Tumor Suppressors Is Structurally and Functionally Conserved in Humans and Yeast *. *Journal of Biological Chemistry*, *272*(47), 29403-29406. https://doi.org/10.1074/jbc.272.47.29403

Liao, Y. C., Fernandopulle, M. S., Wang, G., Choi, H., Hao, L., Drerup, C. M., Patel, R., Qamar, S., Nixon-Abell, J., Shen, Y., Meadows, W., Vendruscolo, M., Knowles, T. P. J., Nelson, M., Czekalska, M. A., Musteikyte, G., Gachechiladze, M. A., Stephens, C. A., Pasolli, H. A., . . . Ward, M. E. (2019). RNA Granules

Hitchhike on Lysosomes for Long-Distance Transport, Using Annexin A11 as a Molecular Tether. *Cell*, *179*(1), 147-164.e120. https://doi.org/10.1016/j.cell.2019.08.050

Loewith, R., & Hall, M. N. (2011). Target of rapamycin (TOR) in nutrient signaling and growth control. *Genetics*, *189*(4), 1177-1201. https://doi.org/10.1534/genetics.111.133363

Loewith, R., Jacinto, E., Wullschleger, S., Lorberg, A., Crespo, J. L., Bonenfant, D., Oppliger, W., Jenoe, P., & Hall, M. N. (2002). Two TOR Complexes, Only One of which Is Rapamycin Sensitive, Have Distinct Roles in Cell Growth Control. *Molecular Cell*, *10*(3), 457-468. https://doi.org/10.1016/S1097-2765(02)00636-6

Maiato, H., Gomes, A. M., Sousa, F., & Barisic, M. (2017). Mechanisms of Chromosome Congression during Mitosis. *Biology (Basel)*, *6*(1). https://doi.org/10.3390/biology6010013

Malia, P. C., Numrich, J., Nishimura, T., González Montoro, A., Stefan, C. J., & Ungermann, C. (2018). Control of vacuole membrane homeostasis by a resident PI-3,5-kinase inhibitor. *Proc Natl Acad Sci U S A*, *115*(18), 4684-4689. https://doi.org/10.1073/pnas.1722517115

McCartney, A. J., Zhang, Y., & Weisman, L. S. (2014). Phosphatidylinositol 3,5-bisphosphate: low abundance, high significance. *Bioessays*, *36*(1), 52-64. https://doi.org/10.1002/bies.201300012

McIntosh, J. R. (2016). Mitosis. *Cold Spring Harb Perspect Biol*, *8*(9). https://doi.org/10.1101/cshperspect.a023218

Merlini, L., Dudin, O., & Martin, S. G. (2013). Mate and fuse: how yeast cells do it. *Open Biology*, *3*(3), 130008. https://doi.org/doi:10.1098/rsob.130008

Mitchison, T., & Kirschner, M. (1984). Dynamic instability of microtubule growth. *Nature*, *312*(5991), 237-242. https://doi.org/10.1038/312237a0

Moore, J. K., Chudalayandi, P., Heil-Chapdelaine, R. A., & Cooper, J. A. (2010). The spindle position checkpoint is coordinated by the Elm1 kinase. *J Cell Biol*, *191*(3), 493-503. https://doi.org/10.1083/jcb.201006092

Morgan, D. O. (1997). CYCLIN-DEPENDENT KINASES: Engines, Clocks, and Microprocessors. *Annual Review of Cell and Developmental Biology*, *13*(1), 261-291. https://doi.org/10.1146/annurev.cellbio.13.1.261

Moyano-Rodríguez, Y., Vaquero, D., Vilalta-Castany, O., Foltman, M., Sanchez-Diaz, A., & Queralt, E. (2022). PP2A-Cdc55 phosphatase regulates actomyosin ring contraction and septum formation during cytokinesis. *Cell Mol Life Sci*, *79*(3), 165. https://doi.org/10.1007/s00018-022-04209-1

Musacchio, A., & Salmon, E. D. (2007). The spindle-assembly checkpoint in space and time. *Nat Rev Mol Cell Biol*, *8*(5), 379-393. https://doi.org/10.1038/nrm2163

Nasmyth, K., & Dirick, L. (1991). The role of SWI4 and SWI6 in the activity of G1 cyclins in yeast. *Cell*, *66*(5), 995-1013. https://doi.org/10.1016/0092-8674(91)90444-4

Nasmyth, K., & Haering, C. H. (2009). Cohesin: its roles and mechanisms. *Annu Rev Genet*, *43*, 525-558. https://doi.org/10.1146/annurev-genet-102108-134233

Nigg, E. A., & Stearns, T. (2011). The centrosome cycle: Centriole biogenesis, duplication and inherent asymmetries. *Nature Cell Biology*, *13*(10), 1154-1160. https://doi.org/10.1038/ncb2345

Noda, T. (2017). Regulation of Autophagy through TORC1 and mTORC1. *Biomolecules*, *7*(3), 52. https://www.mdpi.com/2218-273X/7/3/52

Novarina, D., Guerra, P., & Milias-Argeitis, A. (2021). Vacuolar Localization via the N-terminal Domain of Sch9 is Required for TORC1-dependent Phosphorylation

and Downstream Signal Transduction. *Journal of Molecular Biology*, *433*(24), 167326. https://doi.org/https://doi.org/10.1016/j.jmb.2021.167326

Obara, K., Sekito, T., Niimi, K., & Ohsumi, Y. (2008). The Atg18-Atg2 Complex Is Recruited to Autophagic Membranes via Phosphatidylinositol 3-Phosphate and Exerts an Essential Function*. *Journal of Biological Chemistry*, *283*(35), 23972-23980. https://doi.org/https://doi.org/10.1074/jbc.M803180200

Palmer, R. E., Sullivan, D. S., Huffaker, T., & Koshland, D. (1992). Role of astral microtubules and actin in spindle orientation and migration in the budding yeast, Saccharomyces cerevisiae. *J Cell Biol*, *119*(3), 583-593. https://doi.org/10.1083/jcb.119.3.583

Pereira, G., & Schiebel, E. (2005). Kin4 kinase delays mitotic exit in response to spindle alignment defects. *Mol Cell*, *19*(2), 209-221. https://doi.org/10.1016/j.molcel.2005.05.030

Pereira, G., Tanaka, T. U., Nasmyth, K., & Schiebel, E. (2001). Modes of spindle pole body inheritance and segregation of the Bfa1p–Bub2p checkpoint protein complex. *The EMBO Journal*, *20*(22), 6359-6370. https://doi.org/https://doi.org/10.1093/emboj/20.22.6359

Pfleger, C. M., & Kirschner, M. W. (2000). The KEN box: an APC recognition signal distinct from the D box targeted by Cdh1. *Genes Dev*, *14*(6), 655-665.

Proudfoot, K. G., Anderson, S. J., Dave, S., Bunning, A. R., Sinha Roy, P., Bera, A., & Gupta, M. L. (2019). Checkpoint Proteins Bub1 and Bub3 Delay Anaphase Onset in Response to Low Tension Independent of Microtubule-Kinetochore Detachment. *Cell Reports*, *27*(2), 416-428.e414. https://doi.org/https://doi.org/10.1016/j.celrep.2019.03.027

Queralt, E., Lehane, C., Novak, B., & Uhlmann, F. (2006). Downregulation of PP2A(Cdc55) phosphatase by separase initiates mitotic exit in budding yeast. *Cell*, *125*(4), 719-732. https://doi.org/10.1016/j.cell.2006.03.038

Quilis, I., & Igual, J. C. (2012). Molecular basis of the functional distinction between Cln1 and Cln2 cyclins. *Cell Cycle*, *11*(16), 3117-3131. https://doi.org/10.4161/cc.21505

Riera, A., Barbon, M., Noguchi, Y., Reuter, L. M., Schneider, S., & Speck, C. (2017). From structure to mechanism-understanding initiation of DNA replication. *Genes Dev*, *31*(11), 1073-1088. https://doi.org/10.1101/gad.298232.117

Rivero-Ríos, P., & Weisman, L. S. (2022). Roles of PIKfyve in multiple cellular pathways. *Current Opinion in Cell Biology*, *76*, 102086. https://doi.org/https://doi.org/10.1016/j.ceb.2022.102086

Rudge, S. A., Anderson, D. M., & Emr, S. D. (2004). Vacuole Size Control: Regulation of PtdIns(3,5)P2 Levels by the Vacuole-associated Vac14-Fig4 Complex, a PtdIns(3,5)P2-specific Phosphatase. *Molecular biology of the cell*, *15*(1), 24-36. https://doi.org/10.1091/mbc.e03-05-0297

Rudge, S. A., Anderson, D. M., & Emr, S. D. (2004). Vacuole size control: regulation of PtdIns(3,5)P2 levels by the vacuole-associated Vac14-Fig4 complex, a PtdIns(3,5)P2-specific phosphatase. *Mol Biol Cell*, *15*(1), 24-36. https://doi.org/10.1091/mbc.e03-05-0297

Sambrook, J., Fritsch, E. F., & Maniatis, T. (1989). *Molecular cloning: a laboratory manual*. Cold spring harbor laboratory press.

Scholey, J. M., Civelekoglu-Scholey, G., & Brust-Mascher, I. (2016). Anaphase B. *Biology (Basel)*, *5*(4). https://doi.org/10.3390/biology5040051

Seshan, A., & Amon, A. (2005). Ras and the Rho effector Cla4 collaborate to target and anchor Lte1 at the bud cortex. *Cell Cycle*, *4*(7), 940-946. https://doi.org/10.4161/cc.4.7.1785

Sherman, F. (1991). [1] Getting started with yeast. In *Methods in Enzymology* (Vol. 194, pp. 3-21). Academic Press. https://doi.org/https://doi.org/10.1016/0076-6879(91)94004-V

Shirayama, M., Matsui, Y., Tanaka, K., & Toh-E, A. (1994). Isolation of a CDC25 family gene, MSI2/LTE1, as a multicopy suppressor of ira1. *Yeast*, *10*(4), 451-461. https://doi.org/https://doi.org/10.1002/yea.320100404

Sikorski, R. S., & Hieter, P. (1989). A system of shuttle vectors and yeast host strains designed for efficient manipulation of DNA in Saccharomyces cerevisiae. *Genetics*, *122*(1), 19-27. https://www.ncbi.nlm.nih.gov/pubmed/2659436

Simmons Kovacs, L. A., Mayhew, M. B., Orlando, D. A., Jin, Y., Li, Q., Huang, C., Reed, S. I., Mukherjee, S., & Haase, S. B. (2012). Cyclin-dependent kinases are regulators and effectors of oscillations driven by a transcription factor network. *Mol Cell*, *45*(5), 669-679. https://doi.org/10.1016/j.molcel.2011.12.033

Sommer, R. A., DeWitt, J. T., Tan, R., & Kellogg, D. R. (2021). Growth-dependent signals drive an increase in early G1 cyclin concentration to link cell cycle entry with cell growth. *Elife*, *10*, e64364. https://doi.org/10.7554/eLife.64364

Stegmeier, F., Huang, J., Rahal, R., Zmolik, J., Moazed, D., & Amon, A. (2004). The replication fork block protein Fob1 functions as a negative regulator of the FEAR network. *Curr Biol*, *14*(6), 467-480. https://doi.org/10.1016/j.cub.2004.03.009

Straight, A. F., Marshall, W. F., Sedat, J. W., & Murray, A. W. (1997). Mitosis in living budding yeast: anaphase A but no metaphase plate. *Science*, *277*(5325), 574-578. https://doi.org/10.1126/science.277.5325.574

Strømhaug, P. E., Reggiori, F., Guan, J., Wang, C. W., & Klionsky, D. J. (2004). Atg21 is a phosphoinositide binding protein required for efficient lipidation and localization of Atg8 during uptake of aminopeptidase I by selective autophagy. *Mol Biol Cell*, *15*(8), 3553-3566. https://doi.org/10.1091/mbc.e04-02-0147

Takeda, E., & Matsuura, A. (2018). A substrate localization model for the selective regulation of TORC1 downstream pathways. *Commun Integr Biol*, *11*(2), 1-4. https://doi.org/10.1080/19420889.2018.1475830

Tooley, J., & Stukenberg, P. T. (2011). The Ndc80 complex: integrating the kinetochore's many movements. *Chromosome Res*, *19*(3), 377-391. https://doi.org/10.1007/s10577-010-9180-5

Tsakraklides, V., & Bell, S. P. (2010). Dynamics of pre-replicative complex assembly. *J Biol Chem*, *285*(13), 9437-9443. https://doi.org/10.1074/jbc.M109.072504

Uhlmann, F., Wernic, D., Poupart, M. A., Koonin, E. V., & Nasmyth, K. (2000). Cleavage of cohesin by the CD clan protease separin triggers anaphase in yeast. *Cell*, *103*(3), 375-386. https://doi.org/10.1016/s0092-8674(00)00130-6

Visintin, R., & Amon, A. (2001). Regulation of the mitotic exit protein kinases Cdc15 and Dbf2. *Molecular biology of the cell*, *12*(10), 2961-2974.

Wallroth, A., & Haucke, V. (2018). Phosphoinositide conversion in endocytosis and the endolysosomal system. *J Biol Chem*, *293*(5), 1526-1535. https://doi.org/10.1074/jbc.R117.000629

Weber, S. C., & Brangwynne, C. P. (2012). Getting RNA and protein in phase. *Cell*, *149*(6), 1188-1191. https://doi.org/10.1016/j.cell.2012.05.022

Weisman, L. S. (2003). Yeast Vacuole Inheritance and Dynamics. *Annual Review of Genetics*, *37*(1), 435-460. https://doi.org/10.1146/annurev.genet.37.050203.103207

Yamamoto, A., DeWald, D. B., Boronenkov, I. V., Anderson, R. A., Emr, S. D., & Koshland, D. (1995). Novel PI(4)P 5-kinase homologue, Fab1p, essential for normal vacuole function and morphology in yeast. *Molecular biology of the cell*, *6*(5), 525-539. https://doi.org/10.1091/mbc.6.5.525

Zetterberg, A., & Larsson, O. (1985). Kinetic analysis of regulatory events in G1 leading to proliferation or quiescence of Swiss 3T3 cells. *Proceedings of the National Academy of Sciences*, *82*(16), 5365-5369. https://doi.org/doi:10.1073/pnas.82.16.5365

Zhu, H., Fang, K., & Fang, G. (2009). Microtubule amplification in the assembly of mitotic spindle and the maturation of kinetochore fibers. *Communicative & Integrative Biology*, *2*(3), 208-210. https://doi.org/10.4161/cib.2.3.7875